ABSTRACT

A RESONANT CAVITY HIGH FREQUENCY OSCILLOMETER

by Dante Anthony Costanzo

A high frequency oscillometer operating at 100 megacycles per second was developed. A reentrant cavity was employed as the resonant circuit element. High frequency voltage was induced in the cavity by inductive coupling of the cavity to a constant voltage and constant frequency generator. The current flowing in the cavity was indicated by a tuned detector circuit which was capacitatively coupled to the cavity. The high frequency energy received by the detector probe is rectified and applied to the grid circuit of a dc amplifier tube which is part of a modified Wheatstone Bridge circuit. Bridge unbalance current is linearily related to signal intensity.

One electrode of a precision variable condenser was directly connected to the inner cylinder and the other electrode was connected to the outer cylinder of the cavity. Connected in parallel with the electrodes of the precision variable condenser was a condenser-type cell. When the oscillometer was initially tuned to resonance, a change in conductivity and/or dielectric constant in the solution contained in the cell detuned the oscillometer. Resonance was reestablished by adjustment of the precision condenser as indicated by maximum detector current.

Dante Anthony Costanzo

The changes in instrument responses, effective cavity current, cell capacitance at resonance, and cell capacitance at half power points are related to changes in admittance of the cell-solution network.

Equivalent circuits are proposed to represent cavity, detector and cell-solution networks. A qualitative interpretation of instrument responses in terms of these circuits is presented.

Instrument performance was tested with a simulated titration of an aqueous solution of hydrochloric acid with sodium hydroxide and a simulated titration of a glacial acetic acid solution of sodium acetate with perchloric acid. Dielectric constants of some pure organic solvents were determined by means of direct capacitance measurements.

# A RESONANT CAVITY HIGH FREQUENCY OSCILLOMETER

by

Dante Anthony Costanzo

A THESIS

Submitted to
Michigan State University
in partial fulfillment of the requirements
for the degree of

DOCTOR OF PHILOSOPHY

Department of Chemistry

1967

ACKNOWLEDGEMENTS

The author wishes to express his appreciation to his major professor, Dr. Andrew Timnick, for his encouragement and guidance given throughout this investigation and in the preparation of this thesis.

Acknowledgement is also extended to Mr. Arthur H. Johnson for his helpful suggestion pertaining to instrument design and to the late Mr. Frank Betts for his cooperation and supervision in the shop.

A debt of gratitude is due to the author's wife, Donna Lee, for her patience, understanding and encouragement through his graduate studies.

A special acknowledgement is extended to the Analytical Chemistry Division of the Oak Ridge National Laboratory for the preparation of the drawings contained herein.

# VITA

The author, Dante Anthony Costanzo, was born April 26, 1932, in Cleveland, Ohio. He attended elementary, grade and high school in Lakewood, Ohio. He graduated from Lakewood High School in 1950. He attended Michigan State University from 1950 to 1954 and received a Bachelor of Science degree in 1954 with a major in chemistry. He received a Forest Acker's scholarship (1951-52) and a Superior Student scholarship (1952-54) during his undergraduate studies. He continued in attendance at Michigan State University from 1954 until 1959 in pursuit of an advanced degree. He was a graduate teaching assistant during the school periods 1954 through 1959.

The author is a member of the Society of Sigma Xi, the Society of Sigma Pi Sigma, RESA, the American Association for the Advancement of Science, the American Chemical Society, and the American Institute of Chemists.

TABLE OF CONTENTS

page

LIST OF TABLES

LIST OF FIGURES

page

page

LIST OF APPENDICES

# INTRODUCTION

Oscillometry is a term applied to a class of physico-chemical measurements which employs high frequency oscillators as a power source and reactive coupling of such circuits with test solutions by means of electrodes isolated from the sample. Instruments which are suitable for making high frequency measurements are named oscillometers and the methods of the class are characterized as oscillometric methods.[1]

In the oscillometric method of analysis, the vessel containing the solution to be analyzed is placed between the plates of a capacitor (condenser-type cell) or in the field of a coil (coil-type cell). The cell may be part of a resonance circuit of a high frequency oscillator, or may be part of a resonance circuit excited by high frequency energy from an external oscillator. The oscillators operate in the megacycle per second (Mc/sec) frequency region at either a fixed frequency or at variant frequencies depending upon specific circuitry.

A change in composition of test solution contained within the cell is indicated by a change in the oscillometer response. The response is associated with the electrochemical properties of the test sample and is effected by the entire chemical system between the electrodes. The instrument is responsive to the dielectric constant and/or to the conductivity of the test solution, depending upon the specific circuitry.

Oscillometer responses which may be observed to follow the course of a titration, to evaluate dielectric constants, to monitor flowing streams or chromatographic effluents, etc., are: effective tank circuit current or voltage, cell capacitance, oscillator plate current or grid

current and bias, and frequency. The oscillometer response measured is related to either the total admittance current or to the real or imaginary part of the admittance current flowing through the high frequency cell containing the test sample. Those oscillometer responses related to the real part of the admittance current are proportional to the $Q$-factor of the circuit, and those responses related to the imaginary part are proportional to the susceptance.

Several excellent reviews are available which describe the present state of instrumentation and applications of the oscillometric method of analysis.[1-15]

The principles and theoretical foundation of the oscillometric methods of analysis have been discussed by several authors.[16-25] Reilly and McCurdy[13,24] quantitatively developed in a perspicuous manner, the theory underlying the high frequency measurements when employing a condenser type cell. The authors sucessfully employed a twin-T impedance bridge to obtain absolute values of electrical quantities for a condenser-type cell to test their theory.

Reilly and McCurdy[13,24] have shown that the optimum working concentration, that concentration in which the instrument responds in a nearly linear manner with changes in solution composition, is directly proportional to the operating frequency of the oscillometer and to the geometry of the cell. To extend the instrument response to higher concentrations, higher operating frequencies must be employed.

Many instruments have been described which operate in the frequencies between 1-30 Mc/sec.[21,26,28] These instruments may be employed for concentration measurements of solutions equivalent in conductance

to an aqueous 0.06 M NaCl solution. In instruments operating in this frequency range, ordinary inductances and capacitances are employed in resonant circuit construction. Above 30-40 Mc/sec, the distributed capacitances and inductances of circuit connectors and components become critical and ordinary circuits are no longer usable. To circumvent this difficulty, coaxial lines, transmission lines and cavity resonators are employed to construct stable oscillators.

Johnson and Timnick,[29] and Pungor,[30] constructed half-wavelength coaxial-line oscillators operating at approximately 125-130 Mc/sec. Lane[31] and Fisher, Kelley, Stelzner and Wagner[32] designed instruments operating at 200 to 250 Mc/sec which include parallel-transmission-line oscillators. Pancek,[33] Stelzner,[34] Blaedel and Malmstadt,[35] and Huber and Cruse[19] utilized concentric line oscillators operating at frequencies between 350-500 Mc/sec.

Works, Daken, and Baggs,[36] in 1945, adapted a cavity resonator to the measurement of dielectric constants and power factors of solid dielectric materials at 200 Mc/sec. A signal generator was employed as a source of high frequency energy to excite two cavities, one, a measuring cavity into which the sample was inserted, and the other, a calibrated wavemeter. Parallel crystal diodes in conjunction with a high sensitivity galvanometer were employed to indicate a current proportional to the voltage in the cavity. Voltage, wavemeter, and heterodyning methods were employed to determine dielectric constants and power factors. An oscilloscope replaced the high sensitivity galvanometer in the frequency modulation method to determine dielectric constants and power factors.

Johnson[37] adapted a cavity resonator obtained from a U.S. Navy Model OAO-2 radar test equipment frequency meter to the measurement of dielectric constants and power factors of solid dielectric materials. Johnson loosely coupled an oscillator operating at a fixed frequency of 100 Mc/sec to the cavity resonator. A General Radio Type 1690-A dielectric sample holder, into which the sample was inserted, was connected to the cavity. A crystal diode and vibrating reed electrometer with current sensitivity of $10^{-15}$ amperes, was employed in the detector circuit.

Blaedel and Malmstadt[35] and Huber and Cruse[19] described oscillometers operating at 350 and 415 Mc/sec respectively. Each oscillometer contained two oscillators, a reference oscillator and a working oscillator. The reference oscillator operated at a fixed frequency and employed a cavity resonator. The working oscillator, employed a concentric line as the resonant circuit element. The sample cell was coupled to the working oscillator, and as the composition of the sample varied, the resonant frequency of the working oscillator varied. Changes in beat frequency between these two oscillators, reflected changes in sample composition.

A reentrant cylindrical cavity resonator similar to that described by Johnson[37] was adopted as the resonant circuit element of the oscillometer developed and employed in this investigation.

Statement of Problem. This study was undertaken to; (1) construct a prototype oscillometer to operate in the 100 Mc/sec frequency range which employs a cavity resonator as the resonant circuit element, (2) to elucidate the nature of the instrument response for an instrument

operating in this frequency range, (3) to test the performance of the oscillometer by means of practical physico-chemical measurements on aqueous and nonaqueous systems.

## THEORY

Series Resonance If a sinusoidal voltage is applied to a series combination of resistance, inductance and capacitance as shown in Fig. 1,[38-40] the current flowing in the circuit is given by

$$I = \frac{E}{R + j\left(\omega L - \frac{1}{\omega C}\right)} \tag{1}$$

where $I$ is the current in amperes, $E$ is the applied voltage in volts, $R$ is the resistance in ohms, $L$ is the inductance in henries, $C$ is the capacitance in farads, $\omega$ is the angular frequency equal to $2\pi f$, where $f$ is the frequency in cycles per second, and $j$ is equal to $(-1)^{1/2}$.

Effective impedance Z, the retarding effect on current flow, can be described by the complex quantity

$$Z = R + j\left(X_l - X_c\right) \tag{2}$$

where $X_l$ is the inductive reactance in ohms, equal to $\omega L$ and $X_c$ is the capacitive reactance equal to $\frac{1}{\omega C}$. The effective impedance is the vector sum of resistance and reactance and has both magnitude and phase. The magnitude of the impedance is given by

$$Z = \left[R^2 + \left(\omega L - \frac{1}{\omega C}\right)^2\right]^{1/2} \tag{3}$$

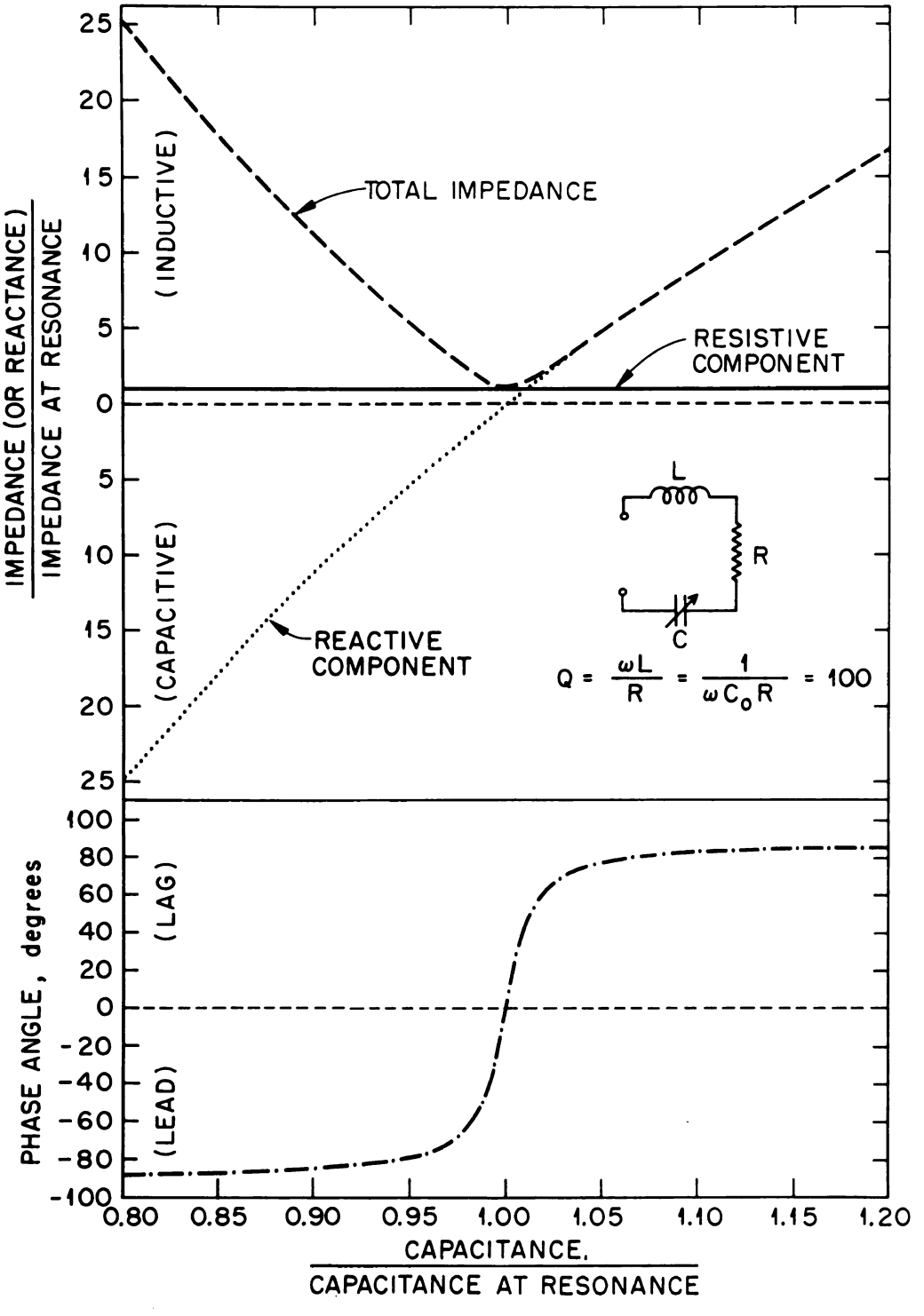


Figure 1. Magnitude and Phase Angle of the Impedance of a Series Resonant Circuit as a Function of Capacitance

The applied voltage is the vector sum of the voltage drops across each circuit component, the values of which are given by

$$E_r = IR \tag{4}$$

$$E_l = j\omega LI \tag{5}$$

$$E_c = \frac{I}{j\omega C} \tag{6}$$

where $E_r$ is the voltage across resistance, $R$, and $E_l$ and $E_c$, are the voltage across the inductance, $L$, and capacitance, $C$, respectively.

The phase angle between the applied voltage and the current is different for each circuit component. The current through the capacitive branch leads the voltage by 90°; the current through the inductive branch lags the voltage by 90°; and the current through the resistive branch is in phase with the current. The phase angle, $\theta$, between the applied voltage and resultant current flowing in the $RLC$ series network is given by

$$\tan \theta = \frac{\omega L - \frac{1}{\omega C}}{R} \tag{7}$$

The current flowing in the circuit will be a maximum when the inductive reactance is equal to the capacitative reactance or,

$$\omega L = \frac{1}{\omega C} \tag{8}$$

in which case the circuit is said to be resonant. The frequency at

which the circuit is resonant is called the resonance frequency and is equal to

$$(9) \qquad f_o = \frac{1}{2\pi\sqrt{LC}}$$

where the subscript zero denotes the value at resonance.

The series resonance circuit represents to a sinusoidal voltage of the resonant frequency an impedance which is a minimum and purely ohmic. Therefore, the resultant current is in phase with the applied voltage ($\theta = 0$) at the resonant frequency, and

$$(10) \qquad I_0 = \frac{E_{applied}}{R}$$

At resonance the voltage across either the inductance $L$ or capacitance $C$ is given by

$$(11) \qquad E_l \text{ or } E_c = E_{applied} \cdot Q$$

The ratio of the inductive reactance or capacitative reactance to the resistance $R$, is called the circuit $Q$, so

$$(12) \qquad Q = \frac{X}{R} = \frac{\omega L}{R} = \frac{1}{\omega CR}$$

and is defined by

$$(13) \qquad Q = \frac{2\pi \text{ energy stored per cycle in circuit}}{\text{energy dissipated per cycle in circuit}}$$

The circuit $Q$ is a measure of the energy dissipated in the circuit due to the ohmic resistance.

When a sinusoidal voltage is applied to a series $RLC$ network as represented in Fig. 1, the circuit may be tuned to resonance, as indicated by maximum circuit current, by varying the frequency, inductance or the capacitance (Equation 8). In this discussion only the effect of capacitative tuning upon circuit response will be considered.

To illustrate the effect of capacitative tuning on circuit behavior, the universal resonance curves, Fig. 1, 2 and 3, were constructed.[40] In universal resonance curves relative quantities rather than absolute quantities are usually interpreted. In the figures cited, relative quantities (except $\tan \theta$) are plotted against fractional tuning, $\gamma$, defined as

$$(14) \qquad \gamma = \frac{C}{C_o}$$

where $C$ is the actual capacitance and $C_o$ is capacitance at resonance. These curves which apply to any series resonance circuits, are independant of frequency or the ratio of inductance to capacitance.

The universal resonance curves are obtained by means of the expression (see Appendix I for sample derivation)

$$(15) \qquad \frac{Z}{Z_o} = \sqrt{1 + Q^2 \left(1 - \frac{1}{\gamma}\right)^2}$$

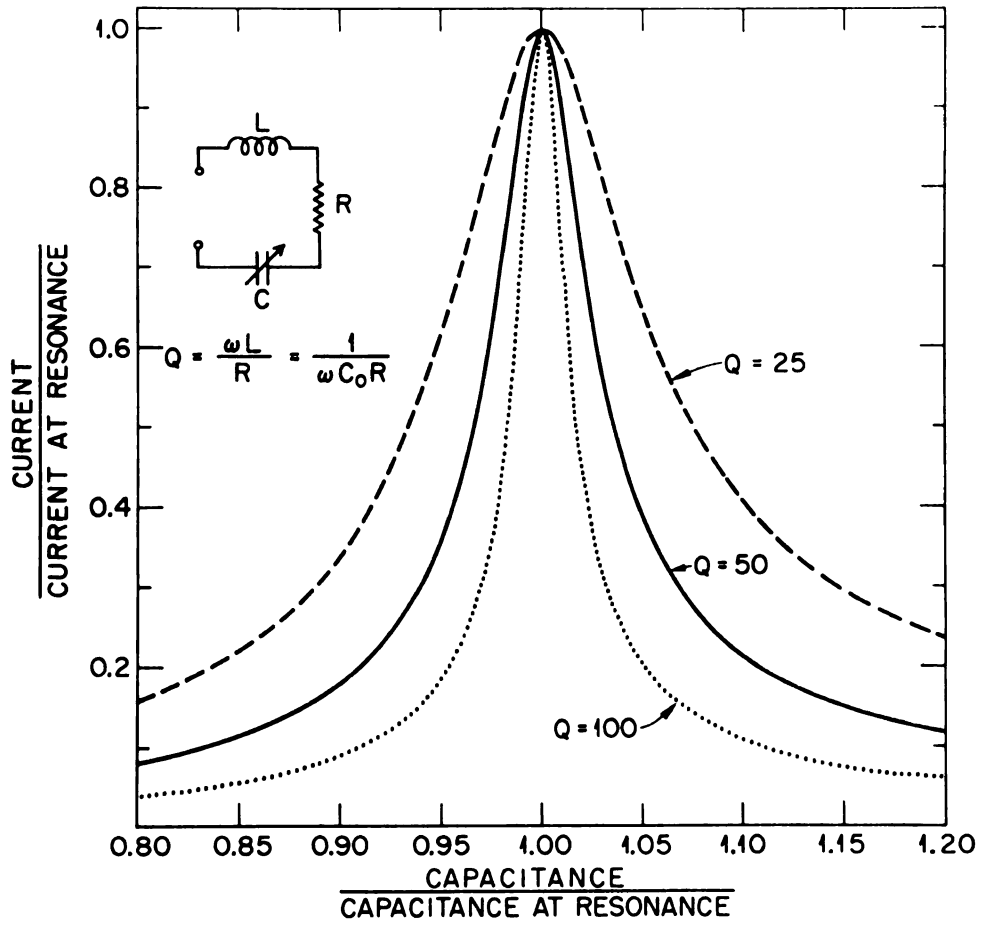


Figure 2. Current Flowing in a Series Resonant Circuit as a Function of Capacitance at Constant Resistance

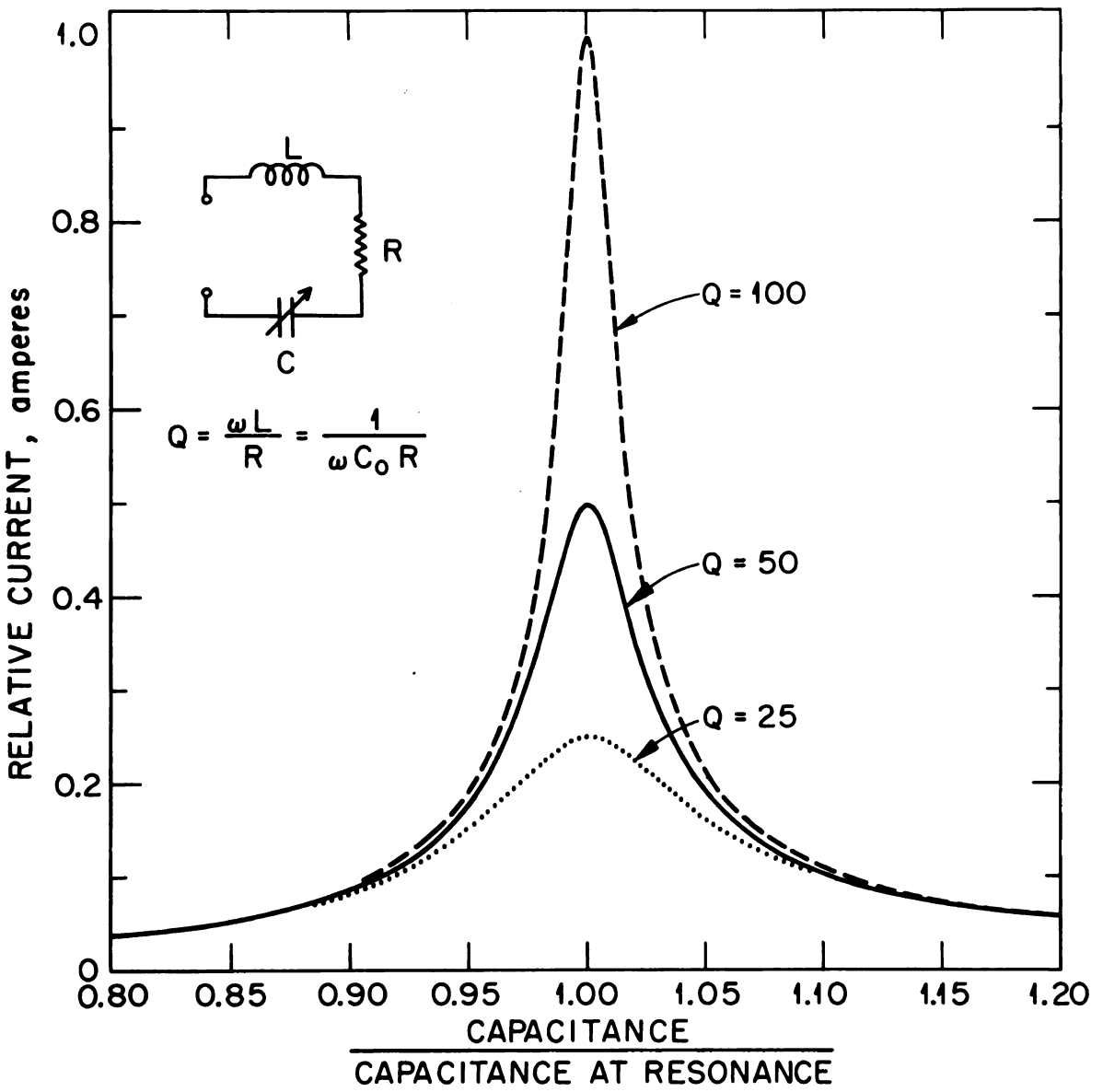


Figure 3. Current Flowing in a Series Resonant Circuit as a Function of Capacitance at Constant Inductive Reactance

(16) $$\frac{X}{Z_o} = Q\left(\frac{f}{f_o} - \frac{f_o}{f}\right)$$

(17) $$\tan\theta = Q\left(\frac{f}{f_o} - \frac{f_o}{f}\right)$$

(18) $$\frac{I}{I_o} = \frac{1}{\sqrt{1 + Q^2\left(\frac{f}{f_o} - \frac{f_o}{f}\right)^2}}$$

where $Z$ and $X$ are the actual impedance and reactance, respectively, of the circuit, $I$ is the actual current flowing in the circuit, $Z_o$ is the characteristic impedance at resonance, and $I_o$ is the current flowing at resonance.

Fig. 1 shows the magnitude and phase angle of the impedance of a series resonant circuit as a function of capacitance. The impedance is broken up into the resistive and reactive components. The resistive component is constant and independent of the circuit capacitance.

At resonance, the reactance curve passes through zero, as does the phase angle curve, and the characteristic impedance is a minimum, equal to the ohmic resistance of the circuit.

Below resonance, the circuit is capacitive, the current leads the applied voltage and the phase angle is negative. Above resonance, the circuit is inductive, the current lags the applied voltage and the phase angle is positive.

The resonance curves in Fig. 2 show the current flowing as a function of capacitance for series resonant circuits of different circuit $Q$ values. The higher the circuit $Q$ the sharper is the curve. The sharper the resonance curve, the more sensitive is the current response

of a series *RLC* circuit tuned to resonance to changes in circuit parameters.

The width of the resonance curves corresponding to 0.707 of the current at resonance is related to the circuit $Q$ by the expression

$$(19) \qquad \left(\gamma_2 - \gamma_1\right)_{0.707} = \frac{\left(C_2 - C_1\right)_{0.707}}{C_0} = \frac{2Q}{Q^2 - 1}$$

where $\gamma_2$ and $\gamma_1$, the half power points, are the values of the fractional tuning on either side of the resonance curves corresponding to 0.707 of the current at resonance. Accordingly, $C_2$ and $C_1$ are the capacitance values on either side of the resonance curve corresponding to 0.707 of the current at resonance, and $C_0$ is the capacitance at resonance. If the circuit $Q$ is much greater than unity, the width of the resonance curve is approximately equal to

$$(20) \qquad \left(\gamma_2 - \gamma_1\right)_{0.707} = \frac{\left(C_2 - C_1\right)_{0.707}}{C_0} = \frac{2}{Q}$$

Fig. 3 shows the relationship between the relative current and the capacitance for series resonant circuits for which the frequency of the applied voltage and the circuit inductance are constant but $Q$ factors of the circuits differ. The current at resonance is directly proportional to the circuit $Q$. Far removed from resonance, the current flowing is nearly independent of the circuit $Q$. The width of the resonance curves corresponding to 0.707 of the current at resonance again is given by equation (19).

Parallel Resonance If a sinusoidal current $I$ is applied to a parallel network of resistance $R$, inductance $L$ and capacitance $C$, as shown in Fig. 4, the voltage across the parallel network is given by[38-40]

$$V = \frac{I}{\frac{1}{R} + j\left(\omega C - \frac{1}{\omega L}\right)} \tag{21}$$

The net admittance of the circuit, $Y$, the reciprocal of the effective circuit impedance, can be described by a complex quantity

$$Y = \frac{1}{R} + j\left(\omega C - \frac{1}{\omega L}\right) \tag{22}$$

where $Y$ is the admittance in mhos, equal to $\frac{1}{Z}$ the reciprocal of the impedance offered by the circuit, $\frac{1}{R}$ is the conductance in mhos, equal to the real part of the admittance, and $\left(\omega C - \frac{1}{\omega L}\right)$ is the susceptance in mhos, equal to the imaginary part of the admittance.

The magnitude of the admittance is given by

$$Y = \sqrt{\left(\frac{1}{R}\right)^2 + \left(\omega C - \frac{1}{\omega L}\right)^2} \tag{23}$$

and the phase angle of the admittance is given by

$$\tan \theta = R\left(\omega C - \frac{1}{\omega L}\right) \tag{24}$$

The voltage across the parallel network will be a maximum when the imaginary term of the admittance, the susceptance, is equal to zero, in which case the circuit is said to be resonant. The frequency at which this occurs is given by equations (8) and (9).

The circuit $Q$ for the parallel resonant circuit is given by

$$Q = \frac{R}{X_0} = \frac{R}{\omega L_0} = \omega C_0 R \tag{25}$$

where $X_0$ denotes the reactance of the inductive or capacitive branch at resonance. For a large circuit $Q$, the parallel circuit requires that $R >> X_0$, whereas, for the series circuit, $R << X_0$.

The impedance offered by the parallel $RLC$ network, represented by the fundamental circuit in Fig. 4, can be expressed in the form of an equivalent resistance and equivalent reactance as represented by equivalent series circuit in Fig. 4.

The characteristic impedance of the parallel combination is given by

$$Z = \frac{R}{1 + R^2\left|\omega C - \frac{1}{\omega L}\right|^2} - j\,\frac{R^2\left|\omega C - \frac{1}{\omega L}\right|}{1 + R^2\left|\omega C - \frac{1}{\omega L}\right|^2} \tag{26}$$

If the voltage, impedance, or phase angle are expressed in terms of the circuit $Q$ and the fractional capacitive tuning, universal resonance curves which will be independent of the frequency or the ratio of the inductance and capacitance may be obtained for any parallel circuit by means of the expressions (See Appendix I for sample

derivation)[40]

$$\frac{Z}{Z_0} = \frac{V}{V_0} = \frac{1}{\sqrt{1 + Q^2(\gamma - 1)^2}} \tag{27}$$

$$\frac{R_{eq}}{Z_0} = \frac{1}{1 + Q^2(\gamma - 1)^2} \tag{28}$$

$$\frac{X_{eq}}{Z_0} = \frac{Q(\gamma - 1)}{1 + Q^2(\gamma - 1)^2} \tag{29}$$

$$\tan \theta = Q(\gamma - 1) \tag{30}$$

where $R_{eq}$ and $X_{eq}$ are the equivalent series resistance and reactance for the equivalent *RLC* circuit.

Fig. 4 shows the magnitude and phase angle of the impedance of a parallel resonant circuit as a function of capacitance. The impedance is broken up into the equivalent resistive and reactive components.

At resonance, the reactance and phase angle curves pass through zero and the total impedance and resistance curves are a maximum, the characteristic circuit impedance

$$Z_0 = R. \tag{31}$$

Below resonance the circuit is capacitive. The current leads the resultant voltage. The phase angle is negative.

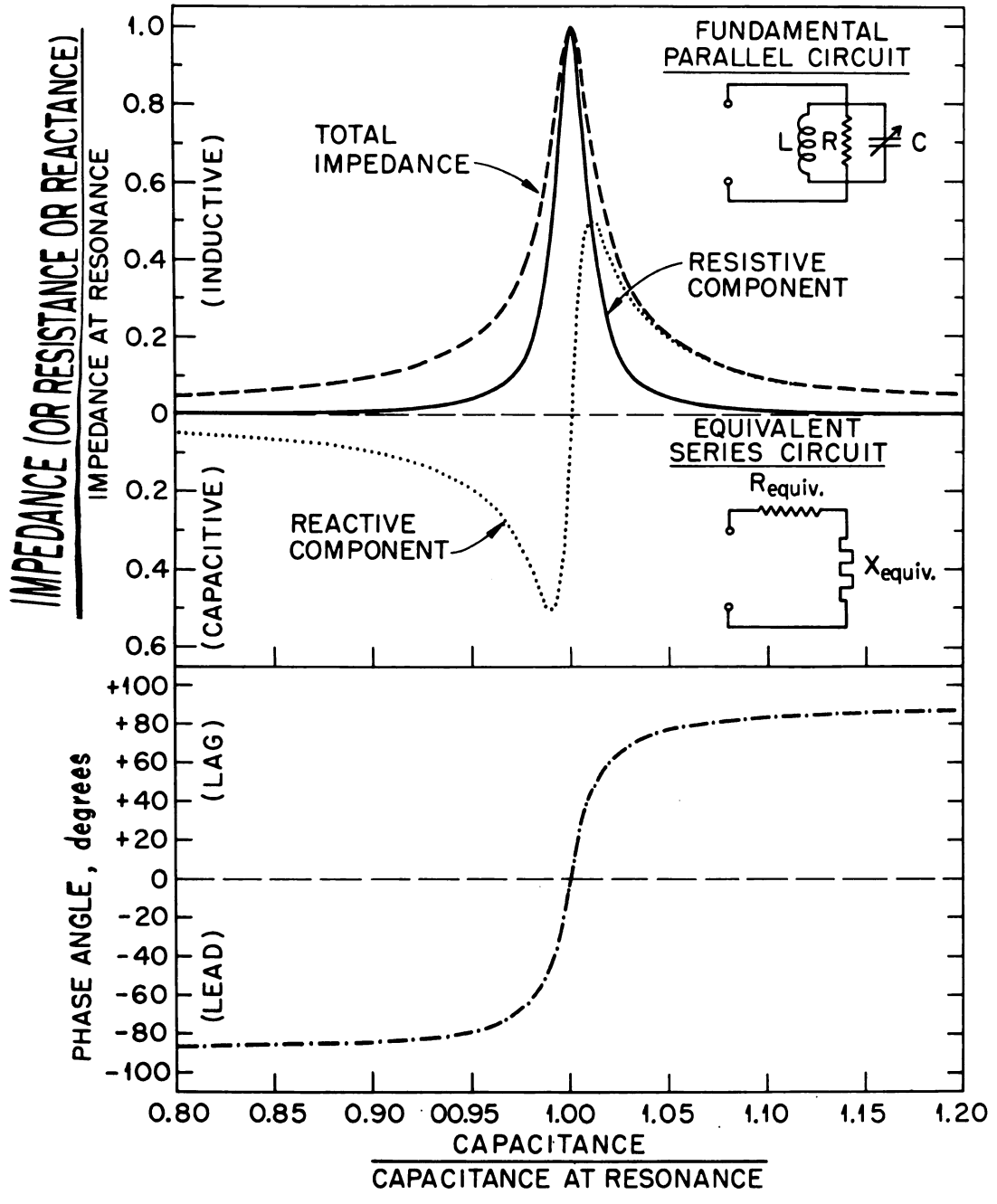


Figure 4. Magnitude and Phase Angle of the Impedance of a Parallel Resonant Circuit as a Function of Capacitance

Above resonance the circuit is inductive. The current lags the resultant voltage. The phase angle is positive.

The reactance curve exhibits a minimum at a capacitance value corresponding to

$$C_{(min)} = C_0\left(1 - \frac{1}{Q}\right) \tag{32}$$

and a maximum at a capacitance value corresponding to

$$C_{(max)} = C_0\left(1 + \frac{1}{Q}\right). \tag{33}$$

The variation of voltage across the parallel circuit with capacitive tuning is identical to the variation of the equivalent impedance of the parallel network (equation (25).

The width of the voltage (equivalent to the impedance) resonance curve, at 0.707 of the voltage at resonance, is related to the circuit Q by

$$\left(\gamma_2 - \gamma_1\right)_{0.707} = \frac{\left(C_2 - C_1\right)_{0.707}}{C_0} = \frac{2}{Q} \tag{34}$$

where $\gamma_2$ and $\gamma_1$, represent the values of the fractional tuning and $C_2$ and $C_1$ correspond to the absolute values of the capacitances on either side of resonance at 0.707 of the maximum voltage.

The variation of voltage with capacitance for the parallel resonant circuit is similar to the variation of current with capacitance for

the series resonant circuit. At resonance, the actual voltage of the parallel circuit varies with the circuit $Q$ in the exact manner as does the current for the series resonant circuit (Fig. 3).

The only difference between the series resonant circuit, Fig. 1, and the parallel resonant circuit, Fig. 4, is that for series resonance, the inductance $L$ and capacitance $C$ are in series as seen from the source of electromagnetic oscillation (the generator) while for parallel resonance, $L$ and $C$ are in parallel as seen from the generator.

The circuit as shown in Fig. 1, would still be a series resonance circuit if resistance $R$ were placed in parallel with either $L$ or $C$, in which case the electrical behavior of the circuit, represented by the resonance curves, would hardly be changed provided that the circuit $Q$ was not altered. Also, the circuit as shown in Fig. 4 would still be a parallel resonance circuit if resistance $R$ were placed in series with either $L$ or $C$.

Cavity Resonator Cavity resonators are characterized by any closed surface having conducting walls which can sustain or support oscillating electromagnetic fields within them when excited by external generators.[38] Resonators of this type are considered as standard resonant circuit elements at high frequencies because of their perfect shielding, low power loss, high shunt impedance and adaptability to various electronic systems.

Fig. 5 shows schematically a reentrant type hybrid coaxial cavity resonator.[19,41] The cavity consists of two concentric cylindrical conductors shorted at one end, and each closed at the other end by plane conducting disks at right angles to their axis to form a gap.

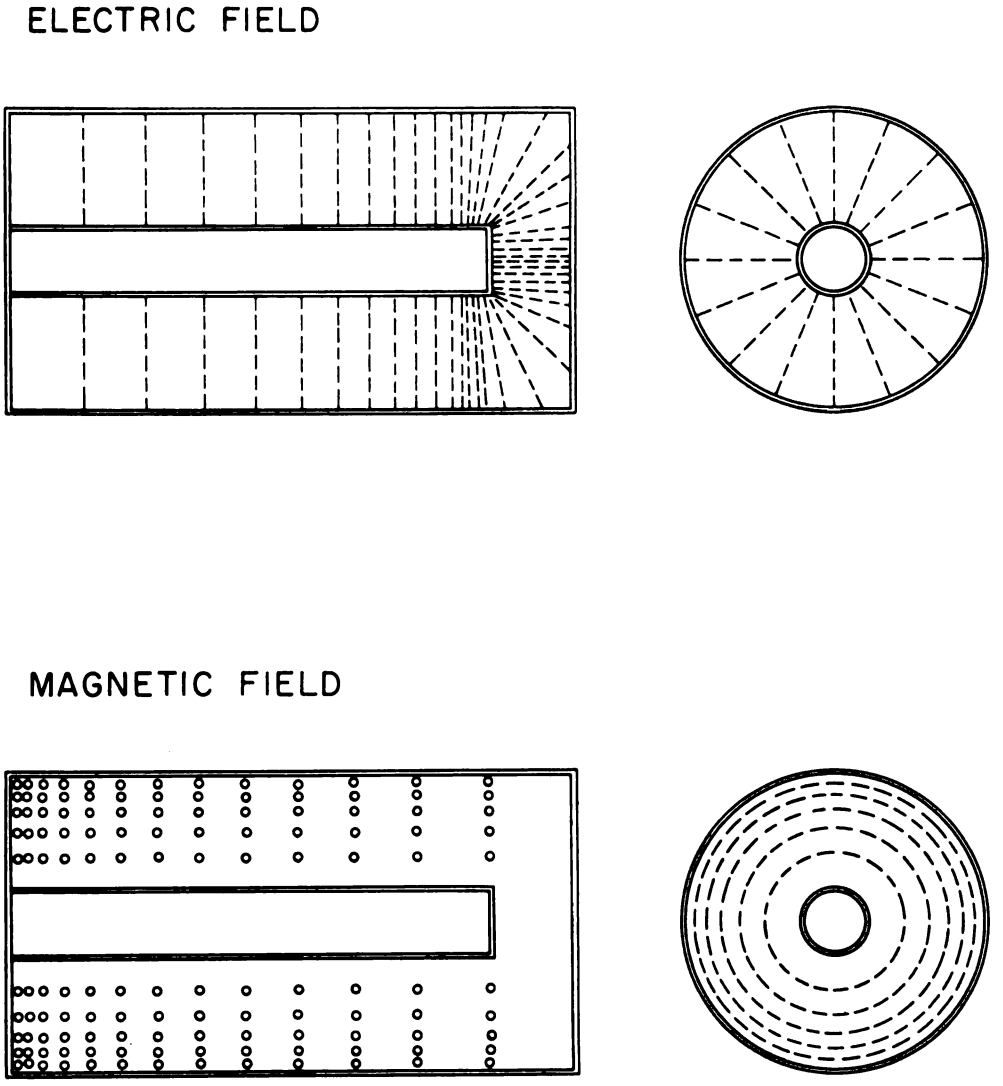


Figure 5. Electromagnetic Field Configuration in a Cylindrical Reentrant Cavity

The hybrid type cavity is a transition between the nonentrant "perfect" cylindrical cavity and the "perfect" coaxial cavity.[41]

In this investigation, the end closure of the inner conductor, which forms the gap, was removed to decrease the capacitance associated with the gap. Barrow and Mieher[41] have shown that a hybrid cylindrical coaxial cavity modified in this manner behaves electrically like the hybrid type.

When the cavity is excited by electrical oscillations, oscillating electrical and magnetic fields are induced and sustained in the radial and axial planes within the cavity as shown in Fig. 5.[19, 41]

The cavity may have an infinite number of natural frequencies of oscillation, and may oscillate in more than one mode at any given frequency.[41, 42] However, any cavity will have certain allowed resonance frequencies. The value of these frequencies and the mode of oscillation are determined by the shape and dimensions of the cavity resonator. For any given type or shape of a cavity, the resonant frequency will be inversely proportional to its mechanical dimensions.

The simple types of cavity resonators have been analyzed in detail by use of Maxwell's equations and pertinent engineering information, has been derived.[43,44] Although the electrical behavior and response of the "hybrid" type cavity have been determined, adequate analysis or comprehensive electrical measurements for this type have not been reported.[41]

The probable configuration of the electrical and magnetic fields of the lowest mode of oscillation existing in a hybrid coaxial cavity resonator is schematically shown in Fig. 5.[19,41]

The electrical lines of forces are most dense in the axial position between the gap formed by the conducting end closure disks of the concentric cylindrical conductors. The electric lines of force are equally distributed in a radial plane and decrease in density toward the shorted end of the coaxial section. For the modified hybrid type, in which the conducting disk of the inner conductor is removed, the electric lines of force are most dense in a radial plane nearest the open end of the inner conductor.

The magnetic lines of force are orthagonal to the electric lines of force and are most dense at the shorted end of the coaxial section. The magnetic lines of force decrease in density in the axial direction toward the gap, and decrease in density in a radial direction away from the axis.

Between the components of the electric and magnetic fields existing within an excited cavity, there exist linear relationships which correspond to relationships between the voltage and current in "lumped" *RLC* networks. It is possible therefore, to synthesize *RLC* networks which have an impedance function similar to that of a cavity. Accordingly, it is possible to represent the cavity by an equivalent *RLC* network which is independent of the type of cavity.[44]

The values of circuit parameters, inductance $L$, and capacitance $C$ are functions of the reactance and depend on shape and dimensions of the cavity.[40]

If the modified cavity may be considered analogous in electrical behavior to a coaxial line, the capacitance, inductance, and impedance associated with the cavity will depend on the ratio of the radii of the

concentric cylinders. Also, the capacitance, $C$, will depend on the length of the gap and the dielectric constant of the medium enclosed by the cavity. The inductance $L$, will depend on the permeability of the medium. The impedance $Z$, will depend on the resistivity, the dielectric constant and permeability of the medium.

The shunt resistance, $R$, for a reentrant cavity is a function of the loss in the circuit and is approximately given by[40]

$$(35) \quad R = \frac{1{,}065\left(\frac{x}{\lambda}\right)^2 \ln \frac{b}{a}}{\frac{x}{a}\left(1 + \frac{a}{b}\right) + \ln \frac{b}{a}} \cdot \frac{\lambda}{\delta}$$

where

$R$ = shunt resistance, ohms
$x$ = length of coaxial section, cms
$\lambda$ = wave length, cms
$a$ = outside radius of inner cylindrical conductor
$b$ = inside radius of outer cylindrical conductor
$\rho$ = resistivity of the conductors, abohms (e m u) per $cm^3$
$\delta = \sqrt{\rho/\pi\omega}$ = "skin depth"
$\omega = 2\pi f$
$f$ = frequency, cycles per second

The high frequency resistance depends therefore not only on the dimensions of the cavity and resistivity of the conducting surfaces but also upon the frequency. The current in the cavity flows only in a thin surface layer of the conducting walls and depends on the total surface area of the conducting walls.

The circuit $Q$ of the cavity can be conveniently defined by equation (13) and has the same significance as for the "lumped" resonance circuits. In terms of the magnetic field $H$ within the cavity, the circuit

$Q$ is given by[40]

$$(36) \qquad Q = \frac{2\sqrt{2}}{\rho/\pi\omega} \cdot \frac{\int H \, dv}{\int H \, da}$$

where $H$ = magnetic intensity
$\rho$ = resistivity of conducting walls, abohms per $cm^2$
$\omega = 2\pi f$
$f$ = frequency, cycles/sec
$v$ = volume of cavity, $cm^3$
$a$ = area of the inner surface of the cavity, $cm^2$

The $Q$ of a cavity therefore is determined by the volume to surface ratio of the cavity, the resistivity of the conductors, and the mode and frequency of oscillation.

The resonant wave length of a reentrant cavity resonator as shown in Fig. 5 is given by[40]

$$(37) \qquad \lambda_0 = 2\pi \left( \frac{x \, a^2}{d} \cdot ln \frac{b}{a} \right)^{1/2}$$

where $\lambda_0$ = wavelength for resonance, cm
$x$ = length of cavity
$a$ = radius of inner cylindrical conductor
$b$ = radius of outer cylindrical conductor
$d$ = distance between end closures (length of gap)

In practice, the circuit parameters of a cavity resonator are not only a function of the characteristic impedance of a cavity but also a function of the impedance coupled into the cavity by external circuits (i.e., the signal generator, detector, and load). Accordingly, the circuit $Q$, and the resonant frequency of the cavity resonator are a function of the impedance coupled into the cavity from the voltage

source, the detector, and the load.

Cavity resonators are coupled to external circuits by means of small loop or rod coupling probes, inserted through holes into the metal enclosure, which are connected to external circuits by coaxial lines.[38,44]

The loop probe which provides coupling with the magnetic field, is oriented within the cavity so as to enclose magnetic flux lines corresponding to the desired mode of operation. If an alternating current is passed through the loop, the excited cavity will support oscillation of the desired mode. Conversely, oscillations existing in an excited cavity will induce a voltage in the loop.

The rod probe, which provides coupling with the electric field, is oriented to coincide with the electric lines of force. Maximum coupling is obtained in the axial position within the gap of a "hybrid" resonator. For the case of the modified "hybrid" resonator as employed in this investigation, maximum coupling is obtained in radial position nearest the open end of the inner conductor.

A voltage applied to the rod probe will also excite oscillations within the cavity, and conversely, oscillations in an excited cavity will induce a voltage in the rod probe.

The size and shape of the probe, and the location and orientation of the probe within the cavity, will determine not only the degree of coupling (energy transfer), but will also determine the mode of oscillation employed. By suitable location and orientation of the probe, definite information about field configuration may also be obtained.

The modified hybrid cavity and cavities in general may be conveniently represented by either the equivalent admittance *RLC* network or the equivalent impedance *RLC* network shown in Fig. 6A.[46] As will be shown, either choice of cavity representation is equivalent when one considers the mode of operation and the observed electrical behavior of the cavity.

In Fig. 6B is shown the equivalent circuit drawn to represent a signal generator inductively coupled to a cavity by means of a loop probe.[43] In this representation, $\dot{V}_1$ is the applied voltage of the signal generator, $R_1$ is the equivalent series resistance of the loop, $L_1$ is equivalent inductance of the loop, $L_2$ is the total equivalent inductance of the cavity, $R_2$ is the total equivalent series resistance of the cavity and $C_2$ is the total equivalent series capacitance of the cavity. $M_{12}$ is the mutual inductance between the inductors $L_1$ and $L_2$.

The impedance representation was selected for convenience only. The electrical behavior for the cavity network would not be appreciably altered if the admittance form of the cavity were selected in which $R_2$, would be in parallel with $C_2$.

The electrical behavior of the inductively coupled circuits shown in Fig. 6B can be calculated with the aid of the following rules:[38]

Rule 1. As far as the signal generator circuit is concerned, the effect that the presence of the coupled cavity circuit has is exactly as though an impedance $(\omega M_{12})^2/Z_2$ had been added in series with the signal generator resistance and inductance, (where $Z_2$ is equal to series impedance of the cavity circuit when considered by itself)

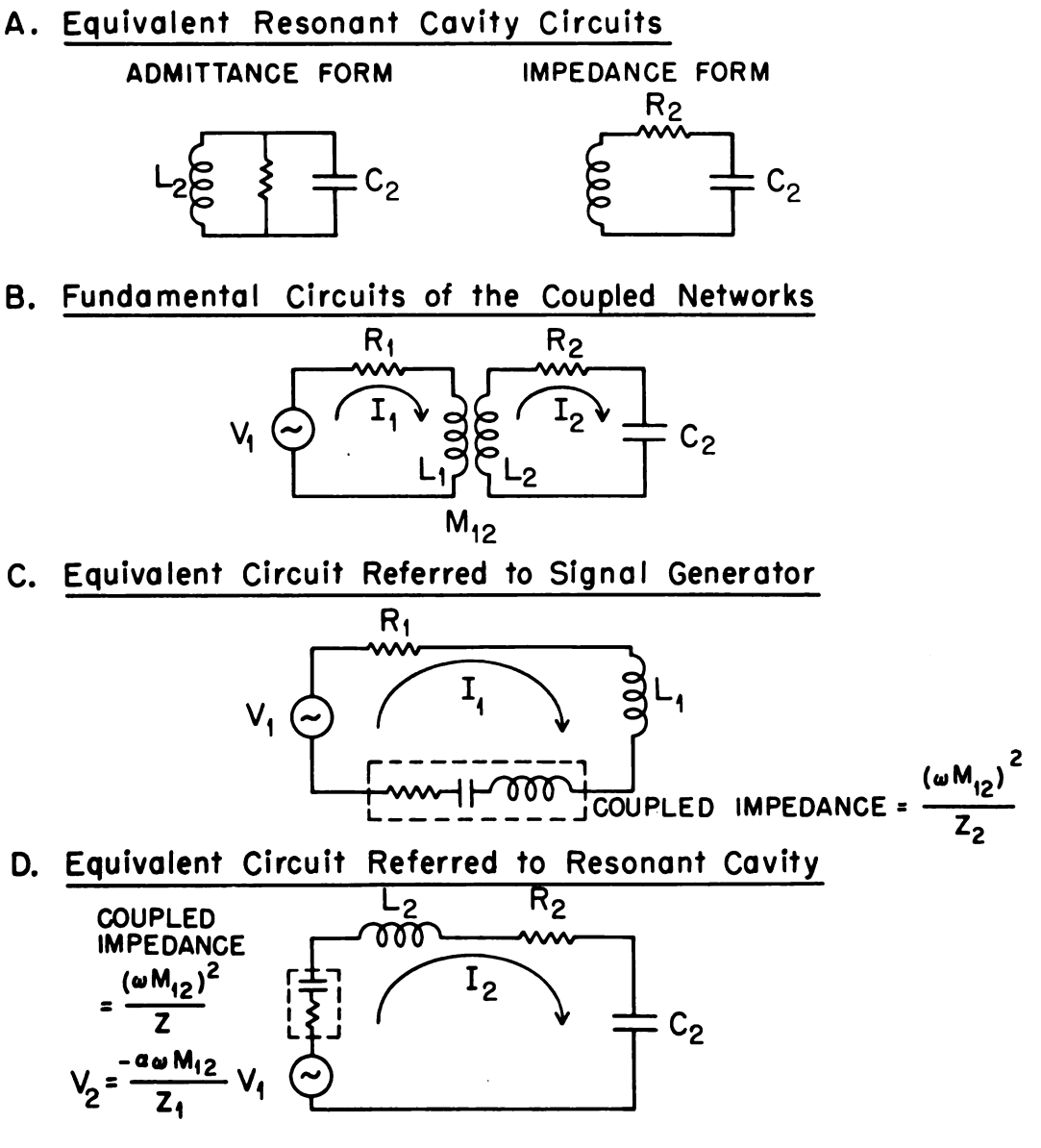


Figure 6. Application of Kirchhoff's Law to Simplify the Electrical Behavior of the Coupled Signal Generator-Resonant Cavity Network

Rule 2. The voltage induced in the cavity circuit by the signal generator current, $I_1$, has a magnitude of $\omega M_{12} I_1$ and lags the current that produces it by 90°. In complex quantity notation, the induced voltage is $-j\omega M_{12} I_1$.

Rule 3. The cavity current is exactly the same current that would flow if the induced voltage were applied in series with the cavity inductance, $L_2$, and if the signal generator circuit were absent.

These rules may be demonstrated by writing down the circuit equations to represent the voltage relationship for the signal generator and cavity circuits. According to Kirchhoff's law,[47,48] these equations are

$$V_1 = \left(Z_1\right) I_1 + j\omega M_{12} I_2 \tag{38}$$

and

$$0 = \left(Z_2\right) I_2 + j\omega M_{12} I_1 \tag{39}$$

where $Z_1$ is the series impedance of the signal generator loop, equal to $R_1 + j\omega L_1$ and $Z_2$ is the series impedance of the cavity equal to $R_2 + j\left(\omega L_2 - \frac{1}{\omega C_2}\right)$. Solving the pair of equations to eliminate $L_2$, yields

$$V_1 = \left(Z_1 + \frac{\left(\omega M_{12}\right)^2}{Z_2}\right) I_1 \tag{40}$$

As referred to the signal generator the equivalent series impedance $Z_{(equiv)}$ of the coupled circuits is the ratio of the signal generator

voltage to the signal generator current, thus

$$(41) \qquad Z_{(equiv)} = \frac{V_1}{I_1} = Z_1 + \frac{\left|\omega M_{12}\right|^2}{Z_2}$$

The term $\frac{\left|\omega M_{12}\right|^2}{Z_2}$ represents the coupled impedance arising from the presence of the cavity (refer to Fig. 6C).

It is evident from equation (40) that the current flowing in the signal generator circuit is given by

$$(42) \qquad I = \frac{V_1}{Z_1 + \left|\omega M_{12}\right|^2 / Z_2}$$

A second current relationship which may be derived by simultaneous solution of equation (38) and (39), is for the value of the current flowing in the cavity as given by

$$(43) \qquad I_2 = \frac{-j\omega M_{12} V_1}{Z_1 Z_2 + \omega M_{12}^2}$$

Rearrangement of the terms of equation (43) yields

$$(44) \qquad I_2 = \frac{-j \frac{\omega M_{12}}{Z_1} \cdot V_1}{Z_2 + \frac{\left|\omega M_{12}\right|^2}{Z_1}} = \frac{V_2}{Z_{2(equiv)}}$$

The significance of equation (44) is that the actual circuit shown in Fig. 6B may now be represented by the series equivalent circuit shown

in Fig. 6D, in which the current and voltage relationships are referred to the cavity. This equivalent circuit representation permits one to explain the electrical behavior of the cavity in terms of the cavity circuit parameters, $L_2$, $R_2$, and $C_2$, at constant applied voltage $V_1$. This equivalent circuit may also be derived by use of Thévenin theorem which states that:[48]

> Any linear network containing one or more sources of voltage and having two terminals behaves, in so far as a load impedance connected across the terminals is concerned, as though the network and its generators were equivalent to a simple generator having an internal impedance $Z$ and a generator voltage $E$, where $E$ is the voltage that appears across the terminals when no load impedance is connected and $Z$ is the impedance that is measured between the terminals when all sources of voltage in the network are short circuited.

In the equivalent circuit representation shown in Fig. 6D, the equivalent cavity circuit is represented as $R_2$, $L_2$, $C_2$ in series with an impedance $\frac{(\omega M_{12})^2}{Z_1}$ which represents the equivalent impedance coupled into the cavity by the signal generator. The equivalent signal generator voltage, as given by

$$V_2 = \frac{-j\omega M_{12}}{Z_1} V_1, \tag{45}$$

behaves as if it were placed in series with an equivalent series impedance given by

$$Z_{2(equiv)} = Z_2 + \frac{(\omega M_{12})^2}{Z_1} \tag{46}$$

Thus, as seen from the signal generator, the cavity capacitance, $C_2$, and inductance $L_2$ are in series. Therefore, a cavity resonator will be analagous in electrical behavior to a series resonant circuit (Fig. 1, 2 and 3) and may be represented by the idealized series resonant circuit.

Cavity resonators may be tuned to resonance by varying the frequency of the applied voltage or by coupling reactance into the cavity. At resonance, the current flowing in the cavity is a maximum. A probe which couples the cavity to a detector, is used to determine the relative magnitude of the current flowing in the cavity.

A more detailed discussion of the electrical behavior of the cavity resonator is contained in the section "Results and Discussion".

Electrical Properties of the Condenser-Type Cell and Solution. To interpret and evaluate changes in oscillometer response to changes in solution parameters, it is most convenient to represent the cell-solution combination as an equivalent circuit in which the electrical properties of the cell and solution are represented by lumped values of capacitance and resistance (or conductance). In this manner, changes in electrical properties of the equivalent circuit may be related to changes in conductivity and dielectric constant of the test solution. In turn, changes in oscillometer response, which result from the change in the electrical properties of the cell-solution load, may be related to the changes in the electrical properties of the equivalent cell-solution circuit.

A summary of the treatment of the electrical properties of the condenser-type cell and solution accomplished by Reilly and McCurdy follows.[13,24]

A condenser-type cell was employed in the oscillometer. The vessel containing solution to be analyzed is placed between the plates of a coaxial condenser. In essence, the cell is a parallel plate condenser whose electrodes' surfaces are separated by three units of dielectric two thicknesses of the vessel wall and the test solution as schematically shown in Fig. 7.

The fundamental equivalent circuit to represent the cell-solution combination is given in Fig. 7, in which the electrical properties are represented as lumped values of capacitance and resistance; $C_g$ is the capacitance due to the dielectric properties of the glass walls of the vessel, $C_s$ is the total capacitance due to the dielectric properties of the solution; $R_g$ is the resistance due to the glass vessel walls, and $R_s$ is the total resistance due to the test solution.

If the resistance $\left(R_g\right)$ due to walls of the vessel is assumed to be so large that it makes a negligible contribution to the cell-solution high frequency response, the cell-solution network may be reduced to the fundamental equivalent circuit shown in Fig. 7A. The net admittance of the fundamental equivalent circuit is given by

$$(47) \qquad Y = \frac{\frac{1}{R_s}\omega^2 C_g^2}{\frac{1}{R_s^2} + \omega^2\left(C_g + C_s\right)^2} + j\,\frac{\frac{\omega C_g}{R_s^2} + \omega^3 C_g C_s\left(C_g + C_s\right)}{\frac{1}{R_s^2} + \omega^2\left(C_g + C_s\right)^2}$$

where $Y$ is the admittance in mhos; $R_s$ equals the total solution resistance in ohms; $C_g$ is the capacitance due to the dielectric properties of the walls of the vessel in farads; $C_s$ is the total capacitance due to the solution, in farads; $\omega$ is the angular frequency, equal to $2\pi f$, where

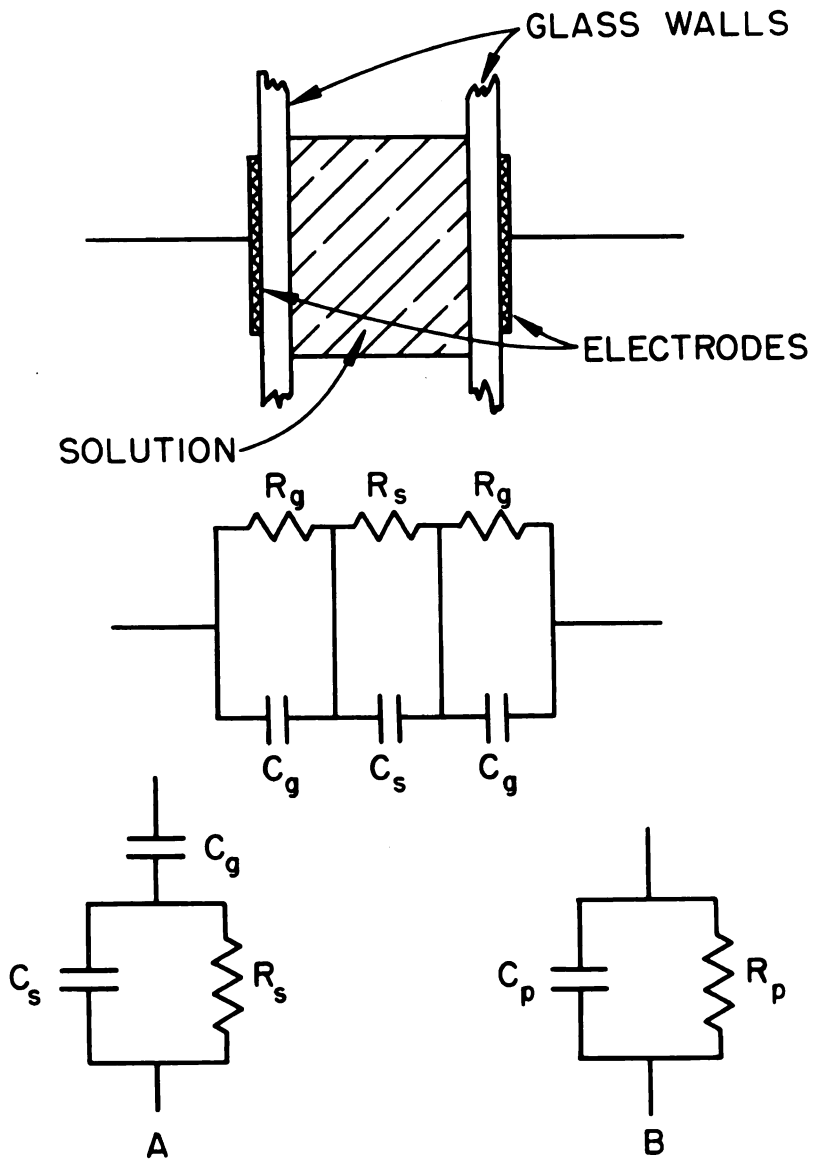


Figure 7. Equivalent Circuit of Condenser-Type Cell and Solution: $C_g$ and $R_g$, Capacitance and Resistance of Glass Walls: $C_s$ and $R_s$, Capacitance and Resistance of the Solution (A) Fundamental Equivalent Circuit, (B) Parallel Equivalent Circuit of A

$f$ is the frequency in cycles per second; and $j$ is the operator equal to $(-1)^{1/2}$.

The net admittance is a complex quantity, equal to the sum of a real and imaginary term, and may be conveniently represented by the general equation

$$Y = G_p + j\, B_p \tag{48}$$

The real part of the admittance, $G_p$, is the conductance term and is equal to $\frac{1}{R_p}$, the reciprocal of the parallel equivalent resistance. The imaginary part of the admittance, $B_p$ is the susceptance term and is equal to $\omega C_p$, where $C_p$ is the parallel equivalent capacitance.

Thus, it is possible to reduce the fundamental equivalent circuit of Fig. 7A to the simplified equivalent circuit of Fig. 7B. The parallel equivalent conductance, $G_p$, is given by

$$G_p = \frac{1}{R_p} = \frac{K\omega^2 C_g^{\,2}}{K_2 + \omega^2 \left[C_g + C_o\varepsilon\right]^2} \tag{49}$$

and the parallel equivalent capacitance, $C_p$, is given by

$$C_p = \frac{K^2 C_g + \omega^2 C_g C_o \varepsilon \left[C_g + C_o\varepsilon\right]}{K^2 + \omega^2 \left[C_g + C_o\varepsilon\right]^2} \tag{50}$$

where $K$ (equal to $\frac{1}{R_s}$) is equal to the low frequency conductivity of the

solution (in mhos); $C$ is the capacitance of the sample space of the vessel containing air; and $\varepsilon$ is the dielectric constant of the medium contained in the cell. The $G_p$ term and the $C_p$ terms, given by equation (49) and (50) respectively, are identical to the real and imaginary terms of the admittance (equation (47) with the exception of the quantities $K$ (equal to $\frac{1}{R_s}$) and $C_o\varepsilon$ (equal $C_s$).

The high frequency conductance $(G_p)$ and the susceptance $(\omega C_p)$ terms of the admittance of the parallel equivalent circuit (Fig. 7B) operate independently of each other. Consequently, it is possible to evaluate each quantity individually in terms of the electrochemical properties of the solution.

The high frequency conductance term $G_p$ is predominately governed by the electrochemical behavior of ions in which electrical energy is converted to heat energy when ions migrate through a voltage gradient.

The susceptance term $(\omega C_p)$ is governed primarily by the electrochemical behavior of molecules in which intra-molecular displacement of charges take place under the influence of an applied voltage gradient.

Equations (49) and (50) state that the parallel equivalent high frequency conductance and the parallel equivalent capacitance are functions of the frequency $f$, the solution parameters $K$ and $\varepsilon$, and the cell parameters $C_g$ and $C_o$. In this investigation, we are concerned only with the effects of $f$, $K$, and $\varepsilon$ upon the oscillometer response. A single cell was constructed and employed throughout the investigation.

Fig. 8 shows the expected relationship between $G_p$ and $C_p$ and $K$. Reasonable values of $f$, $C_g$, $C_v$, and $\varepsilon$, were substituted into equations

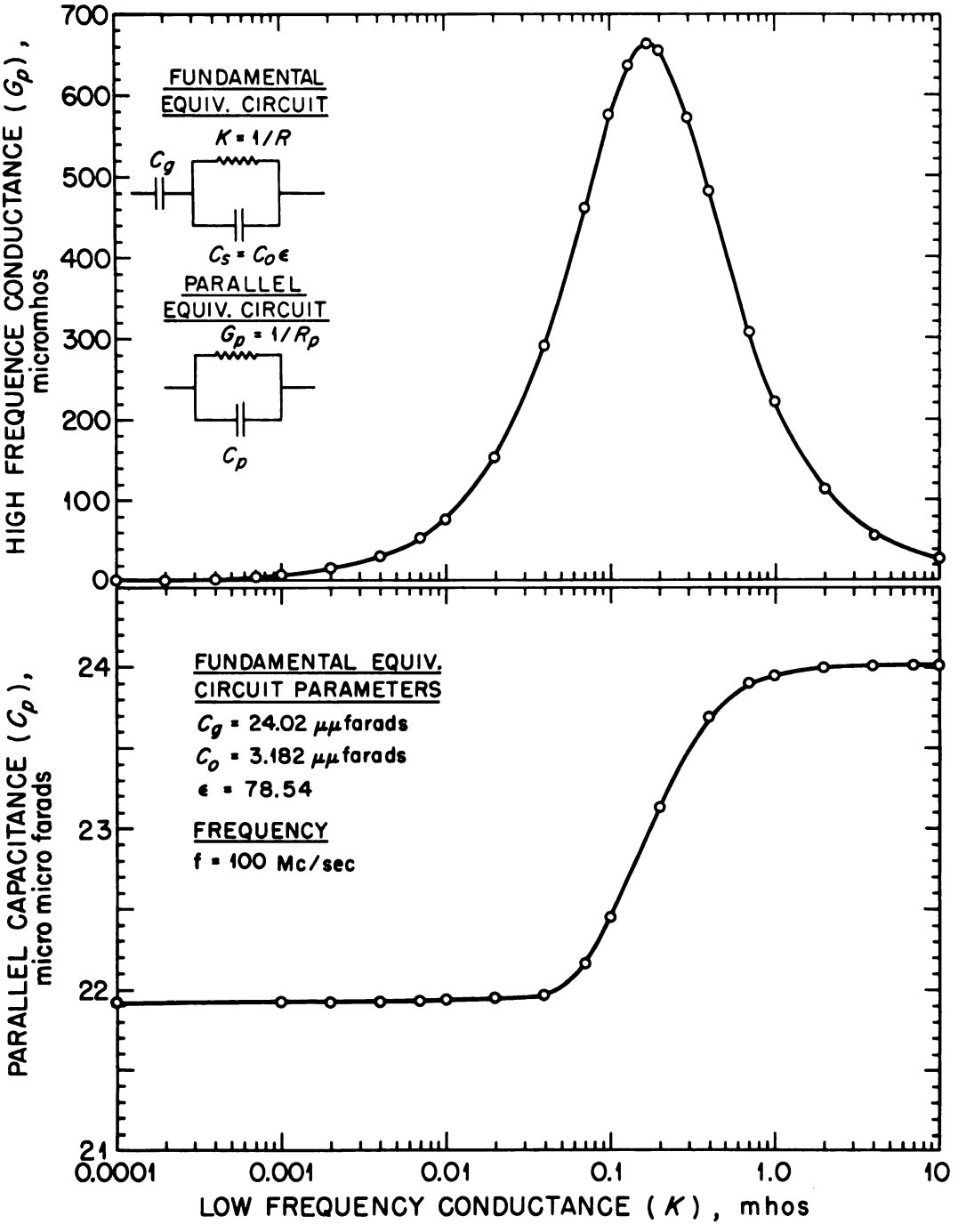


Figure 8. High Frequency Parallel Equivalent Capacitance and Conductance as a Function of the Fundamental Equivalent Circuit Low Frequency Conductance

(49) and (50) to obtain the theoretical curves. The dielectric constant of the solution, $\varepsilon$, is assumed to be constant and independent of the solution conductivity, $K$.

At very small or very large values of the low frequency solution conductivity, $K$, the limit of the high frequency conductance approaches zero,

$$\lim_{\infty \leftarrow K \rightarrow 0} G_p = 0 \tag{51}$$

At a value of the low frequency conductance equal to

$$K_{(peak)} = \omega\left(C_g + C_o\varepsilon\right) \tag{52}$$

the high frequency conductance is a maximum and is equal to

$$G_{p(max)} = \frac{\omega C_g^2}{2\left(C_g + C_o\varepsilon\right)} \tag{53}$$

The value of $K$ for which $G_p$ is a maximum is obtained by differentiating the expression for $G_p$, given by equation (49), with respect to $K$, equating $\frac{dG_p}{dK}$ equal to zero, and solving the resulting expression for $K$.

When the value of the low frequency conductivity approaches zero, the parallel equivalent capacitance approaches a limit given by

$$\lim_{K \to 0} C_p = \frac{C_g C_o \varepsilon}{C_g + C_o \varepsilon} \tag{54}$$

When the value of $K$ becomes very large, $C_p$ approaches a limit given by

$$\lim_{K \to \infty} C_p = C_g \tag{55}$$

The difference in the extreme values of the equivalent parallel capacitance $\Delta C_p$, as expressed by equation (54) and (55), is equal to

$$\Delta C_p = \frac{C_g^2}{C_g + C_o \varepsilon} \tag{56}$$

The value of $K$ at the mid-point, where the parallel equivalent capacitance is half way between the extremes, is found by setting

$$C_{p(mid\text{-}point)} = C_g - 1/2\ \Delta C_p = \frac{K^2 C_g + \omega^2 C_g C_o \varepsilon \left(C_g + C_o \varepsilon\right)}{K^2 + \omega^2 \left(C_g + C_o \varepsilon\right)^2} \tag{57}$$

Thus, the value of $K$ at the mid-point is equal to

$$K_{(mid\text{-}point)} = \omega \left(C_g + C_o \varepsilon\right) \tag{58}$$

A comparison of equations (52) and (58) show that the maximum value of the parallel high frequency conductance, $G_{p(max)}$, and the mid-point parallel equivalent capacitance value, $C_{p(mid\text{-}point)}$, occur at the same

value of the low frequency conductance, or

$$K_{(peak)} = K_{(mid\text{-}point)} = \omega\left(C_g + C_o\varepsilon\right) \tag{59}$$

From a comparison of equation (53) and (56), it follows that the relationship between $G_{p(max)}$ and $\Delta C_p$ is given by

$$G_{p(max)} = \frac{\omega \Delta C_p}{2} \tag{60}$$

Equations (52), (54) and (53) show that the magnitudes of $K_{(peak)}$, $K_{(mid\text{-}point)}$, and $G_{p(max)}$, respectively, are directly proportional to the frequency, where as, $\Delta C_p$ (equation 56) is independent of the frequency. A decrease in the frequency will result in a proportional decrease in the magnitude of $G_{p(max)}$, $K_{(peak)}$ and $K_{(mid\text{-}point)}$. The magnitude of $\Delta C_p$ will remain constant with a change in frequency.

Equations (53) and (56) show that a decrease in the dielectric constants of the medium will result in an increase in the magnitude of $G_{p(max)}$ and $\Delta C_p$. The magnitudes of $K_{(peak)}$ and $K_{(mid\text{-}point)}$, will decrease with a decrease in the dielectric constant of the medium.

# EXPERIMENTAL

Preparation of Reagents. a. Aqueous Solutions. Laboratory distilled water was passed through a "Deminizer" ion exchange column and distilled from alkaline potassium permanganate in an all glass apparatus. This double distilled water was used for all aqueous solution preparations.

Reagent grade hydrochloric acid was used to prepare a stock solution which was compared to a standard sodium hydroxide solution.

A dilute sodium hydroxide solution, free of carbonate, was prepared from a filtered, saturated sodium hydroxide solution. The dilute sodium hydroxide solution was standardized against primary grade potassium acid phthalate to the phenolphthalein end point.

Reagent grade sodium chloride and barium chloride dihydrate, dried at 105°, were used to prepare stock solutions of known concentrations.

Optical grade lanthanum sesquioxide, ignited to constant weight, was dissolved in the minimum of hydrochloric acid to prepare a stock solution of lanthanum chloride.

Dilute solutions of sodium chloride, barium chloride, lanthanum chloride, and hydrochloric acid were prepared by diluting desired aliquots of the respective stock solutions.

b. Acetous Solutions. Glacial acetic acid, acetic anhydride, and perchloric acid, 70-73%, conforming to A.C.S. specifications were used in the acetous solution preparations.

Acetic anhydride was added to glacial acetic acid to remove water. Glacial acetic acid thus treated was used in all acetous solution preparations.

An acetous stock solution of perchloric acid was prepared and standardized against primary grade potassium acid phthalate to the crystal violet endpoint.[49]

Eastman Kodak p-nitroaniline was recrystallized from a mixture of equal volumes of water and ethyl alcohol until the uncorrected melting point of the solid remained constant to within 0.5°C of the accepted value of 148°C.[50] An acetous stock solution was prepared and its concentration was determined by a potentiometric titration with standard acetous perchloric acid as titrant.

Reagent grade anhydrous sodium acetate was dissolved in the treated glacial acetic acid and the concentration of this stock solution was determined by potentiometric and low-frequency conductometric titration with standard acetous perchloric acid as titrant.

Dilute solutions of perchloric acid, sodium acetate and p-nitroaniline were prepared by diluting desired aliquots of the respective stock solutions with the treated glacial acetic acid.

c. Methanolic Solutions. Commercial methanol was refluxed over grignard alloy and fractionally distilled and the middle fraction of the anhydrous methanol collected.[49]

Reagent grade sodium chloride was used to prepare a saturated methanolic stock solution. The concentration of the stock solution was determined by evaporating an aliquot of the stock solution at 105°C and weighing the residue.

Dilute solutions of methanolic sodium chloride were prepared by diluting a desired aliquotof the stock solution with the anhydrous methanol.

Weights calibrated against Bureau of Standards calibrated weights, N.B.S. Test No. 87925, were used in all weighing.

All solutions were prepared at 25°C. Calibrated pipets, burets, and volumetric flasks were used for all solution preparation and the titrations.

Purification of Solvents used in Dielectric Constant Measurements. Double distilled water was redistilled and collected in an all quartz apparatus.

Mallinckrodt, thiophene free, benzene was recrystallized three times from its own melt.[51] The benzene was refluxed over phosphorous pentoxide and fractionally distilled. The purified benzene was stored over metallic sodium ribbons.

Eastman Kodak chlorobenzene was repeatedly shaken with concentrated sulfuric acid in a separatory funnel until no brown coloration of the sulfuric acid was observed.[52] The solvent was washed successively with water, 2 M $K_2CO_3$ and water. The material was dried over calcium chloride for several days and fractionally distilled.

Baker Chemical purified nitrobenzene was recrystallized five times from its own melt.[52] The material was dried over phosphorous pentoxide and fractionally distilled under reduced pressure.

Eastman Kodak (White Label) 1, 2-dichloroethane was washed with 4 M NaOH and then with water.[53] The material was dried for several weeks over calcium chloride and fractionally distilled, while protected from sunlight, under reduced pressure.

Baker Chemical acetone was purified by the Shipsey-Werner method which involves the solvation of sodium iodide by acetone to form sodium

iodide triacetonate.[54] Acetone was saturated with anhydrous sodium iodide at ambient temperature and the excess solid removed by decantation. The saturated solution was cooled to -10°C and the solid sodium iodide triacetonate was separated on a filter, transferred to a distillation apparatus and the acetone was distilled and collected in fractions.

Resonant Cavity Oscillometer. The oscillometer and auxillary instrumentation employed in this investigation is shown in Fig. 9.

The oscillometer consists of a signal generator, reentrant cavity resonator, cell assembly, and detector. The cell assembly includes the condenser-type cell, thermostated by a circulating water bath, and the dielectric sample holder. The detector components include the detector probe capacitor and high sensitivity galvanometer.

Auxilliary equipment, used to obtain classical conductance measurements, are the conductivity bridge and cell, and the capacitance decade box.

In Fig. 10 is shown a top view of the chassis upon which the cavity resonator and some associated electrical circuit components are mounted.

A schematic diagram of the electrical circuit of the oscillometer is shown in Fig. 11. The parts list for the oscillometer (Fig. 11) is given in Appendix II.

The operating procedure for the cavity resonator oscillometer is given in Appendix III.

Signal Generator. A Hewlett-Packard Model 608 A VHF signal generator was used as a source of high frequency energy to excite the cavity resonator. The pertinent electrical specifications and operating procedures

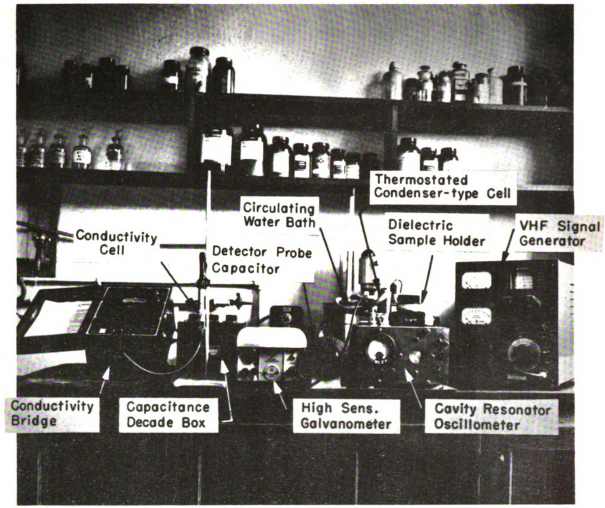


Figure 9. Resonant Cavity High Frequency Oscillometer and Instrumental Set Up

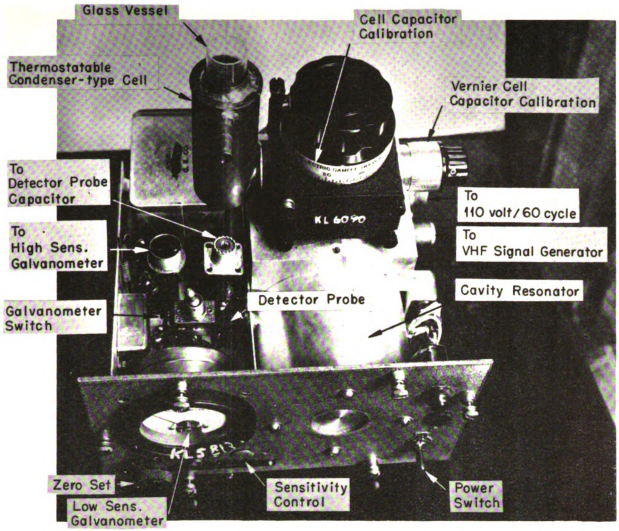


Figure 10. Resonant Cavity High Frequency Oscillometer

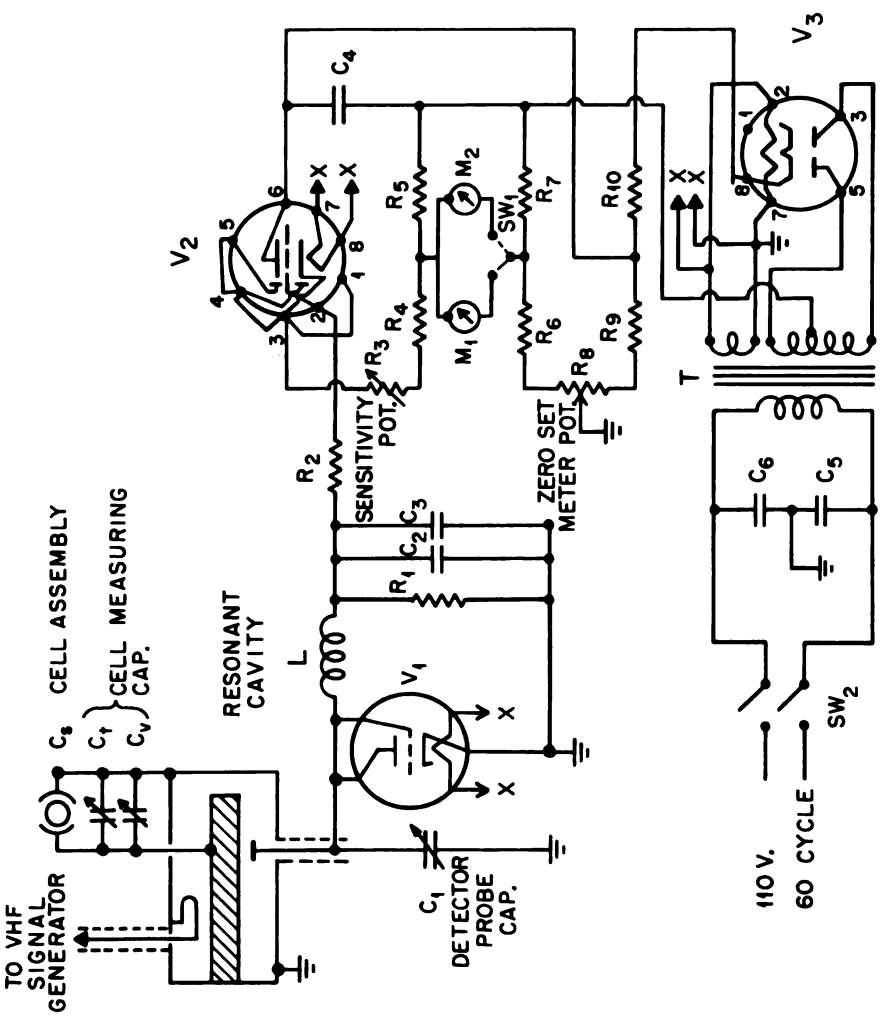


Figure 11. Circuit Diagram of the Resonant Cavity High Frequency Oscillometer

for the signal generator are given in Appendices IV and V respectively.

The Type N RF output connector of the signal generator was replaced with a more conventional Amphenol 83-1H (Series UHF) connector. The signal generator was connected to the cavity resonator and other equipment by means of an RG8/U coaxial cable terminated at both ends with Amphenol 83-1SP (Series UHF) connectors.

The operating frequencies of the signal generator, as indicated on the frequency dial, were compared and agreed very closely with known frequencies originating from a U.S. Army Signal Corps Model 1-222-A signal generator which contained an internal quartz crystal calibrating oscillator.

Since RF voltage measuring equipment was not available, a high frequency voltage detector[37,55,56] employing a 1N-34A crystal diode was constructed and used to determine the stability of the signal generator output voltage at 5 Mc/sec frequency intervals between 75 and 150 Mc/sec.

The voltage stability tests were performed in the following manner. The signal generator was tuned to the desired frequency and the attenuator adjusted to give a voltmeter indication at the "Set Level". At 100 Mc/sec the relative output voltage as indicated by the crystal diode detector was measured at 10 minute intervals over a two hour period and every hour thereafter for 10 hours. At all other frequencies, the output voltage was measured at 10 minute intervals over a one hour period. For all practical purposes the output voltage of the signal generator was constant at a given frequency. However, it was necessary to retune the signal generator to the desired frequency and readjust the voltage control before every measurement to insure that the values corresponded to the desired

frequency and output voltage.

Due to the nonlinear frequency response of the crystal diode detector, it was impossible to compare the relative magnitude of output voltage at the various frequencies even though the signal generator output voltage was adjusted to the "Set Level" meter indication. Consequently, the signal generator output voltmeter indication was employed as a measure of the relative output voltage at all frequencies. The exact value of the output voltage could not be determined because the impedance terminating at the output terminal of the signal generator was not known.

The output voltage of the signal generator was adjusted to the "Set Level" meter indication for all high frequency measurements obtained with the oscillometer. Necessary adjustments of the signal generator were made prior to each individual measurement to insure that values obtained corresponded to the desired frequency and output voltage.

Cavity Resonator. A silver plated brass reentrant cavity resonator (Fig. 12) was obtained from a U.S. Navy Model OAO-2 radar test equipment frequency meter (manufactured by The Liebel-Florsheim Co., Cincinnati, Ohio).

As the resonant circuit element of the radar test equipment, the cavity provided for frequency measurement between 105 to 127 Mc/sec. The cavity was capacitatively tuned to resonance by inserting an iron rod plunger into a flared open end of the inner conductor. The plunger was driven by a vernier screw.

The cavity resonator was modified to be operable in the 100 Mc/sec frequency region as the resonant circuit element of the oscillometer by removing the capacitance associated with the iron plunger and flared end

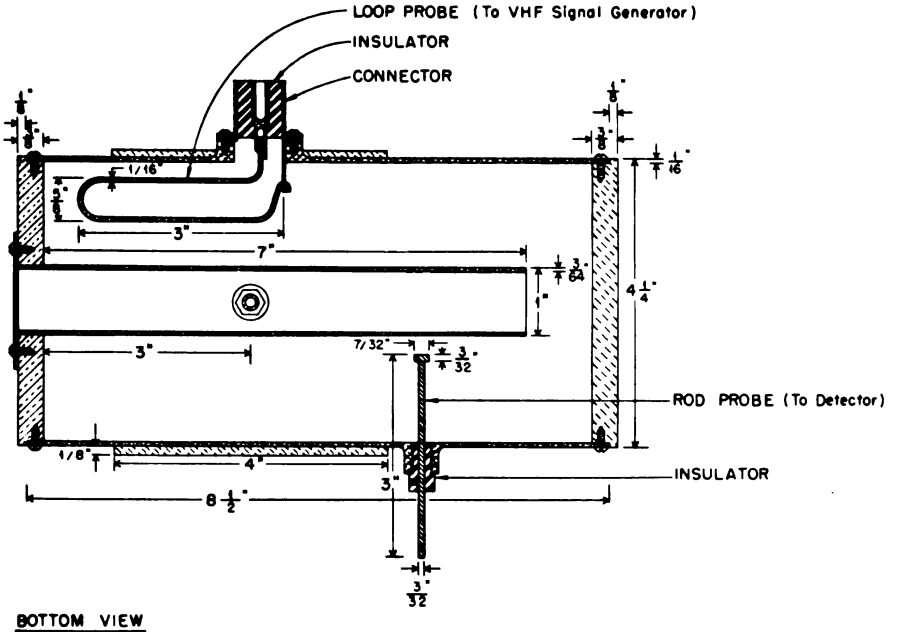


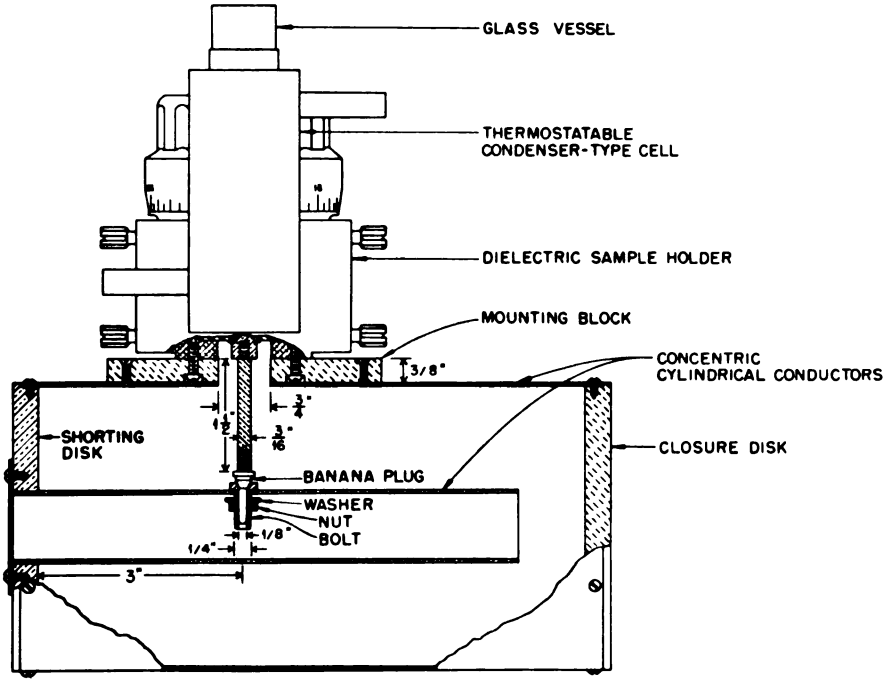


Figure 12. Longitudinal Cross-Section Views of the Cavity Resonator

of the inner conductor.

The conducting disk to which the iron plunger and vernier screw were attached, was replaced by a solid machined aluminum disk. The inside surface of the conducting disk was polished to insure minimum resistance to the current path of the conducting surface.

The flared end of the inner concentric conductor was removed and the length of the inner conductor selected so that the cavity could be employed in the 100 Mc/sec frequency region as the resonant circuit element of the oscillometer, and to obtain maximum circuit $Q$.[37]

The cavity was rigidly mounted on the chassis provided in the Model OAO-2 frequency meter and contained in a metal enclosure.

The signal generator was inductively coupled to the cavity resonator by terminating the coaxial cable, connected between the output terminal of the signal generator and the cavity resonator in a loop as shown in Figs. 12 and 13. Silver was used as the loop material, in preference to other metals, to insure minimum resistance to current flow.

The loop was located in the same position as provided in the Model OAO-2 frequency meter. The plane of the loop was oriented in the axial and radial direction within the cavity (orthagonal to the magnetic flux lines existing in the excited cavity).

The dimensions of the loop were selected to give a maximum degree of coupling (energy transfer) and minimum power loss as experimentally indicated by a maximum of the detector current and sharpness of response curve when the trail loops were employed in the oscillometer at 100 Mc/sec. The length of the loops were experimentally observed to be more critical than the width, in increasing the degree of coupling.

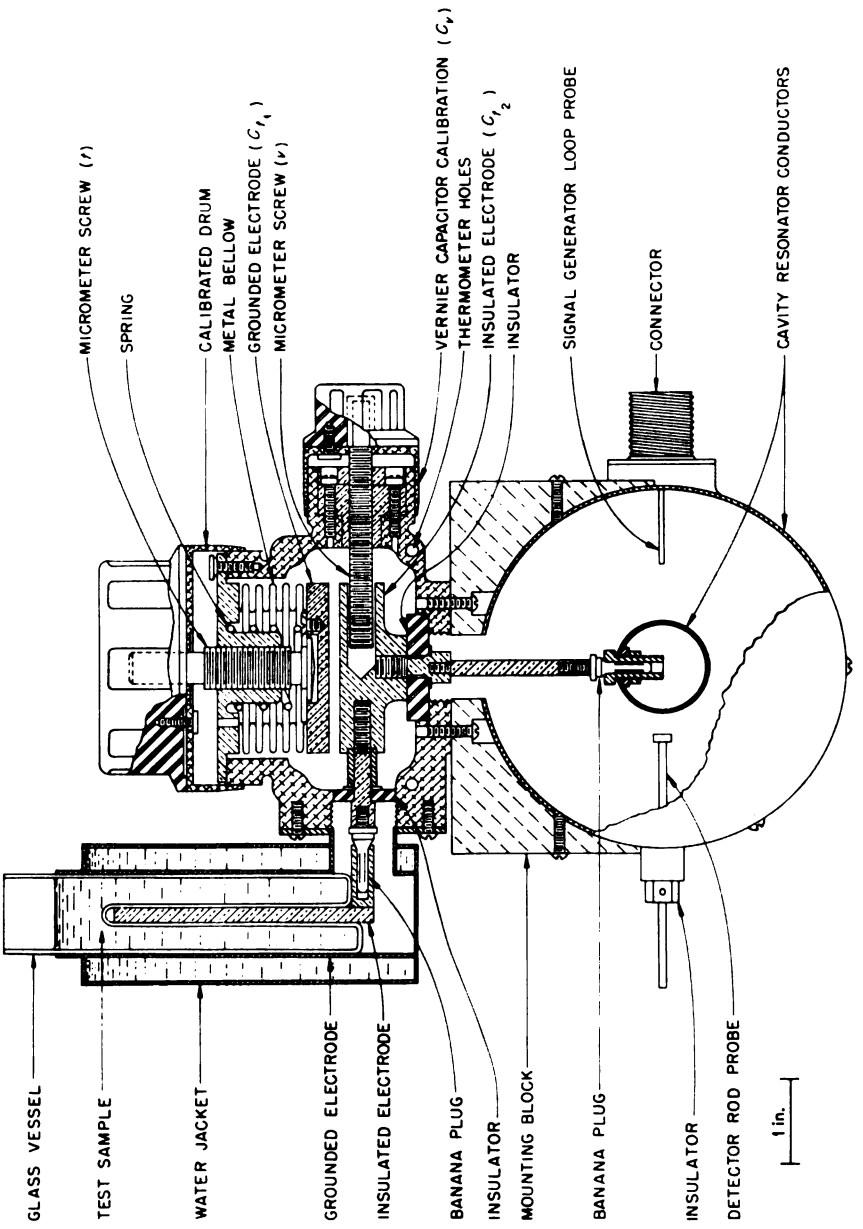


**Figure 13. Cross-Section View of the Cell-Dielectric Sample Holder-Cavity Resonator Assembly**

Cell Assembly. In Fig. 13 is shown a cross-sectional view of the cell assembly employed in the oscillometer. The cell assembly consists of a thermostatable cell and a General Radio Type 1690-A dielectric sample holder (manufactured by General Radio Co., Cambridge, Mass.). The cell assembly is schematically represented in Fig. 11 by capacitors $C_s$, $C_t$ and $C_v$, where $C_s$ represents the capacitance contributed by the condenser-type cell and test solution, and $C_t$ and $C_v$, the variable capacitors of the dielectric sample holder.

The condenser-type cell was experimentally designed to meet two requirements: (1) the cell could be employed for high frequency measurements between 75 to 150 Mc/sec with air as the dielectric contained in the cell to determine instrument operating characteristics; and (2) the cell could be employed for high frequency measurements at 100 Mc/sec of pure and conducting liquids whose dielectric constants were between 1 and 80.

The dielectric sample holder was used to measure changes in cell capacitance because: (1) it contained calibrated variable capacitors ($C_t$ and $C_v$); (2) the unit was provided with a vernier capacitor which could be employed for susceptance variance measurements;[57,58] (3) the unit could be connected to the cavity and cell with a minimum of distributed capacitance; and (4) the unit could be rigidly attached to the cavity and cell.

The high frequency condenser-type cell is shown in Fig. 14. The inside wall of the jacket of the vessel holder serves as one electrode of the coaxial condenser and the right angle rod, which protrudes into the finger of the borosilicate vessel served as the other plate. The

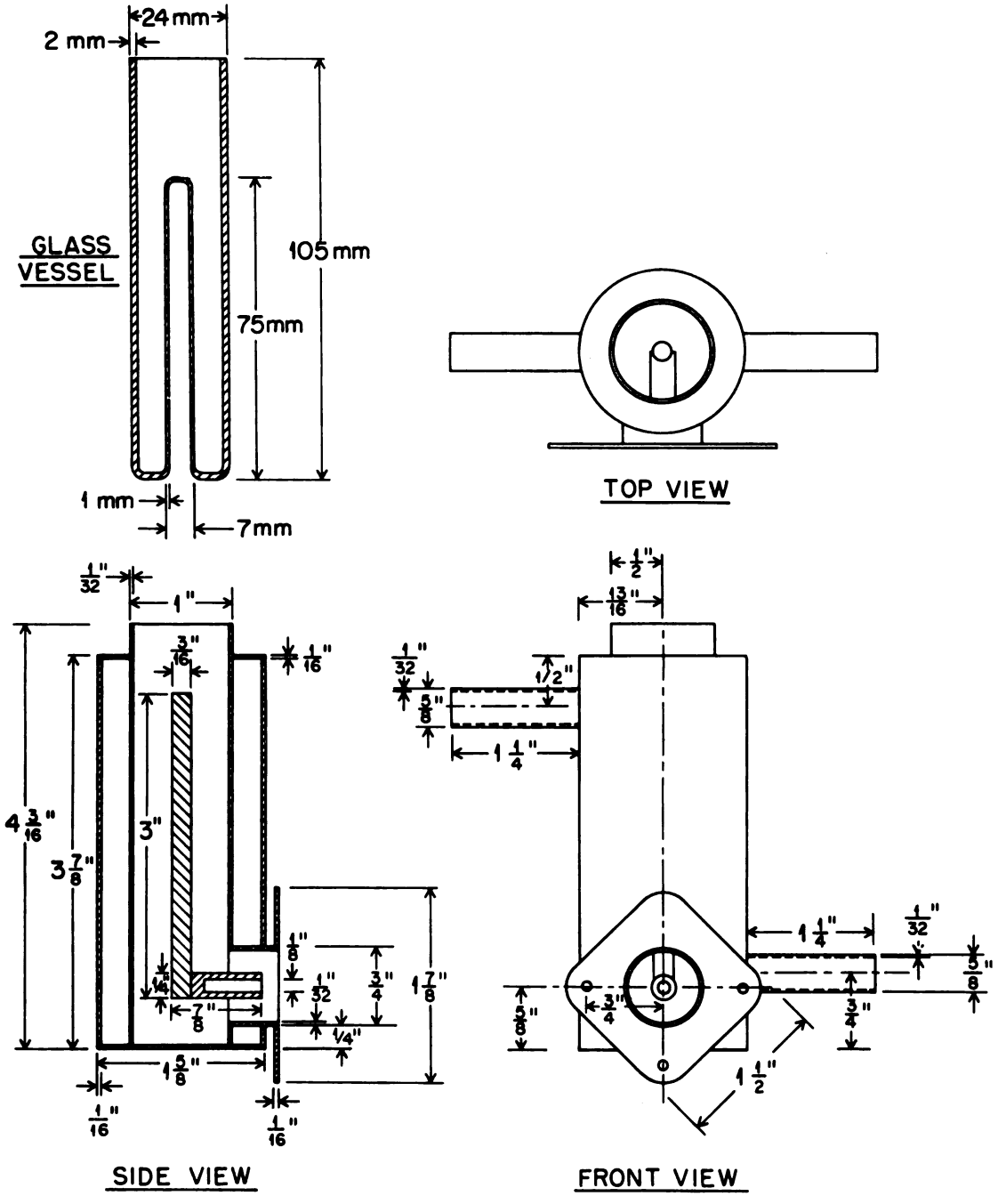


Figure 14. High Frequency Condenser-Type Cell

cell holder was machined to very close tolerance to insure a constant resistance and capacitance to the current path between the vessel wall and electrode.

The borosilicate vessel, constructed to represent an annular sample space, was reproducibly positioned in the holder by alignment of markings placed on the surface of the vessel and on the lip of the holder.

The condenser-type cell was attached to the dielectric sample holder as shown in Fig. 13. The plates of the cell are connected in parallel to the capacitors $C_t$ and $C_v$ of the dielectric sample holder. The parallel capacitance network formed by the cell and sample holder is represented in Fig. 11 by $C_s$, $C_t$, and $C_v$. It was assumed that in connecting the dielectric sample holder cell assembly to the resonant cavity, the net capacitive contribution of the assembly, $C_t + C_v + C_s$, is in parallel to the total equivalent capacitance of the resonant cavity circuit.

A cross sectional view of the General Radio Type 1690-A dielectric sample holder, employed as measuring capacitors $C_t$ and $C_v$ is shown in Fig. 13. The main micrometer capacitor $(C_t)$ is formed by two electrodes, 2.000 ± 0.0025 inches in diameter. The surfaces are ground optically flat within a few wavelengths. The lower electrode is positioned by a Vycor insulator. The upper electrode is positioned by the micrometer type screw. The screw is surrounded by a flexible copper tube, or metal bellow, to insure low and constant resistance and inductance in the current path to the movable electrode which is at ground potential.

The spacing in mils between the electrodes is read directly on the drum and barrel. The air capacitance as a function of spacing is given by

$$(61) \qquad C_t = \frac{706.4}{t}$$

where $C_t$ is the calculated air capacitance in picofarads, and $t$ is the spacing between the electrode surfaces in mils. A correction curve (Fig. 15) was provided with the dielectric sample holder, giving the measured deviations from the calculated values over the range 300 mils to 10 mils spacing. The corrections in picofarads are added algebraically to the capacitance corresponding to readings of the drum and barrel.

A vernier capacitor $(C_v)$ is formed by the micrometer screw projecting into a hole in the ungrounded electrode. Micrometer screw travel is measured in terms of 500 divisions, each corresponding very closely to 0.01 picofarads.

In Table I is given the calibration data for the vernier screw capacitor. The correction chart was provided by the Standardizing Laboratory, General Radio Company.

The figures in the body of the table are corrections in picofarads to be added algebraically to the readings of the vernier capacitor dial and drum for capacitance differences. When these corrections are applied, the resultant calibration is internally consistant to 0.002 picofarads or 0.1%, whichever is the greater. Thus, capacitance differences may be measured to 0.004 picofarads.

The calibration data was obtained at 1000 cycles per second with the low potential or shield terminal grounded. Each setting was approached in the direction of increasing scale reading to eliminate any possible

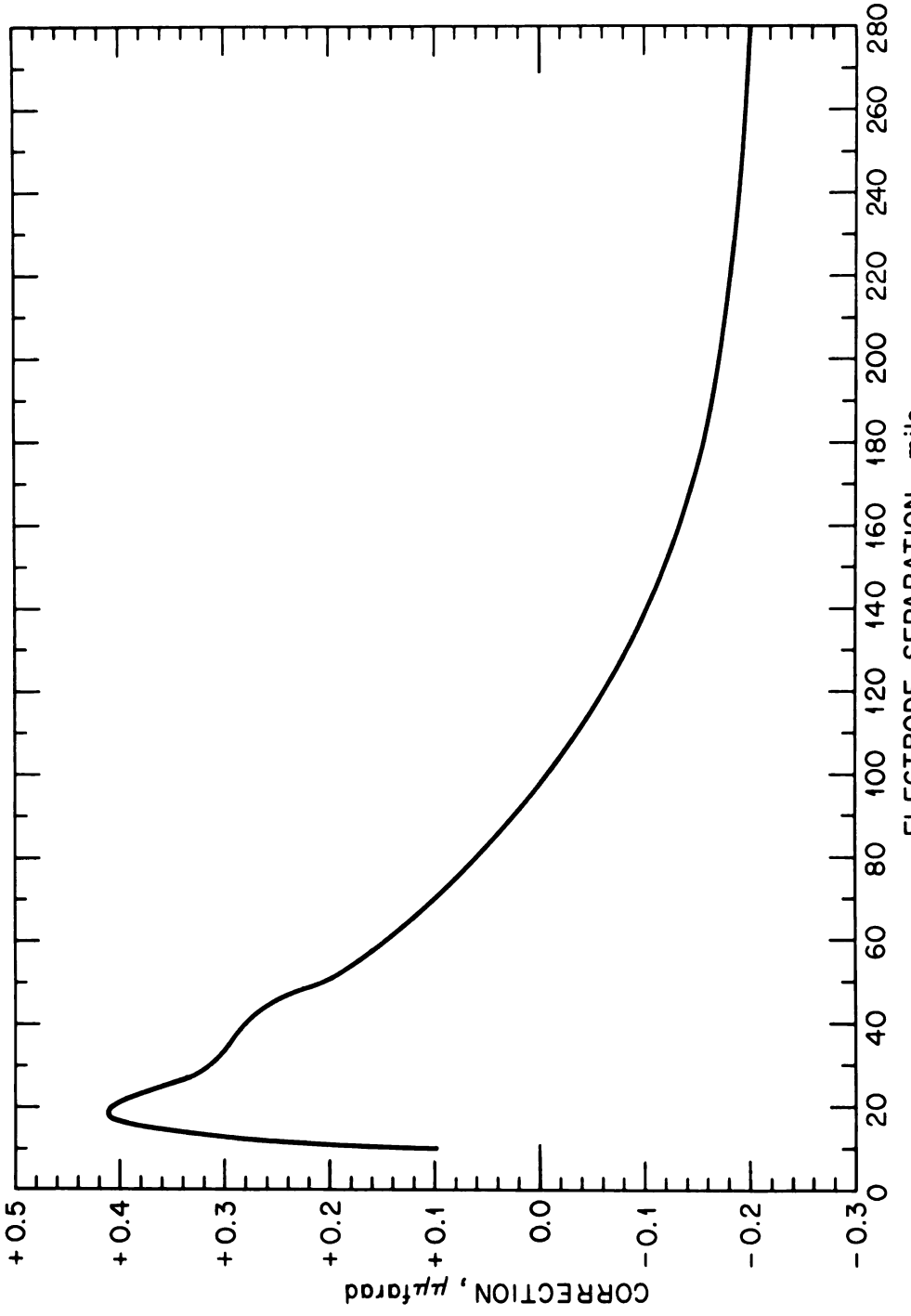


Figure 15. Dielectric Sample Holder Micrometer Capacitance Calibration (Type 1690-A, Serial No. 438)

Table I. Vernier Capacitor Calibration: Dielectric Sample Holder, Type No. 1690-A, Serial No. 438

Correction in Micromicrofarads

| Drum Divisions | Dial Divisions | | | | |
|---|---|---|---|---|---|
| | 0 | .10 | .20 | .30 | .40 |
| 0. | .000 | -.010 | -.023 | -.031 | -.036 |
| 0.50 | -.030 | -.039 | -.054 | -.060 | -.064 |
| 1.00 | -.059 | -.066 | -.082 | -.085 | -.087 |
| 1.50 | -.082 | -.086 | -.106 | -.107 | -.108 |
| 2.00 | -.104 | -.108 | -.132 | -.131 | -.133 |
| 2.50 | -.131 | -.136 | -.156 | -.156 | -.158 |
| 3.00 | -.155 | -.161 | -.179 | -.182 | -.184 |
| 3.50 | -.180 | -.186 | -.202 | -.207 | -.210 |
| 4.00 | -.205 | -.212 | -.225 | -.232 | -.234 |
| 4.50 | -.228 | -.236 | -.246 | -.255 | -.259 |
| 5.00 | -.252 | | | | |

error due to residual backlash. The amount of backlash is less than 1/2 dial division.

The maximum capacitance that can be measured by the sample holder is 100 picofarads. With the electrodes in contact, shorted together, the zero capacitance of the cell holder is approximately 11 picofarads.

The dielectric sample holder was rigidly mounted on an aluminum block which was attached to the cylindrical surface of the cavity by four screws threaded into the outer cavity wall (Fig. 13). The ends of the screws were contoured to the internal conducting surface of the cavity to minimize disturbance of the electromagnetic field and insure low resistance in the current path on the conducting surface.

The ungrounded plate of the sample holder was connected to the inner concentric cylinder of the cavity by a rod which screwed into the plate and connected to the inner conductor by means of a banana plug.

In practice, the cavity resonator is capacitatively tuned to resonance (the operating frequency of a signal generator) by capacitance displacement of the main micrometer capacitor $(C_t)$ and vernier capacitor $(C_v)$ of the sample holder.

It was assumed that resonance was attained when the detector meter indicated the maximum reading. The detector current decreased when the cavity was capacitatively detuned by means of the sample holder $(C_t$ or $C_v)$ or by introducing a sample into the cell $(C_s)$.

The net capacitance of the cell assembly parallel circuit represented by the cell and sample holder (Fig. 11) is the sum of the capacitance $C_s$, $C_t$, and $C_v$ associated with the cell and sample holder.

When the cavity is initially tuned to resonance, a change in the

cell capacitance will result in the detuning of the cavity. To retune the oscillometer to resonance, an amount of capacitance equal to the change in cell capacitance must be removed from the cell assembly by adjustment of $C_t$ and $C_v$.

In tuning the cavity to resonance, the main micrometer capacitor ($C_t$) was always adjusted to a graduated dial division and the vernier capacitor ($C_v$) used to obtain precise capacitance balance. The vernier capacitor was used in the susceptance variance method to determine the cell capacitance difference at the half-power points.[57,58] To obtain this cell capacitance difference, the cavity was tuned to half power points on either side of resonance by adjusting $C_v$ to values corresponding to 0.707 of the maximum detector current. The difference in capacitance values corresponding to the half points is proportional to the circuit $Q$. (Refer to Appendix VII, equation (A-29)

When the cavity was tuned to resonance, the net capacitance of the dielectric sample holder ($C_t$ and $C_v$) was assumed to be equal to the difference in capacitance values of $C_t$ and $C_v$. The reason for calculating the net capacitance of the sample holder as the difference rather than the sum of the values is because the vernier capacitor dial is graduated in increasing units of capacitance as the vernier screw is withdrawn. Therefore, the net capacitance of the sample holder decreases as the vernier screw is withdrawn.

Detector Circuit. Several crystal diode detector circuits employing a 1N-34A crystal diode were designed and constructed, and used to measure relative current flowing in the excited cavity resonator.[37] This type of detector proved to be unsatisfactory due to its poor response. The

magnitude of the response was dependent upon the values of the capacitance and resistance used in the circuits, as well as the frequency of the signal actuating the crystal diode detector. The detector circuit appeared to behave as if it were a resonant circuit. The poor response was probably due also in part to the inherent nature of the crystal diode. In all cases, the high frequency response of the detector was insufficient to obtain accurately necessary current measurements with available current measuring instruments.

The electrical circuit diagram of the detector employed in the oscillometer is shown in Fig. 12. The circuit is identical with that used in the Model OAO-2 frequency meter with exception of $C_1$, $M_2$ and $SW_1$.

A variable air capacitor ($C_1$) was connected to the plate circuit of the high frequency detector tube ($V_1$). The capacitance-inductance network formed by the cavity, probe and detector capacitor served as a resonant coupling device by means of which the magnitude of the energy transfer (coupling) from the excited cavity to the detector could be increased above that obtainable with the Model OAO-2 detector.

The capacitor was connected externally to the chassis containing the cavity resonator by means of a coaxial cable, and contained in a metal enclosure. Accurate and reproducible positioning of capacitor ($C_1$) was provided by a 10-turn, 500-division precision dial.

In practice, the value of capacitance $C_1$ was experimentally selected so that reactance of the detector circuit was equal to zero, as indicated by optimum detector current at resonance.

A high sensitivity galvanometer ($M_2$) was incorporated into the bridge circuit of the detector by means of a switch ($SW_1$), to obtain more

accurate measurement and to extend the measurable current range above that obtainable with the microammeter ($M_1$) of the frequency meter. The current sensitivity of the galvanometer ($M_2$) was 0.0051 microamps/mm, and the current range, 0-500 microamps.

The low sensitivity meter ($M_1$), 0-30 microamps, was used at the start of an experiment when preliminary measurements were necessary. The high sensitivity galvanometer ($M_2$) was used for experimental current measurements. The meters were disconnected from the bridge circuit by switch ($SW_2$), to prevent accidental damage to the meters, during preliminary adjustments.

The detector was coupled to the cavity resonator by means of a small brass rod probe extending into the cavity (Figs. 12 and 13). The probe was fixed in a plastic insulating plug which was screwed into the probe hole provided in the Model OAO-2 frequency meter.

The end of the probe was terminated with a circular disk, as shown in Fig. 12, to provide greater capacitative coupling with the inner conductor of the cavity. The dimensions of the probe and the spacing between the probe and the inner conductor were experimentally selected so that energy transfer (coupling) was of sufficient magnitude to make possible accurate high frequency measurement by means of the detector current. The dimensions of the probe were of necessity kept small in order to minimize capacitance reactance being coupled into the cavity. The probe was connected to the plate circuit of the high frequency diode detector tube ($V_1$).

High frequency energy received by the coupling rod probe is rectified by the high frequency detector tube ($V_1$). The rectified D.C. voltage

build-up across the load resistor $R_1$ and capacitors ($C_2$, $C_3$) is applied to the grid circuit of the D.C. amplifier tube ($V_2$). The D.C. amplifier tube is wired so that its internal plate-cathode resistance is in series with one arm of a Wheatstone bridge. The bias on the grid of $V_2$ will determine the value of the internal plate-cathode resistance. When there is unbalance in the bridge, current will flow which is indicated by meters $M_1$, $M_2$. There is a linear relationship between the high frequency signal actuating the detector circuit and the galvanometer indication.

Variable resistor ($R_s$), "Sens. Control", is used to vary the sensitivity of the bridge response to provide meter indications of desired magnitude for a high frequency signal of a given magnitude.

Potentiometer ($R_8$), "Zero Set", is used to balance the bridge circuit (to zero the meter indication) of the detector when the cavity resonator is detuned from any signal. The "Zero Set" control must be readjusted for every change of the setting of the "Sens. Control" when the cavity is detuned.

Incidental Instrumentation. A Beckman thermometer calibrated against a platinum resistance thermometer was used for temperature indication and as a reference to adjust the thermo-regulators of the constant temperature baths to 25°.

A constant temperature bath was employed to maintain test solutions at 25° prior to measurement in the oscillometer.

A Precision Scientific Co. circulating water bath was employed to thermostat the high frequency condenser-type cell at 25°. The thermoregulator supplied with the bath was replaced by a "Red Top" (inert

atmosphere) thermo-regulator.

Other instruments used included a Simpson Model 221 volt-ohm-milliameter, Heathkit Model O-7 oscilloscope, Sargeant recorder, Cat. No. 5-72150, Phaostron microammeter, D.C., 0-30 microamp range, and a Beckman Model M-2 pH meter and glass electrodes.

Oscillometer Response Measurements. The oscillometer responses that were measured and used to determine the electrical behavior of the oscillometer, and related to changes in composition of the test sample are: the cell capacitance, the cell capacitance difference at the half power points, and the detector current.

For a given dielectric material, $s$, contained in the cell, the cell capacitance, $\Delta C_s$, is equal to the difference in capacitance between the main dial, $C_t$, and the vernier screw, $C_v$, of the dielectric sample,

$$\Delta C_s = \left(C_t - C_v\right)_s. \tag{62}$$

For a given frequency and arbitrarily selected value of the detector probe capacitance (Fig. 11), the oscillometer is tuned to resonance by adjusting $C_t$ and $C_v$ to obtain maximum effective detector current. The main dial, $C_t$, was always adjusted to a graduated marking on the drum and the vernier screw, $C_v$, used to obtain precisely resonance.

A change in the conductivity and/or dielectric constant of the test solution will detune the oscillometer from resonance. To retune the oscillometer, $C_t$ and $C_v$ are readjusted to obtain maximum effective detector current. Since the condenser cell is in parallel to the capacitors $C_t$ and $C_v$, the change in cell capacitance is equal and opposite

in sign to the change in equivalent parallel capacitance, $C_p$ (equation (50) of the cell-solution load.

A change in the detector probe capacitance will also result in detuning the oscillometer from resonance. To reestablish resonance, $C_t$ and $C_v$ are adjusted to obtain maximum effective detector current. The change in cell reactance, $\Delta X_s = \left|\frac{1}{\omega \Delta C_s}\right|$, which is necessary to reestablish resonance, is equal and opposite in sign to the change in equivalent reactance coupled into the resonant cavity by coupled detector circuit.

The cell capacitance difference at the half power points, $\Delta C_{0.707}$, is equal to the difference in cell capacitance values which correspond to 0.707 of the optimum effective detector current, on either side of resonance, as given by

$$(63) \qquad \Delta C_{0.707,s} = \left| \left(C_t - C_v\right)_{s,1} - \left(C_t - C_v\right)_{s,2} \right|_{0.707}$$

where $\left(C_t - C_v\right)_{s,1}$ and $\left(C_t - C_v\right)_{s,2}$ are the two values of the cell capacitance corresponding to 0.707 of the optimum detector current at resonance. In general, the magnitude of $\Delta C_{0.707}$ is less than 5 picofarads. Therefore, it is possible to fix $C_t$ and then use the vernier screw, $C_v$, to precisely determine $\Delta C_{0.707}$.

The capacitance difference at the half power points, $\Delta C_{0.707}$ is related to the total high frequency equivalent conductivity, $G_t$ of the oscillometer and is given by (Refer to Appendix VII)

$$\Delta C_{0.707} = \frac{2G_t}{\omega} \tag{64}$$

The capacitance difference at the half power points is related to the $Q$-factor of the oscillometer as given by

$$\Delta C_{0.707} = \frac{2C_{total(res)}}{Q} \tag{65}$$

where $C_{total(res)}$ is the total equivalent capacitance of the oscillometer network at resonance. (Refer to equation (34), THEORY)

The detector current which is measured actually corresponds to the meter indication of the detector bridge circuit (Fig. 11). The meter indication is linearly related to the voltage drop across the detector probe capacitance which actuates the detector circuit. The meter indication is therefore linearly related to the current flowing in the resonant portion of the detector circuit.

Since it is possible to show that the voltage across the detector probe capacitance is directly proportional to the voltage across the resonant cavity capacitance (which is represented by the dielectric sample holder), the meter indication is linearly related to the voltage drop across the dielectric sample holder as represented by $C_t$ and $C_v$. Therefore, it is possible to use the meter indication to the Susceptance-Variance Method[57,58] to determine the capacitance difference at the half power points.

For a given resonance frequency, the detector current at resonance, will be an inverse function of the total equivalent resistance of the

oscillometer network. The relationship between the detector current and the equivalent circuit parameters is discussed in detail in the section, DISCUSSION AND RESULTS.

Effect of Detector Probe Capacitance Upon the Oscillometer Responses. The effect of the detector probe capacitance upon the oscillometer responses was determined at 5 Mc/sec intervals between the frequency range 75-105 Mc/sec in the following manner.

The clean, empty, borosilicate vessel was inserted and positioned in the cell assembly. The frequency of the signal generator was adjusted to 75 Mc/sec and the output voltage adjusted to the "Set Level". (Refer to Appendix V). The detector probe capacitance was adjusted to zero as indicated by the 10-turn (500-division) dial. The oscillometer was tuned to resonance by adjustment of the cell capacitance ($C_t$ and $C_v$). Resonance was indicated by a maximum effective detector current. After having determined the maximum effective detector current, the cell capacitance difference at half power points was measured. The resonance values of the detector probe capacitance, cell capacitance, and the detector current, as well as the cell capacitance difference at half power points were recorded.

The detector probe capacitance was readjusted to a higher capacitance value. The oscillometer was retuned to resonance by adjustment of the cell capacitance. The second set of resonance values of the detector probe capacitance, cell capacitance and detector current were recorded and then the cell capacitance difference at half power points measured. This procedure was repeated until the change in the oscillometer responses between successive values of the detector probe capacitance was negligible.

The above procedure was repeated at 5 Mc/sec intervals between the frequency range 75-105 Mc/sec. For each frequency, sufficient data was obtained in order to define the shape of the oscillometer response curve and to determine the value of the detector probe capacitance which will yield optimum detector current at resonance.

Evaluation of Cell Capacitance Measurements. The data used to determine the reproducibility in positioning of the vessel in the coaxial condenser cell holder was obtained in the following manner.

The resonant frequency was arbitrarily set at 100 Mc/sec. The detector probe capacitance was adjusted to a predetermined value to yield optimum detector current at resonance. The main dial $C_t$ was set arbitrarily to a spacing equal to 24.5 mils, which corresponds to a capacitance value for $C_t$ equal to 29.198 picofarads. The empty vessel was positioned in the cell assembly by alignment of the mark on the glass vessel with a mark on the lip of the cell holder. The oscillometer was tuned to resonance by adjustment of $C_v$. The value of $C_v$ was noted. The vessel was removed and the $C_v$ setting changed. The vessel was reinserted and positioned in the cell assembly and the oscillometer retuned to resonance by adjustment of $C_v$. The procedure was repeated several times. A total of twenty measurements were obtained in this manner.

The data used to determine reliability of the cell capacitance measurements at resonant frequencies of 100 and 120 Mc/sec were obtained in the following manner.

The clean, dry, empty vessel was inserted and positioned in the cell assembly. The detector probe capacitance was set at a predetermined value to yield optimum detector current at resonance. The vernier screw $C_v$ of

the dielectric sample holder was set at zero and the main dial $C_t$ adjusted to obtain resonance. The main dial $C_t$ was readjusted to the nearest graduated marking on the drum and $C_v$ then adjusted to reestablish resonance. The values of $C_t$ and $C_v$ were noted. The oscillometer was detuned by selecting a different setting of $C_t$ which corresponded to the second graduated marking on the drum. Again $C_v$ was used to retune the oscillometer to resonance. This procedure was repeated until the limit of the vernier screw was reached.

Evaluation of Cell Parameters, $C_g$ and $C_o$. The method suggested by Reilly and McCurdy[13,24] was employed to evaluate the cell constants $C_g$, the capacitance due to walls of the borosilicate vessel, and $C_o$, the capacitance contribution of the annular sample space of the borosilicate vessel containing air. The dielectric constant of air was assumed to be equal to one.

The cell parameters were experimentally obtained at 5 Mc/sec intervals between 75 and 105 Mc/sec by means of the derived expressions: (See Appendix VII for sample derivation)

$$C_g = \frac{\left[\Delta C_s - \Delta C_{Hg}\right]\left[\varepsilon_s - 1\right]}{\varepsilon_s\left[\frac{\Delta C_s - \Delta C_{Hg}}{\Delta C_a - \Delta C_{Hg}}\right] - 1} \tag{66}$$

and

$$C_o = \frac{C_g^2 - C_g\left[\Delta C_a - \Delta C_{Hg}\right]}{\Delta C_a - \Delta C_{Hg}} \tag{67}$$

Where: $\Delta C_a$ = capacitance, vessel containing air, picofarads.
$\Delta C_s$ = capacitance, vessel containing benzene, picofarads.
$\Delta C_{Hg}$ = capacitance, vessel containing mercury, picofarads.
$\varepsilon_s$ = dielectric constant of benzene at 25°, equal to 2.275.

The cell capacitance values, $\Delta C_a$, $\Delta C_{Hg}$, and $\Delta C_s$ necessary to evaluate $C_o$ and $C_g$ were obtained in the following manner.

The signal generator was adjusted to the desired frequency. The clean, dry, empty vessel was inserted and positioned in the cell assembly. The oscillometer was tuned to resonance by adjustment of $C_t$ and $C_v$. The cell capacitance, $\Delta C_a$, for the empty cell was noted. Mercury was then introduced into the vessel and the oscillometer retuned to resonance. The cell capacitance, $\Delta C_{Hg}$, for the vessel containing mercury was noted.

The vessel was removed from the cell assembly, and the mercury removed. The vessel was rinsed several times with concentrated acid and water, and then dried at 105°.

The clean, dry, empty vessel was inserted and positioned in the cell assembly and the oscillometer tuned to resonance. The cell capacitance, $\Delta C_a$, for the empty vessel was compared to the previous value to insure proper positioning of the vessel. Benzene was introduced in the vessel and the oscillometer retuned to resonance. The cell capacitance, $\Delta C_s$, for benzene contained in the vessel was noted.

Having obtained the cell capacitance values for air, mercury and benzene, the values $\Delta C_a$, $\Delta C_{Hg}$, and $\Delta C_s$ were inserted into equation (66) and the value of $C_g$ calculated.

Having determined $C_g$, the values of $C_g$, $\Delta C_a$, and $\Delta C_{Hg}$ were inserted into equation (67) and the value of $C_o$ calculated.

Dielectric Constant Measurements. The dielectric constants of benzene, acetic acid, 1, 2 diehloroethane, chlorobenzene, acetone, and nitrobenzene were experimentally evaluated at 100 Mc/sec and 25°.

The dielectric constants, $\epsilon_s$, of the pure liquids were evaluated by substituting appropriate quantities into the expression. (See Appendix VII for sample derivation)

$$\epsilon_s = \frac{C_g\left[\left(\Delta C_a - \Delta C_s\right) + \frac{C_g C_o}{C_g + C_o}\right]}{C_o\left[C_g - \left(\Delta C_a - \Delta C_s\right) - \frac{C_g C_o}{C_g + C_o}\right]} \tag{68}$$

where: $C_g$ = capacitance due to the walls of the vessel, picofarads.
$C_o$ = capacitance, evacuated cell, picofarads.
$\Delta C_a$ = capacitance, cell containing air, picofarads.
$\Delta C_s$ = capacitance, cell containing test liquid, picofarads.

The capacitance values corresponding to the cell parameters, $C_g$ and $C_o$ and cell capacitance $\Delta C_a$ and $\Delta C_s$ were obtained in the manner described in the previous section.

Before and after a sample measurement, the vessel was removed from the cell holder, cleaned with dichromate cleaning solution, washed, and dried. Before introducing a test sample into the vessel, the vessel was positioned into the cell assembly and the air capacitance of the cell determined to insure proper vessel position.

Oscillometer Response Curves. Response curves similar to the theoretical curves shown in Fig. 8 were obtained at 100 Mc/sec for the following systems: (1) aqueous solutions of sodium chloride, barium chloride, and lanthanum chloride, (2) glacial acetic acid solutions of

sodium acetate, perchloric acid, and p-nitro aniline and (3) methanolic solutions of sodium chloride. Response curves at 75 Mc/sec were obtained for aqueous solutions of sodium chloride.

The changes in oscillometer response which were measured for the solutions of varying conductivity were: (1) detector current, (2) cell capacitance, and (3) cell capacitance difference at half power points.

For a given solvent, solute, and frequency, the response curve data was obtained in the following manner.

The clean, dry, cell was positioned in the cell holder and the oscillometer tuned to resonance. The cell capacitance for the empty cell was noted and compared with previous values to indicate proper cell position. The solvent was introduced in the cell and the oscillometer tuned to resonance. The cell capacitance and detector current at resonance were noted. The cell capacitance at half power points was determined. The solvent was removed from the cell by means of a tube connected to a suction apparatus. The cell was filled with solution of electrolyte of a known conductivity and then emptied. The cell was rinsed three times with fresh solution before a second set of readings were measured. The above procedure was repeated several times with solutions of increasing solute concentration.

For all response curve measurements, the value of the detector probe capacitance was selected to yield optimum detector current at resonance.

Low Frequency Conductance Measurements. A Serfass Model RC-M15 conductivity bridge was employed for all aqueous and non-aqueous conductivity measurements.

A glass enveloped dipping type conductivity cell with a cell constant

of 0.0944 $cm^{-1}$ was used. Solutions were contained in an electrolytic beaker immersed in a waterbath maintained at 25 ± 0.02°. A standard molal solution of potassium chloride, prepared from fused potassium chloride dissolved in triply distilled water, was used to evaluate the cell constant.

An Industrial Instruments Model DK-2A MFD capacitance box was connected in parallel with the electrodes of the conductivity cell to obtain sharper bridge balance for conductivity measurements of the concentrated aqueous and non-aqueous solutions. Sharper bridge balance was obtained at 60 than 1000 c.p.s.

The dipping type cell was washed three times with test solution prior to a measurement. Duplicate measurements were obtained for each test solution. The measurements for a given solute-solvent system were obtained in the order of increasing concentration of solute to minimize error in measurements due to absorption of solute on the platinum electrode surfaces.

After a series of measurements for a given solute-solvent system was obtained, the conductivity cell was cleaned and the cell constant redetermined.

The conductivities were measured and the specific conductances were evaluated for the following solutions: (1) aqueous sodium chloride, barium chloride, lanthanum chloride, and aqueous solutions of the simulated titration of hydrochloric acid with sodium hydroxide, (2) acetous sodium acetate, perchloric acid, p-nitro aniline, and acetous solution of the simulated titration of sodium acetate with perchloric acid; and (3) methanolic sodium chloride.

Simulated Titrations. The simulated low frequency conductometric and oscillometric (100 Mc/sec) aqueous titration of sodium hydroxide with standard hydrochloric acid, and acetous titration of sodium acetate with standard perchloric acid were performed in the following manner.

Aliquots of the stock solution to be analyzed (aqueous sodium hydroxide solution or acetous sodium acetate solution) were transferred to fourteen volumetric flasks of equal volume. The solution contained in the first flask was diluted to volume with solvent. A measured amount of titrant was introduced into the second flask to partially neutralize the test reactant and the resulting solution diluted to volume with solvent. Increasing measured amounts of titrant were introduced successively to the remaining twelve flasks and the solutions diluted to volume. The equivalents of titrant introduced into the fourteenth flask was approximately equal to twice the equivalents of reactant present in the aliquot of test solution.

A portion of each of the fourteen solutions was introduced into the conductivity cell and into the oscillometer vessel for measurement as previously described.

The oscillometer response curves were employed to select the proper concentration range in which substance titrated and titrant must fall to obtain straight line oscillometric titration curves.

## RESULTS AND DISCUSSION

The discussion which follows is an attempt to elucidate the nature of the resonant-cavity oscillometer with the aid of a "synthesized" *RLC* network which was derived from the observed electrical behavior of the oscillometer. In the synthesized network, only those circuit parameters or circuit elements which affect oscillometer response are included.

The equivalent network has no physical relationship, part by part, with the cavity resonator or with the associated circuitry and is not even unique. But rather, the equivalent circuit serves only as a model.

In this model, the electrochemical properties of the solution are represented by "lumped" values of resistance, $R$, (or conductance, $G = \frac{1}{R}$) and capacitance, $C$. Circuit analysis of the condenser-type cell and solution network was accomplished by employing the theory of oscillometric measurements developed by Reilly and McCurdy.

With the more conventional resonant circuits that operate at lower frequencies, 1-30 Mc/sec, the conditions of the circuit as represented by voltage and current, can usually be evaluated by direct measurements. However, with the cavity resonator oscillometer, the only A.C. measurements that are easy to make even in principle, are those of impedance, power, and frequency.[47] Consequently, it was necessary to contend with indirect measurements of the circuit current, capacitance, high frequency conductance and $Q$-factor.

In this investigation, only relative electrical measurements were obtained. Consequently, a rigorous quantitative circuit analysis and treatment of the data was not possible. However, by means of the

equivalent circuit models, a qualitative analyses has been accomplished in which the model satisfies relationships between the experimentally observed oscillometer responses.

Equivalent Circuit of the Cavity Resonator Oscillometer. The oscillometer reduced to its essential circuit elements is schematically represented by the double-tuned equivalent circuit shown in Fig. 16. This model satisfies relationships between the experimentally observed oscillometer responses: detector current, equivalent parallel cell capacitance, and the capacitance difference at the half power points.

The cavity resonator is represented in the conventional impedance form as a series *RLC* network in which $L_2$ and $C_2$ are the equivalent distributed inductance and capacitance, respectively, of the cavity at angular frequency $\omega$, and $R_2$, is the equivalent series resistance associated with the cavity at angular frequency $\omega$.

Directly connected to the cavity is the dielectric sample holder consisting of the variable capacitors $C_t$ and $C_v$. The condenser-type cell, connected in parallel to the capacitors of the dielectric sample holder, is represented by the equivalent parallel capacitance, $C_p$, and equivalent parallel shunt conductance, $G_p$ (equal to $\frac{1}{R_p}$).

The signal generator was inductively coupled to the cavity by inserting a loop probe into the cavity enclosure. The distributed inductance of the loop at angular frequency $\omega$ is $L_1$. $R_1$ is the equivalent series resistance of the coil. The mutual inductance between the inductors $L_1$ and $L_2$ is represented by $M_{12}$.

To measure the internal electrical conditions existing in the cavity, a detector-bridge circuit was coupled to the cavity by inserting a rod

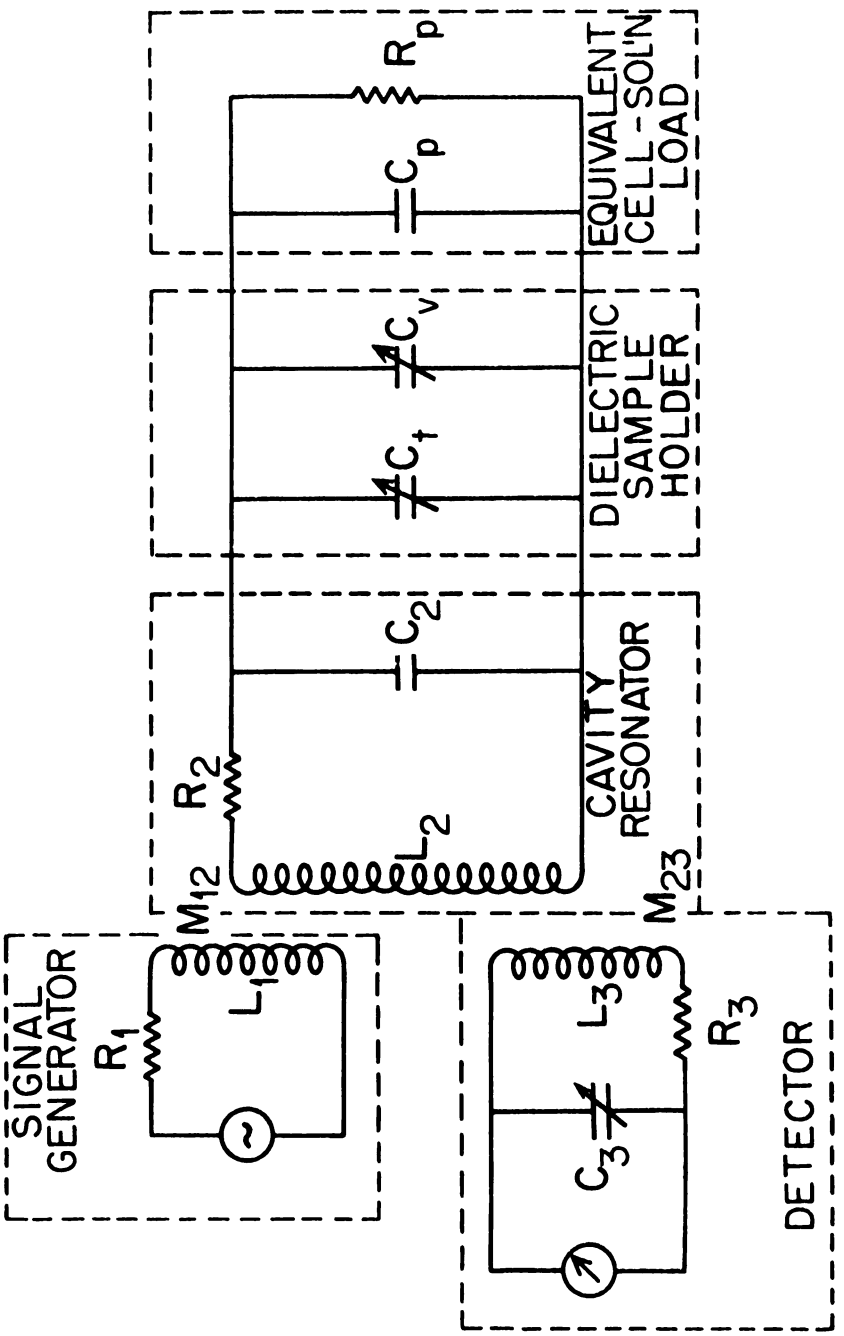


Figure 16. The Fundamental Equivalent Circuit of the Resonant Cavity Oscillometer

probe into the cavity enclosure. This form of coupling may be represented by several different equivalent representation circuits. Since the probe interacts with the electrostatic as well as the electromagnetic fields existing in the excited cavity, an inductive coupling representation has been selected rather than a capacitative coupling representation for convenience and to facilitate circuit analysis.[46] Similar qualitative circuit relationships as developed herein may be obtained by use of other coupling networks representations.

The distributed inductance of the detector probe at angular frequency $\omega$ is represented by $L_3$. The variable detector probe capacitance (Fig. 11) and distributed capacitance of the detector circuit are lumped together and represented by a variable capacitor, $C_3$. The equivalent series resistance of the detector network is $R_3$. The mutual inductance between the cavity and detector inductor is $M_{23}$.

To facilitate the analysis of oscillometer response and more conveniently show the relationships between the voltage, current, and impedance for the network, the fundamental circuit shown in Fig. 16 may be reduced to the fundamental equivalent circuit shown in Fig. 17. The only significant difference between the two fundamental circuit representations is that in Fig. 17, an equivalent series capacitance $C_2'$ and equivalent series resistance $R_2'$ have been substituted for the network consisting of $R_2$, $R_p$, $C_2$, $C_v$, $C_t$ and $C_p$ as shown in Fig. 16.

The equivalent series impedance, $Z'$, for the network consisting of $R_2$, $R_p$, $C_2$, $C_v$, $C_t$ and $C_p$ is given by

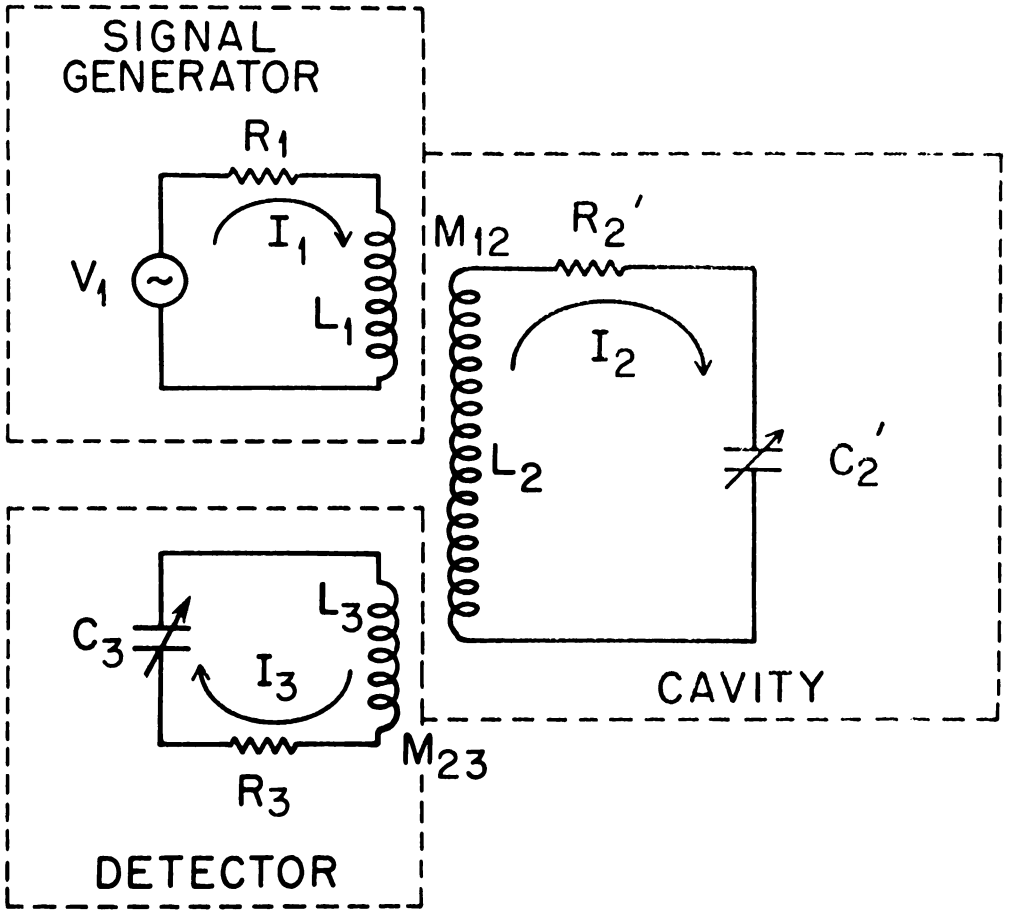


Figure 17. Simplified Equivalent Circuit of the Resonant Cavity Oscillometer

$$(69) \qquad Z' = \left\{ \frac{R_2 + R_p}{1 + \omega^2 \left[ C_2 + C_t + C_v + C_p \right]^2 R_p^2} \right\} - j \left\{ \frac{\omega \left[ C_2 + C_t + C_v + C_p \right] R_p^2}{1 + \omega^2 \left[ C_2 + C_t + C_v + C_p \right]^2 R_p^2} \right\}$$

Equation (69) shows that this network may be represented by an equivalent resistance $R_2'$, which is equal to

$$(70) \qquad R' = R_2 + \frac{R_p}{1 + \omega^2 \left[ C_2 + C_t + C_v + C_p \right]^2 R_p^2} ,$$

and in series with an equivalent capacitive, given by

$$(71) \qquad C_2' = \frac{1 + \omega^2 \left[ C_2 + C_v + C_t + C_p \right]^2 R_p^2}{\omega^2 \left[ C_2 + C_v + C_t + C_p \right] R_p^2}$$

The use of $R_2'$ and $C_2'$ in the development of the circuit theory permits one to use terms in the mathematical expression which are much less cumbersome and less difficult to employ.

When a sinusoidal voltage, $V_i$, is applied to the cavity by means of the signal generator, a voltage will be induced in the cavity via the coupling between inductors $L_1$, and $L_2$ by the current, $I_1$, flowing in the signal generator circuit.

The complex notation of the voltage, $V_2$, induced in the cavity, is

(72) $$V_2 = j\omega M_{12} I_1$$

The induced voltage has a magnitude of $\omega M_{12} I_1$ and lags behind the signal generator current by 90°.

The current $I_2$ flowing in the cavity circuit is exactly the same current that would flow in the cavity, if the induced voltage $V_2$ were applied in series with the inductor $L_2$ and the signal generator circuit were absent.

The current $I_2$ flowing in the energized cavity will in turn induce a voltage, $V_3$, in the detector. The complex notation of the induced detector circuit voltage is given by

(73) $$V_3 = -j\omega M_{23} I_2$$

The current $I_3$ flowing in the detector circuit is the same current that would flow in circuit 3 if the induced voltage, $V_3$, were applied in series with the inductor $L_3$ and the cavity circuit were absent.

If the output $V_1$, of the signal generator is a sinusoidal voltage and all circuit parameters are constant, the following relationships may be written.

(74) $$\left(R_1 + j\omega L_1\right) I_1 + j\omega M_{12} I_2 = V_1$$

(75) $$\left(R_2' + j\left(\omega L_2 - \frac{1}{\omega C_2'}\right)\right) I_2 + j\omega M_{23} I_3 + j\omega M_{12} I_1 = 0$$

$$(76) \qquad \left[R_3 + j\left(\omega L_3 - \frac{1}{\omega C_3}\right)\right] I_3 + j\omega M_{23} I_2 = 0$$

For the sake of simplicity in writing, the following abbreviations are adopted:

$$(77) \qquad Z_1 = R_1 + j\omega L_1, \text{ signal generator impedance}$$

$$(78) \qquad Z_2' = R_2' + j\left(\omega L_2 - \frac{1}{\omega C_2'}\right), \text{ cavity resonator impedance}$$

$$(79) \qquad Z_3 = R_3 + j\left(\omega L_3 - \frac{1}{\omega C_3}\right), \text{ detector circuit impedance}$$

$$(80) \qquad Z_{M_{12}} = j\omega M_{12}, \text{ mutual impedance between the generator and cavity inductors}$$

$$(81) \qquad Z_{M_{23}} = j\omega M_{23}, \text{ mutual impedance between the cavity and detector inductors}$$

Equations (74), (75), and (76) are reduced to

$$(82) \qquad Z_1 I_1 + Z_{M_{12}} I_2 = V_1$$

$$(83) \qquad Z_{M_{12}} I_1 + Z_2 I_2 + Z_{M_{23}} I_2 = 0$$

$$(84) \qquad Z_{M_{23}} I_2 + Z_3 I_3 = 0$$

The simultaneous solution of equations (82), (83), and (84) yield

$$(85) \qquad I_1 = \frac{\left[Z_2 Z_3 - Z_{M_{23}}^2\right] V_1}{Z_1 Z_2 Z_3 - Z_1 Z_{M_{23}}^2 - Z_3 Z_{M_{12}}^2}$$

$$(86) \qquad I_2 = \frac{-Z_{M_{12}} Z_3 V_1}{Z_1 Z_2 Z_3 - Z_1 Z_{M_{23}}^2 - Z_3 Z_{M_{12}}^2}$$

$$(87) \qquad I_3 = \frac{Z_{M_{12}} Z_{M_{23}} V_1}{Z_1 Z_2 Z_3 - Z_1 Z_{M_{23}}^2 - Z_3 Z_{M_{12}}^2}$$

As is evident by equations (85), (86), and (87) the nature and magnitude of the current flow in the various circuits are complex and depend upon the nature and magnitude of the impedances of the individual circuits. However, by means of equations (85), (86), and (87), it is possible to synthesize equivalent networks which are very useful in demonstrating the nature of the interaction and coupling of impedance in the various circuits.

For example, the terms in equation (86) may be rearranged to yield an equivalent expression given by

$$(88) \qquad I_2 = \frac{-\frac{Z_{M_{12}}}{Z_1} V_1}{Z_2' - \frac{Z_{M_{12}}^2}{Z_1} - \frac{Z_{M_{23}}^2}{Z_3}}$$

Equation (88) may be satisfied by an equivalent circuit shown in Fig. 18. This is an equivalent circuit referred to the cavity.

In this simplified equivalent circuit, the equivalent voltage

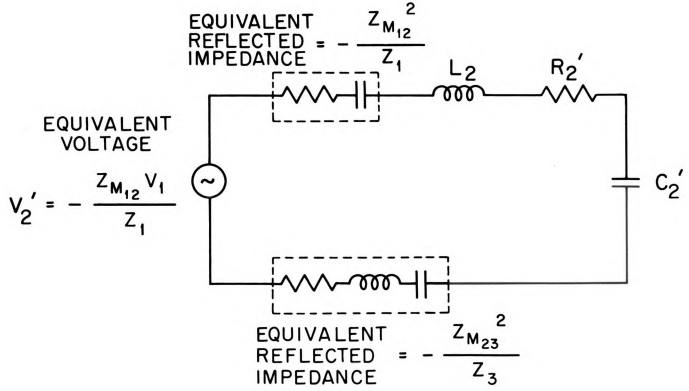


Figure 18. An Equivalent Circuit as Represented by the Expression $I_2 = \frac{-\frac{Z_{M_{12}}}{Z_1} \cdot V_1}{Z_2 - \frac{Z_{M_{12}}^2}{Z_1} - \frac{Z_{M_{23}}^2}{Z_3}}$

source $V_2'$ is represented by the complex quantity $-\frac{Z_{M_{12}}}{Z_1} V_1$. Since the quantities $R_1$, $L_1$, $L_2$ and $M_{12}$ were fixed under conditions of constant applied voltage, $V_1$, at angular frequency $\omega$, the equivalent voltage source, $V_2'$, is a constant voltage whose magnitude is given by

$$(89) \qquad V_2' = \left( \frac{\left[\omega^2 M_{12} L_1\right]^2 + \left[\omega M_{12} R_1\right]^2}{R_1^2 + \omega^2 L_1^2} \right)^{1/2} \cdot V.$$

The equivalent impedance $Z_{(equiv)_2}$ of the network shown in Fig. 3 is that impedance as seen by, or referred to, the cavity and is given by

$$(90) \qquad Z_{(equiv)_2} = Z_2' - \frac{Z_{M_{12}}^2}{Z_1} - \frac{Z_{M_{23}}^2}{Z_3}$$

In equation (90), the quantity $Z_2'$ represents the impedance of the cavity as given by equation (78) and represented in Fig. 1 by the cavity network which consists of the resonant cavity, dielectric sample holder and cell-solution load.

The quantity $-\frac{Z_{M_{12}}^2}{Z_1}$ represents the equivalent series impedance reflected (or coupled) into the cavity by the signal generator, via the mutual inductance, $M_{12}$, of inductance $L_1$ and $L_2$. In complex notation, the equivalent reflected impedance $-\frac{Z_{M_{12}}^2}{Z_1}$ is given by

$$(91) \qquad -\frac{Z_{M_{12}}^2}{Z_1} = Z_{(reflected)_{12}} = \frac{\omega^2 M_{12}^2}{R_1 + j\omega L_1}$$

When the terms of equation (91) are rationalized and grouped into the real and complex parts, one obtains an expression for the equivalent reflected impedance given by

$$(92) \qquad Z_{(reflected)_{12}} = \frac{\omega^2 M_{12}^2 R_1}{R_1^2 + \omega^2 L_1^2} - j \frac{\omega L_1}{R_1^2 + \omega^2 L_1^2}$$

which consists of a resistive component equal to

$$(93) \qquad R_{(reflected)_{12}} = \frac{\omega^2 M_{12}^2 R_1}{R_1^2 + \omega^2 L_1^2}$$

and a reactive component equal to

$$(94) \qquad X_{(reflected)_{12}} = \frac{\omega L_1}{R_1^2 + \omega^2 L_1^2}$$

The reactance reflected into the cavity by the signal generator, $X_{(reflected)_{12}}$, is capacitive in nature as indicated by the negative sign of imaginary term in equation (92).

The net effect of coupling the signal generator to the cavity is to lower the $Q$ of the cavity and to decrease the cavity's capacitive reactance at angular frequency $\omega$.

In equation (90), the quantity $-\frac{Z_{M_{23}}^2}{Z_3}$ represents the equivalent series impedance, $Z_{(reflected)_{23}}$, reflected (or coupled) into the cavity by the tuned detector via the mutual inductance $M_{23}$ of inductors $L_2$ and $L_3$. The equivalent reflected impedance, $Z_{(reflected)_{23}}$, in complex

notation is given by

$$(95) \qquad -\frac{Z_{M_{23}}^{2}}{Z_3} = Z_{(reflected)_{23}} = \frac{\omega^2 M_{23}^{2}}{R_3 + j\left(\omega L_3 - \frac{1}{\omega C_3}\right)}$$

When the terms of equation (95) are rationalized and grouped into the real and complex parts, the equivalent reflected impedance of the detector is given by

$$(96) \qquad Z_{(reflected)_{23}} = \frac{\omega^2 M_{23}^{2} R_3}{R_3^{2} + \left(\omega L_3 - \frac{1}{\omega C_3}\right)^2} - j\,\frac{\omega^2 M_{23}^{2}\left(\omega L_3 - \frac{1}{\omega C_3}\right)}{R_3^{2} + \left(\omega L_3 - \frac{1}{\omega C_3}\right)^2}$$

and consists of a resistive component, $R_{(reflected)_{23}}$, given by

$$(97) \qquad R_{(reflected)_{23}} = \frac{\omega^2 M_{23}^{2} R_3}{R_3^{2} + \left(\omega L_3 - \frac{1}{\omega C_3}\right)^2}$$

and a reactive component, $X_{(reflected)_{23}}$, given by

$$(98) \qquad X_{(reflected)_{23}} = \frac{\omega^2 M_{23}^{2}\left(\omega L_3 - \frac{1}{\omega C_3}\right)}{R_3^{2} + \left(\omega L_3 - \frac{1}{\omega C_3}\right)^2}$$

Although the sign of the imaginary term in equation (96) is negative, the reactance reflected into the cavity by the detector may be either capacitive or inductive in nature and depends upon the magnitude of the detector reactance, the quantity $\left(\omega L_3 - \frac{1}{\omega C_3}\right)$. If $\frac{1}{\omega C_3}$ is greater than $\omega L_3$, the sign of the imaginary term in equation (96) will be positive and the

reactance reflected into the cavity, $X_{(reflected)_{23}}$, will be inductive. Conversely, if $\omega L_2$ is greater than $\frac{1}{\omega C_3}$, the sign of the imaginary term in equation (96) will be negative and the reactance, $X_{(reflected)_{23}}$, will be capacitive in nature.

When the variable capacitor, $C_3$, of the detector (Fig. 16) is adjusted so that the detector circuit is tuned to resonance, when $\omega L_3 = \frac{1}{\omega C_3}$, the reactance reflected into the cavity is equal to zero,

$$X_{(reflected)_{23}} = 0 \tag{99}$$

Under the above stated condition of resonance, the impedance reflected into the cavity is purely resistive in nature and is given by

$$Z_{(reflected)_{23}} = \frac{\omega^2 M_{23}^2}{R_3} \tag{100}$$

A more pertinent discussion of the effect of reflected detector impedance upon the oscillometer response is contained in the sections which follow.

In complex notation, equation (90) is given by

$$Z_{(equiv)_2} = R_2' + j\left(\omega L_2 - \frac{1}{\omega C_2'}\right) + \frac{\omega^2 M_2^2}{R_1 + j\omega L_1} + \frac{\omega^2 M_{23}^2}{R_3 + j\left(\omega L_3 - \frac{1}{\omega C_3}\right)} \tag{101}$$

When the terms of equation (101) are rationalized and grouped into the real and complex parts, one obtains

$$(102)\qquad Z_{(equiv)_2} = \left[R_2' + \frac{\omega^2 M_{12}^2 R_1}{R_1^2 + \omega^2 L_1^2} + \frac{\omega^2 M_{23}^2}{R_3^2 + \left(\omega L_3 - \frac{1}{\omega C_3}\right)^2}\right]$$

$$+j\left[\left(\omega L_2 - \frac{1}{\omega C_2'}\right) - \frac{\omega^2 M_{12}^2 (\omega L_1)}{R_1^2 + (\omega L_1)^2} - \frac{\omega^2 M_{23}^2 \left(\omega L_3 - \frac{1}{\omega C_3}\right)^2}{R_3^2 + \left(\omega L_3 - \frac{1}{\omega C_3}\right)^2}\right]$$

Equation (102) more clearly shows that the double-tuned oscillometer network represented in Fig. 17 is reducible to an equivalent circuit consisting of an equivalent resistive impedance, $R_{(equiv)_2}$ given by

$$(103)\qquad R_{(equiv)_2} = R_2' + \frac{\omega^2 M_{12}^2 R_1}{R_1^2 + (\omega L_1)^2} + \frac{\omega^2 M_{23}^2 R_3}{R_3^2 + \left(\omega L_3 - \frac{1}{\omega C_3}\right)^2}$$

in series with an equivalent reactance, $X_{(equiv)_2}$, given by

$$(104)\qquad X_{(equiv)_2} = \left(\omega L_2 - \frac{1}{\omega C_2'}\right) - \frac{\omega^3 M_{12}^2 L_1}{R_1^2 + (\omega L_1)^2} - \frac{\omega^2 M_{23}^2 \left(\omega L_3 - \frac{1}{\omega C_3}\right)}{R_3^2 + \left(\omega L_3 - \frac{1}{\omega C_3}\right)^2}$$

In equation (103) the quantities $\frac{\omega^2 M_{12}^2 L_1}{R_1^2 + (\omega L_1)^2}$ and $\frac{\omega^2 M_{23}^2 R_3}{R_3^2 + \left(\omega L_3 - \frac{1}{\omega C_3}\right)^2}$ represent the equivalent series resistive impedances, $R_{(equiv)_{12}}$ and $R_{(equiv)_{23}}$ respectively reflected into the cavity by the signal generator and detector (refer to equations (93) and (97). The first term in equation (93), $R_2'$ is equal to the equivalent cavity resistive impedance as shown in Fig. 17 and given by equation (70).

In equation (104) the quantities $\frac{\omega^3 M_{12}^2 L_1}{R_1^2 + \left[\omega L_1\right]^2}$ and $\frac{\omega^2 M_{23}^2 \left[\omega L_3 - \frac{1}{\omega C_3}\right]}{R_3^2 + \left[\omega L_3 - \frac{1}{\omega C_3}\right]^2}$ represent the equivalent series resistive impedance, $R_{(equiv)_{12}}$ and $X_{(equiv)_{23}}$ respectively, reflected into the cavity by the signal generator and detector (refer to equations (94) and (98). The first term in equation (104) is the reactive impedance of the cavity network and for which the equivalent series capacitance, $C_2'$ is given by equation (71).

Condition of Resonance. Resonance in the resonant cavity oscillometer may be obtained when any one circuit parameter, as shown in Fig. 16-18, is so varied as to cause maximum effective detector current under the conditions of constant applied signal generator voltage at angular frequency, $\omega$. For fixed values of $R_1$, $L_1$, $M_{12}$, $L_2$, $R_2$, $C_2$, $C_t$, $C_v$, $R_p$, $C_p$, $M_{23}$, $C_3$, $R_3$, and $L_3$, resonance may be obtained by adjusting the frequency.

In the oscillometer, as represented by the fundamental equivalent circuit shown in Fig. 16, all circuit parameters with the exception of $R_p$, $C_p$, $C_v$, $C_t$ and $C_3$ were held constant and are assumed to operate independently of each other at angular frequency $\omega$. In practice, only the cavity capacitance ($C_t$ and $C_v$) and the detector probe capacitance ($C_3$) may be adjusted to obtain maximum effective detector current ($I_3$) under conditions of constant applied voltage ($V_1$). The equivalent parallel resistance ($R_p$) and capacitance ($C_p$), which represent the cavity cell-solution load, are not used to tune the oscillometer to resonance. However, when the oscillometer is initially tuned to resonance, by proper adjustment of $C_t$, $C_v$ and $C_3$, a change in $R_p$ or $C_p$ will detune the oscillometer. Resonance is restored by adjustment of the cavity capacitance ($C_t$ and $C_v$) to

yield maximum effective detector current.

The relationship between the oscillometer detector current and the cavity cell capacitance ($C_t$ and $C_v$) and the relationship between the oscillometer detector current and the detector probe capacitance ($C_3$) are shown in Fig. 19. All circuit parameters were held constant with the exception of cavity cell capacitance ($C_t$ and $C_v$) and the detector probe capacitance, ($C_3$), under condition of constant applied signal generator voltage and frequency.

As shown in Fig. 19A, for an arbitrarily selected value of cavity cell capacitance ($C_t$ and $C_v$) corresponding to 27.10 picofarads, the detector current is a maximum at a detector probe capacitance value equal to 43.5 picofarads. When the detector current is a maximum, the oscillometer is tuned to resonance. In Fig. 19B, the detector probe capacitance was arbitrarily fixed at a value equal to 43.5 picofarads and the cavity cell capacitance ($C_t$ and $C_v$) varied. Maximum effective detector current occurred at a cavity cell capacitance corresponding to 27.74 picofarads. This detector current response, (Fig. 19, A and B) is typical of that response expected for the double-tuned equivalent circuit representation shown in Fig. 16.

A qualitative interpretation of the oscillometer detector current response may be accomplished most conveniently if the fundamental equivalent circuit representation shown in Fig. 16, 17 and 18 are reduced to the simplified equivalent circuit shown in Fig. 20. In the equivalent circuit representation, the subscripts of the various circuit parameters are consistant with all of the preceding circuit notation in that the

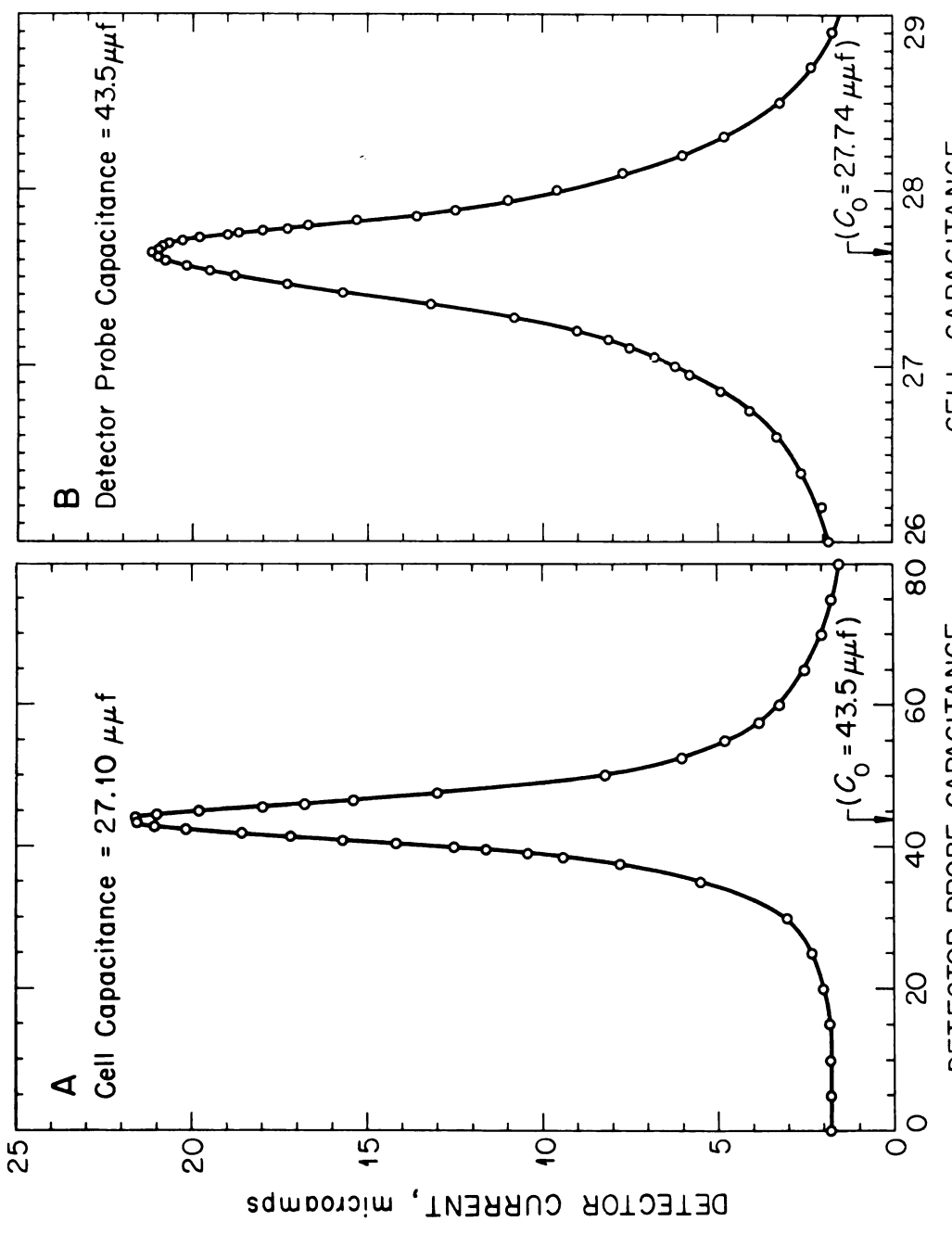


**Figure 19. Detector Current as a Function of: (A) Cell Capacitance; (B) Detector Probe Capacitance (at 100 Mc/sec)**

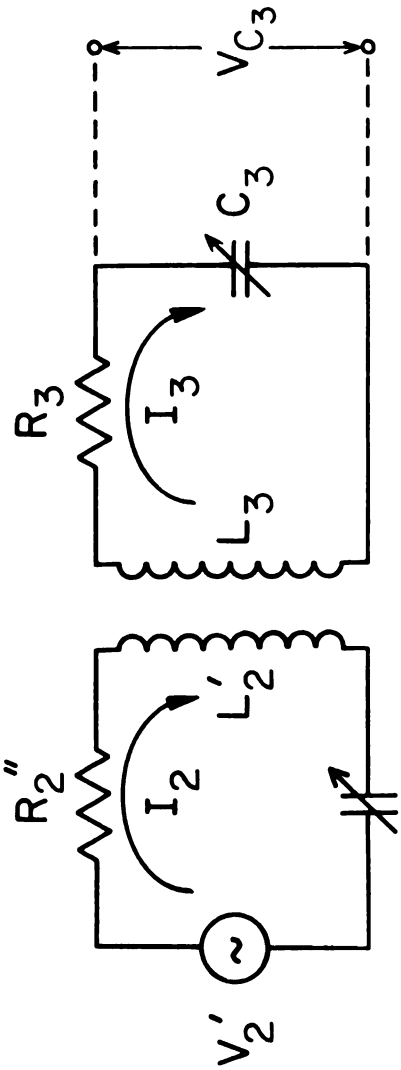


Figure 20. Simplified Equivalent Circuit Representation of the Oscillometer Fundamental Equivalent Circuit (Refer Figure 16)

subscript 2 refers to the equivalent cavity circuit and the subscript 3 refers to the detector circuit. Furthermore, the circuit parameters, $V_2'$, $C_2'$, $L_3$, $M_{23}$, $R_3$ and $C_3$ denote the same quantities as shown or expressed in preceding equations and circuit representations. $R_2''$ and $L_2'$ represent the total equivalent series resistance and inductance, respectively, of the cavity as given by

$$R_2'' = R_2' + \frac{\omega^2 M_{12}^2 R_1}{R_1^2 + \omega^2 L_1^2} \tag{105}$$

and

$$L_2' = L_2 - \frac{\omega^2 M_{12}^2 L_1}{R_1^2 + (\omega L_1)^2} \tag{106}$$

The quantity $R_2''$ includes the resistive term $\frac{\omega^2 M_{12}^2 R_1}{R_1^2 + \omega^2 L_1^2}$ which represents the resistive impedance reflected into the cavity by inductively coupling the signal generator to the cavity. The term $R_2'$ is given by equation (70). The quantity representing $L_2'$ includes a term $\frac{\omega^2 M_{12}^2 L_1}{R_1^2 + (\omega L_1)^2}$ which represents the equivalent reactance reflected into the cavity by the signal generator, via the inductive coupling of the cavity to the generator.

The equation to represent the detector current, $I_3$, may be derived in a manner similar to the derivations of equations (85), (86) and (87), and is given by

$$I_3 = - \frac{Z_{M_{23}} V_2'}{Z_2'' Z_3 - Z_{M_{23}}^2} \tag{107}$$

where:

$$Z_2'' = R_2'' + j\left(\omega L_2' - \frac{1}{\omega C_2'}\right) \tag{108}$$

$$Z_{M_{23}} = j\omega M_{23} \tag{109}$$

$$Z_3 = R_3 + j\left(\omega L_3 - \frac{1}{\omega C_3}\right) \tag{110}$$

In complex notation the detector current is given by

$$I_3 = \frac{-jX_{M_{23}} V_2'}{\left(R_2'' + jX_2'\right)\left(R_3 + jX_3\right) + X_{M_{23}}^2} \tag{111}$$

where:

$$X_{M_{23}} = \omega M_{23} \tag{112}$$

$$X_2' = \omega L_2' - \frac{1}{\omega C_2'} \tag{113}$$

$$X_3 = \omega L_3 - \frac{1}{\omega C_3} \tag{114}$$

When the terms of equation (111) are rationalized and grouped into the real and imaginary parts, one obtains an expression for the detector current given by

$$(115) \qquad I_3 = \frac{\left[X_2'R_3 + X_3R_2''\right] + j\left[R_2''R_3 - X_2'X_3 + X_{M_{23}}^2\right]V_2'X_{M_{23}}}{\left[X_2'R_3 + X_3R_2''\right]^2 + \left[R_2''R_3 - X_2'X_3 + X_{M_{23}}^2\right]^2}$$

The magnitude of the detector current is given by

$$(116) \qquad I_3 = \frac{V_2'X_{M_{23}}}{\left\{\left[X_2'R_3 + X_3R_2''\right]^2 + \left[R_2''R_3 - X_2'X_3 + X_{M_{23}}^2\right]^2\right\}^{1/2}}$$

or

$$(117) \qquad I_3 = \frac{V_2'X_{M_{23}}}{\left[\begin{array}{l} X_2'^2R_3^2 + X_3^2R_2''^2 + R_2''^2R_3^2 + 2R_2''X_{M_{23}}^2 \\ + X_2'^2X_3^2 - 2X_2'X_3X_{M_{23}}^2 + X_{M_{23}}^4 \end{array}\right]^{1/2}}$$

Partial resonance in the coupled circuits, as shown in Fig. 20, is obtained when any one circuit parameter is so varied as to cause maximum effective detector current, $I_3$, under conditions of applied voltage, $V_2'$.

From equation (117), it is evident that in theory, partial resonance may be obtained by adjusting any one of the five circuit parameters $\left(R_2', R_3, X_2', X_3 \text{ or } X_{M_{23}}\right)$, which appear only in the positive terms of the denominator. However, in this discussion we are concerned primarily with the values of $C_2'$ and $C_3$ $\left(\text{or } X_2' \text{ and } X_3\right)$ which will produce partial resonance.

The value of $X_2'$ or $X_3$ which will produce partial resonance may, in general, be found by differentiating the expression for $I_3$ with respect

to the proper $X$, equating $dI/dX$ equal to zero and solving for $X$ in terms of the other parameters. For example, the value of $X_2'$ which will produce partial resonance is given by

$$(118) \qquad \frac{dI_3}{dX_2'} = 0 = -V_2' X_{M_{23}} 1/2 \left[ 2X_2' \left( R_3^2 + X_3^2 \right) - 2X_3 X_{M_{23}}^2 \right]$$

Therefore,

$$(119) \qquad X_2'(res) = \frac{X_3 X_{M_{23}}^2}{R_3^2 + X_3^2} = \frac{X_3 X_{M_{23}}^2}{Z_3}$$

If one substitutes for $X_{M_{23}}$, $X_2'$ and $X_3$, the value given by equations (112), (113) and (114) respectively,

$$(120) \qquad \left( \omega L_2' - \frac{1}{\omega C_2'} \right)_{(res)} = \frac{\left( \omega L_3 - \frac{1}{\omega C_3} \right) \omega^2 M_{23}^2}{R_3^2 + \left( \omega L_3 - \frac{1}{\omega C_3} \right)^2}$$

From equation (120), the value of $C_2'$ to produce partial resonance is obtained and is given by

$$(121) \qquad C_2'(res) = \left( \omega \left[ \omega L_2' - \frac{\left( \omega L_3 - \frac{1}{\omega C_3} \right) \omega^2 M_{23}^2}{R_3^2 + \left( \omega L_3 - \frac{1}{\omega C_3} \right)^2} \right] \right)^{-1}$$

The significance of equation (121) is that for a given value of $C_3$, $C_2'$ must have the value stated to produce maximum detector current, $I_3$.

If the reactance of the detector circuit is equal to zero, by virtue of $\left[\omega L_3 - \frac{1}{\omega C_3}\right] = 0$, then $C_2'$ should be so adjusted so that the reactance of the cavity, $X_2'$, is equal to zero. Thus, the value of $C_2'$ is given by

$$C_2'\left[X_3 = 0\right] = \frac{1}{\omega^2 L_2'} \tag{122}$$

In a similar manner, it may be shown that the value of $X_3$ to produce partial resonance is given by

$$X_{3(res)} = \frac{X_2' X_{M_{23}}^2}{R_2'^2 + X_2'^2} \tag{123}$$

By substituting into equation (123) the values of $X_{M_{23}}$, $X_3$ and $X_2'$ given by equations (112), (113) and (114) respectively, one obtains the value of $C_3$ which will produce partial resonance,

$$C_{3(res)} = \frac{1}{\omega\left[\omega L_3 - \frac{\omega^2 M_{23}^2\left[\omega L_2' - \frac{1}{\omega C_2'}\right]}{R_2''^2 + \left[\omega L_2' - \frac{1}{\omega C_2'}\right]^2}\right]} \tag{124}$$

It is evident from equation (116) that if both the cavity reactance, $X_2'$ and the detector reactance $X_3$ are equal to zero, the detector current will be an optimum and will be equal to

$$I_3\left[X_3 = 0,\ X_2' = 0\right] = \frac{X_{M_{23}} V_2'}{R_2'' R_3 + X_{M_{23}}^2} = \frac{\omega M_{23} V_2'}{R_2'' R_3 + \omega^2 M_{23}^2} \tag{125}$$

The significance of equation (125) is that, if the reactance of the cavity, $X_2'$, and the reactance of the detector, $X_3$, are adjusted to equal zero, and $R_3$ and $X_{M_{23}}$ are fixed, then the detector current will be a function of the total equivalent series resistance, $R_2'$, of the cavity network.

Effect of the Detector Probe Capacitance upon Oscillometer Response. In Fig. 21 is shown the relationship between the detector probe capacitance and the oscillometer responses at 75, 80, 90 and 100 Mc/sec. The data were obtained in the manner described on page 67. Each data point on the cell capacitance and detector current curves correspond to resonance values for the given value of the detector probe capacitance.

In order to conveniently show the relationship between the cell capacitance and the detector probe capacitance at the various frequencies, the difference between the measured cell capacitance, (for a given detector probe capacitance value) and the cell capacitance corresponding to optimum detector current were plotted. For example, at 100 Mc/sec, the detector probe capacitance was arbitrarily adjusted to 39.5 picofarads and the cell capacitance $\{C_t$ and $C_v\}$ were adjusted to obtain maximum effective detector current. The cell capacitance at resonance was equal to 27.843 picofarads. This value corresponds to the minimum of the cell capacitance curve (at 100 Mc/sec) and is equal to -0.109 picofarads (27.843 - 27.942). Therefore, at any given value of the detector probe capacitance, the measured cell capacitance is the algebraic sum of the value obtained from the curve and the cell capacitance at optimum detector current. The cell capacitance at optimum detector current obtained at 75, 80, 90 and 100 Mc/sec are given in Fig. 21.

The relationship between the detector probe capacitance and the

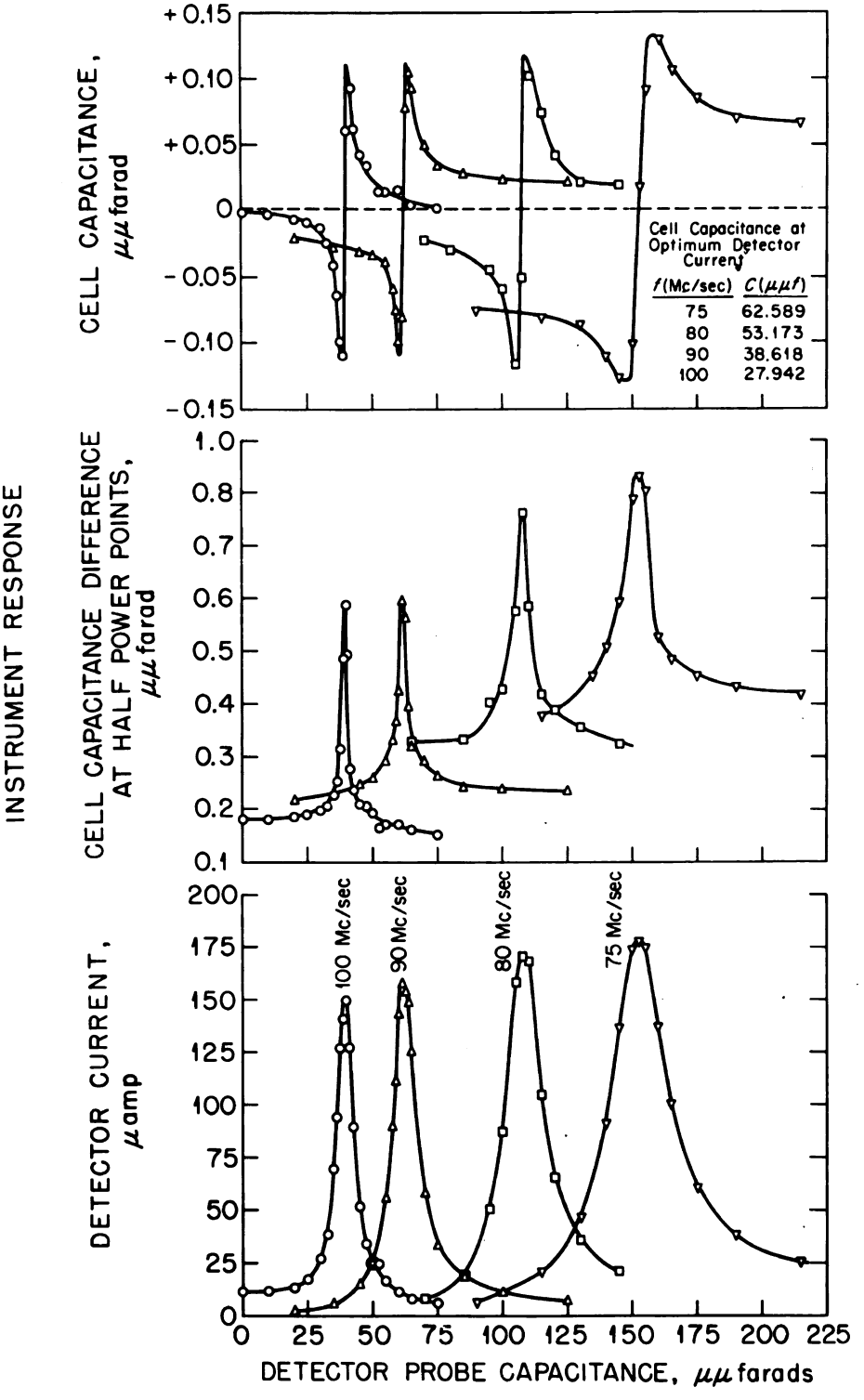


Figure 21. Effect of Detector Probe Capacitance upon Oscillometer Response

oscillometer responses shown in Fig. 21 conformed to the electrical behavior developed for the fundamental equivalent circuit shown in Fig. 16.

For a given value of the detector probe capacitance, the oscillometer is tuned to resonance by adjustment of the resonant cavity cell capacitance. Partial resonance is indicated by a maximum effective detector current (Equation (121). When the reactance of the tuned resonant cavity and the reactance of the tuned detector circuit are equal to zero, the detector current is an optimum (equation (125).

In the preceding section, it was shown that the net effect of coupling a tuned detector circuit to a resonant cavity is to couple an impedance into the resonant cavity network. The equivalent impedance, $Z_{(reflected)_{23}}$, reflected (or coupled) into the cavity by the coupled detector is given by equation (96), and consists of a resistive component given by equation (97), and an equivalent series reactive component given by equation (98). The magnitude of the equivalent resistive and reactive impedance coupled into the resonant cavity will depend not only upon the detector capacitance but also the frequency.

As previously stated on page 87, the reactive impedance reflected into the resonant cavity circuit may be either inductive or capacitive in nature and will depend upon the magnitude of the capacitive reactance term $\frac{1}{\omega C_3}$ as compared to the inductive reactance term $\omega L_3$ of the detector circuit. If $\frac{1}{\omega C_3}$ is greater than $\omega L_3$, the equivalent series reactance reflected into the cavity is inductive in nature by virtue of the negative sign of the reactance term in equation (96). In Fig. 21, the condition $\frac{1}{\omega C_3} > \omega L_3$ corresponds to the negative portion of the cell capacitance curve. If $\frac{1}{\omega C_3}$ is less than $\omega L_3$, the equivalent series

reactance reflected into the cavity will be capacitive in nature. The condition where $\frac{1}{\omega C_3} < \omega L_3$ corresponds to the positive portion of the cell capacitance curve.

When the oscillometer is initially tuned to resonance, a change in the detector capacitance will detune the cavity. If the change in detector capacitance results in an increase in the inductive reactance coupled into the cavity, the cell capacitance value necessary to reestablish resonance will be less than the initial value. If the change in detector capacitance results in an increase in the capacitance reactance coupled into the cavity, the cell capacitance value necessary to reestablish resonance will be greater than the initial value. The change in capacitive reactance of the cavity necessary to reestablish resonance is equal but opposite in sign to the change in the equivalent reactance coupled into the cavity which resulted from the change in detector capacitance.

For a given value of the detector probe capacitance, the value of the cavity capacitance that will produce maximum effective detector current is indicated by equation (121).

By use of equation (119), it is possible to show that the cell capacitance curve should exhibit a maximum and a minimum as shown in Fig. 21. The value of $X_3$ for which $X_2'_{(res)}$ is a maximum or a minimum is obtained by differentiating the expression for $X_2'_{(res)}$, equation (119). with respect to $X_3$, equating $\frac{dX_2'_{(res)}}{dX_3}$ to zero, and solving the resulting expression in terms of $X_3$. For example,

$$\frac{dX_2'_{(res)}}{dX_3} = 0 = -R_3^2 + X_3^2 \tag{126}$$

(127) $$X_3^2 = R_3^2$$

The value of $X_3$ at which $X_2'_{(res)}$ will be a minimum is

(128) $$X_{3(max)} = +R_3$$

The value of $X_3$ at which $X_2'_{(res)}$ will be a maximum is equal to

(129) $$X_{3(min)} = -R_3$$

Therefore, the minimum value of the equivalent cavity reactance is

(130) $$X_2'_{(min)_{(res)}} = -\frac{\omega^2 M_{23}^2}{2R_2}$$

The value of the cavity capacitance which will produce $X_2'_{(min)}$ is given by

(131) $$C'_{X'_{(min)_{(res)}}} = \frac{1}{\omega\left(\omega L_2' - \frac{\omega^2 M_{23}^2}{2R_2}\right)}$$

and corresponds to the maximum on the cell capacitance curve.

The maximum value of the equivalent cavity reactance is

(132) $$X_2'_{(min)_{(res)}} = +\frac{\omega^2 M_{23}^2}{2R_2}$$

The value of the cavity capacitance which will produce $X_2'_{(max)_{(res)}}$ is given by

$$(133) \qquad C'_{X_{(max)_{(res)}}} = \frac{1}{\omega\left(\omega L_2' - \frac{\omega^2 M_{23}^2}{2R}\right)}$$

and corresponds to the minimum on the cell capacitance curve.

The mid-point values between the maximum and the minimum $X_2'_{(res)}$ is given by

$$(134) \qquad X_2'_{(res)_{(mid\text{-}point)}} = 0$$

Therefore, the value of the cavity capacitance corresponding to $X_2'_{(res)_{(mid\text{-}point)}}$ is

$$(135) \qquad C_2'_{(res)_{(mid\text{-}point)}} = \frac{1}{\omega^2 L_2}$$

and is equal to the cavity capacitance at optimum current.

In Fig. 21, the mid-point value between the maximum and minimum cell capacitance corresponds to the optimum current. At optimum detector current the reactance of the tuned detector and tuned resonant cavity network are equal to zero.

The relationship between the detector current and the circuit parameters for the equivalent circuit shown in Fig. 20, is given by equation (117). To show how the detector current at resonance varies with detector probe capacitance, the value $X_2'_{(res)}$ given by equation (119) is substituted for $X_2'$ in equation (117), and the resulting expression solved for

$I_{3(res)}$ in terms of $X_3$, or

$$I_{3(res)} = \frac{X_{M_{23}} V_2'}{\left\{\left[R_2'' R_3 + X_{M_{23}}^2\right] + \frac{\left|R_2'' - X_{M_{23}}\right| \left|X_3\right|^2}{R_3^2 + X_3}\right\}^{1/2}} \tag{136}$$

Furthermore, if the term $\left|\omega L_3 - \frac{1}{\omega C_3}\right|$ is substituted for $X_3$ in the above expression, the effective detector current at resonance, the relationship between $I_{3(res)}$ and the detector capacitance, $C_3$ is given by

$$I_{3(res)} = \frac{X_{M_{23}} V_2'}{\left\{\left[R_2'' R_3 + X_{M_{23}}^2\right] + \frac{\left|R_2'' - X_{M_{23}}\right| \left|\omega L_3 - \frac{1}{\omega C_3}\right|^2}{R_3^2 + \left|\omega L_3 - \frac{1}{\omega C_3}\right|^2}\right\}^{1/2}} \tag{137}$$

As previously stated, the detector current at resonance will be an optimum when $\omega L_3 = \frac{1}{\omega C_3}$. The optimum detector current as given by equation (125) is a function not only of the frequency but also of the magnitude of the equivalent resistive impedance of the detector and cavity networks. If one assumes that the equivalent cavity resistive impedance $R_2''$, equivalent detector resistive impedance $R_3$, and the mutual inductance $M_{23}$, operate independently of one another, the optimum detector current at resonance should increase with a decrease in the frequency.

At very large values of the detector capacitance, the detector current at resonance approaches a limit given by

$$\lim_{C_3 \to \infty} I_{3(res)} = \left\{\frac{X_{M_{23}} V_2'}{\left[R_2'' R_3 + X_{M_{23}}^2\right]^2 + \frac{\left|R_2'' - X_{M_{23}}\right| \omega L_3^2}{R_3^2 + \omega^2 L_3^2}}\right\}^{1/2} \tag{138}$$

When the detector capacitance approaches very small in magnitude, $I_{3(res)}$ approaches a limit given by

$$\lim_{C_3 \to 0} I_{3(res)} = \frac{X_{M_{23}} V_2'}{\left(R_2'' R_3 + X_{M_{23}}^2\right)^2 + \left(R_2'' - X_{M_{23}}\right)^2}^{1/2} \tag{139}$$

A comparison of equations (136) and (139) indicates that the detector current response curve should not be symmetrical as shown in Fig. 21.

Also, the relationship between the capacitance difference at the half power points and the detector probe capacitance, shown in Fig. 21, is similar in nature to that predicted for the equivalent network shown in Fig. 16. The change in capacitance difference at the half power point is related to the resistive impedance reflected into the cavity by the coupled detector.

The resistive component of the equivalent impedance reflected into the cavity network by the coupled detector is given by equation (97). When the detector reactance is equal to zero, the resistive impedance reflected into the cavity by the coupled circuit will be a maximum as given by

$$R_{(reflected)_{23(max)}} = \frac{\omega^2 M_{23}^2}{R_3} \tag{140}$$

In turn, the total equivalent series resistance, $R_{2(equiv)_{(max)}}$, of the cavity-detector network, as referred to the cavity (Fig. 18) will be a maximum as given by

$$(141) \qquad R_{2(equiv)_{(max)}} = R_2' + \frac{\omega^2 M_{12}^2 R_1}{R_1^2 + \omega^2 L_1^2} + \frac{\omega^2 M_{23}^2}{R_3}$$

When the equivalent series resistance of the cavity network is a maximum, the $Q$-factor for the cavity will be a minimum and is equal to

$$(142) \qquad Q_{(min)} = \frac{\omega L_2'}{R_{2(equiv)_{(max)}}} = \frac{}{\omega C_2' R_{2(equiv)_{(max)}}}$$

Therefore, the capacitance difference at the half power points will be a maximum when the detector reactance is equal to zero, and is equal to

$$(143) \qquad \Delta C_{0.707(max)} = \frac{2C'_{(res)}}{Q_{(min)}}$$

where $C_2'_{(res)}$ is equal to the total equivalent cavity capacitance at optimum detector current.

In each curve of Fig. 21, the cell capacitance difference at the half power points is shown to increase with an increase in the detector probe capacitance, to exhibit a maximum and then to decrease there after. The maximum of the response curve corresponds exactly to the optimum detector current and to the mid-point between the maximum and minimum cell capacitance values. When the cell capacitance difference at the half power points is a maximum, the value of the detector probe capacitance corresponds to a reactance for the tuned portion of the detector circuit equal to zero.

The oscillometer response curves shown in Fig. 21 are used to determine the detector probe capacitance needed to obtain optimum detector

current at resonance for use in oscillometric titrations and dielectric constant measurements. The detector current is used not only to determine the cell capacitance at resonance but also the cell capacitance difference at the half-power points. Therefore, it is most desirable to select a detector probe capacitance which will result in maximum readability of the detector current in order to obtain precise measurement of these quantities.

In Table II are given the capacitance data which show the relationship between the resonant frequency and the values of the cell capacitance and detector probe capacitance which are necessary to obtain optimum detector current. However, as shown in Fig. 21 (cell capacitance difference at half power points), the $Q$-factor of the oscillometer is a minimum when the detector probe capacitance is selected to yield optimum detector current at resonance. When the $Q$-factor is a minimum, the oscillometer is least sensitive to changes in circuit parameter. To obtain maximum sensitivity in oscillometer response to changes in circuit parameters, one should select a detector probe capacitance value which will result in a minimum capacitance difference at half-power points (or maximum $Q$). However, in practice, this was not possible due to the lack in sensitivity of the detector measuring circuit.

Cell Capacitance Measurements - Reliability and Precision Data. In Table II are given the resonant cell capacitance data obtained at a frequency of 100 Mc/sec for different values of the main dial capacitor, $C_t$, and vernier screw capacitor, $C_v$. The data were obtained as described on page 68.

As shown in Table III, the corrected cell capacitance, $\left(C_t - C_v\right)_{(corr)}$,

Table II. Relationship Between the Resonant Frequency Cell Capacitance and Detector Probe Capacitance at Optimum Detector Current

| Frequency Mc/sec | Detector Probe Capacitance picofarads | Cell Capacitance picofarads |
|---|---|---|
| 75 | 152.5 | 62.589 |
| 80 | 108.0 | 54.663 |
| 85 | 80.5 | 45.319 |
| 90 | 62.0 | 38.618 |
| 95 | 49.0 | 32.986 |
| 100 | 39.7 | 27.942 |
| 105 | 32.5 | 23.575 |

Table III. Reliability of the Cell Capacitance Measurements: Resonant Frequency, 100 Mc/sec

| a) $C_t$ mil | b) $C_{t(calc)}$ μμf | c) $C_{t(corr)}$ μμf | d) $C_{t(meas)}$ μμf | e) $C_{v(corr)}$ μμf | f) $(C_t - C_{v(corr)})$ μμf |
|---|---|---|---|---|---|
| 25.5 | 27.706 | 28.058 | 0.125 | 0.121 | 27.937 |
| 25.0 | 28.260 | 28.618 | 0.736 | 0.680 | 27.937 |
| 24.5 | 28.837 | 29.199 | 1.343 | 1.257 | 27.942 |
| 24.0 | 29.438 | 29.806 | 1.968 | 1.862 | 27.944 |
| 23.5 | 30.064 | 30.440 | 2.635 | 2.492 | 27.948 |
| 23.0 | 30.717 | 31.198 | 3.420 | 3.237 | 27.961 |
| 22.5 | 31.400 | 31.786 | 3.954 | 3.746 | 28.040 |
| 22.0 | 32.114 | 32.506 | 4.652 | 4.411 | 28.095 |

NOTE:

a) The spacing between the plates of the main drum $C_t$ of the dielectric sample holder, mils.

b) The calculated capacitance of $C_t$; $C_t = \frac{706.5}{t}$, μμf (where $t$ equals the spacing in mils).

c) The corrected value of $C_t$ (see Fig. 15, EXPERIMENTAL).

d) The measured value of the vernier screw, $C_v$.

e) The corrected value of $C_v$, (see Table I, EXPERIMENTAL).

f) The difference between the corrected values of $C_t$ and $C_v$.

increases with increasing values of $C_t$ and $C_v$. In theory, the cell capacitance, $|C_t - C_v|$, should be constant at a given frequency and independent of the absolute magnitude of $C_t$ or $C_v$. Since $|C_t - C_v|$ is not constant, one must assume that the capacitance values, $C_{t_{(corr)}}$ and $C_{v_{(corr)}}$, are in error.

The values of $C_{t_{(corr)}}$ and $C_{v_{(corr)}}$ given in Table III corresponds to corrected values for $C_{t_{(calc)}}$ and $C_{v_{(meas)}}$. The corrections applied to the experimentally derived capacitance values, $C_{t_{(calc)}}$ and $C_{v_{(meas)}}$ were obtained from the calibration data supplied by the manufacturer of the dielectric sample holder (Table I and Fig. 15). As stated on page 56, the calibration data were obtained at 1000 cycles per second rather than at 100 Mc/sec. The calibration data correct for nonparallelism of the main dial electrodes, and stray capacitance associated with the main dial capacitor, $C_t$, and vernier screw capacitor, $C_v$.[59,60] As evident from the data given in Table III, the calibration data obtained at 1000 cycles per second is not applicable to capacitance measurements at 100 Mc/sec.

It is interesting to note that if one employs the uncorrected values, $C_{t_{(calc)}}$ and $C_{v_{(meas)}}$ to evaluate $|C_t - C_v|$, a smaller difference is observed between the extremes of the cell capacitance $|C_{t_{(calc)}} - C_{v_{(meas)}}|$ as compared to $|C_t - C_v|_{(corr)}$. The difference in the extreme values of $|C_{t_{(calc)}} - C_{v_{(meas)}}|$ is equal to 0.119 picofarads as compared to 0.158 picofarads for the extreme values of $|C_t - C_v|_{corr}$.

In Table IV are given the data for the resonance cell capacitance measurements at a frequency of 120 Mc/sec.

A comparison of the data in Table III and IV shows that at 120 Mc/sec

Table IV. Reliability of the Cell Capacitance Measurements: Resonant Frequency, 120 Mc/sec

| $C_t$ | $C_{t\,(calc)}$ | $C_{t\,(corr)}$ | $C_{v\,meas}$ | $C_{v\,(corr)}$ | $(C_t - C_v)_{(corr)}$ |
|---|---|---|---|---|---|
| 68.5 | 10.314 | 10.422 | 0.000 | 0.000 | 10.422 |
| 68.0 | 10.390 | 10.499 | 0.068 | 0.061 | 10.431 |
| 66.5 | 10.467 | 10.579 | 0.155 | 0.138 | 10.441 |
| 67.0 | 10.545 | 10.659 | 0.246 | 0.219 | 10.440 |
| 66.5 | 10.624 | 10.740 | 0.328 | 0.295 | 10.445 |
| 66.0 | 10.704 | 10.822 | 0.391 | 0.355 | 10.467 |
| 65.5 | 10.786 | 10.906 | 0.467 | 0.435 | 10.471 |
| 65.0 | 10.869 | 10.991 | 0.540 | 0.501 | 10.490 |
| 64.0 | 11.039 | 11.165 | 0.728 | 0.669 | 10.496 |
| 63.0 | 11.214 | 11.345 | 0.895 | 0.831 | 10.514 |
| 62.0 | 11.395 | 11.531 | 1.070 | 1.006 | 10.525 |
| 60.0 | 11.775 | 11.921 | 1.473 | 1.385 | 10.536 |
| 57.0 | 12.395 | 12.556 | 2.101 | 1.993 | 10.563 |
| 53.0 | 13.330 | 13.512 | 3.082 | 2.922 | 10.590 |
| 48.0 | 14.719 | 14.945 | 4.510 | 4.281 | 10.664 |

the difference between the extreme values of $\left(C_t - C_v\right)_{(corr)}$ is equal to 0.442 picofarads, whereas, at 100 Mc/sec, the difference is equal to 0.158 picofarads. At 120 Mc/sec, the extreme values of $\left(C_t - C_v\right)_{(corr)}$ corresponds to a difference in electrode spacing of $C_t$, equal to 29.5 mils. At 100 Mc/sec, the difference in the electrode separation, which corresponds to the extreme value of $\left(C_t - C_v\right)_{(corr)}$, is equal to 2.5 mils.

One may assume that since the two frequencies are of the same order of magnitude and the range in resonance values of $C_v$, employed at 100 and 120 Mc/sec is the same, the error in the cell capacitance measurements is primarily associated with the main dial capacitor $C_t$. In all probability, the magnitude of the error will depend upon the separation of the electrodes of $C_t$. A comparison of the extreme values of $\left(C_t - C_v\right)_{(corr)}$ observed at 120 and 100 Mc/sec show that the difference in extreme values of $\left(C_t - C_v\right)_{(corr)}$ increase with an increase in the separation of the electrodes of the main dial capacitor.

No attempt was made to calibrate the main dial capacitor, $C_t$, or the vernier screw capacitor, $C_v$, in this investigation. All cell capacitance values were corrected using the calibration data supplied by the manufacturer of the dielectric sample holder. The corrected cell capacitance values were employed in the cell parameter, dielectric constant, response curve and titration measurements.

In a test to establish the reproducibility in positioning the empty vessel in the cell assembly from twenty measurements, the mean value for $\left(C_t - C_v\right)_s$ was 27.942 ± 0.0004 picofarads. The necessary data for the test were obtained as described on page 68.

Evaluation of Cell Parameters, $C_g$ and $C_o$. In Table V are given the values of the cell parameters, $C_g$ and $C_o$, which were determined at 5 Mc/sec frequency intervals between 75 and 105 Mc/sec. The method suggested by Reilly and McCurdy[13,24] was used to derive the cell parameters $C_g$, the capacitance due to the walls of the borosilicate vessel, and $C_o$, the capacitance contribution of the annular sample space of the vessel containing only air. This method is described on page 69.

As shown in Table V, the values obtained for $C_g$ and $C_o$ vary with the resonant frequency and are not constant as one would expect. The difference in the values of $C_g$ and $C_o$ are due to the erroneous cell capacitance values of $\Delta C_{Hg}$, $\Delta C_a$, and $\Delta C_5$ (benzene) used in the calculations (refer to equations (66) and (67). Since, for any of the given frequencies, the magnitudes of the errors associated with the individual values of $C_t$ and $C_v$ were not known, it was not possible to determine the effect of the errors in the calculations of $C_g$ and $C_o$.

Effect of Solution Parameters and Resonant Frequency upon the Oscillometer Response. When the oscillometer is initially tuned to resonance, a change in solution parameters, (conductivity or dielectric constant) or a change in the resonant frequency will result in a change in the oscillometer response at resonance. The change in oscillometer response can be interpreted most conveniently in terms of the net change in electrical properties of the cell-solution network as discussed on page 71.

An increase in the parallel equivalent conductance of the cell-solution network will result in a corresponding increase in the total equivalent conductance of the oscillometer as measured by the cell capacitance difference at half power points $\left(\Delta C_{0.707}\right)$ and given by equation

Table V. Evaluation of Cell Parameters $C_g$ and $C_o$

| Frequency | $C_g$ [a] | $C_o$ |
|---|---|---|
| | picofarads | picofarads |
| 75 | 20.72 | 3.224 |
| 80 | 21.33 | 3.118 |
| 85 | 21.78 | 2.966 |
| 90 | 22.51 | 3.017 |
| 95 | 23.25 | 3.144 |
| 100 | 24.02 | 3.182 |
| 105 | 24.74 | 3.157 |

a) Average of three determinations.

(A-28). The increase in the total equivalent conductance of the oscillometer $\left(G_t = \frac{\omega L C_{0.707}}{2}\right)$ is exactly equal to the change in the equivalent conductance of the cell-solution network (equation (49).

The change in cell capacitance at resonance which occurs with a change in solution parameters will be exactly equal to but opposite in sign to the change in the equivalent capacitance, $C_p$, of the cell-solution network (equation (50).

The relationship between the detector current at resonance and the solution parameters is somewhat complex in nature. However, it can be shown than an increase in the equivalent parallel conductance, $G_p$, of the cell-solution network will result in an increase in the equivalent series resistance of the cavity network as given by equation (70). In turn, an increase in the equivalent series resistance of the cavity circuit will result in a decrease in the detector current as given by equation (117).

In the discussion which follows, the effect of solution parameters and resonant frequency upon oscillometer response are interpreted in terms of the parallel equivalent conductance $(G_p)$ and the parallel equivalent capacitance $(C_p)$ of the admittance of the cell-solution equivalent circuit shown in Fig. 7B.

Throughout the discussion which follows, the capacitance difference at half power points, $\Delta C_{0.707}$, will be used synonomously with the high frequency conductance term, $G_p$. Where appropriate, the conversion from $\Delta C_{0.707}$ to $G_p$ will be made.

Effect of Solution Conductivity upon Oscillometer Response. In Fig. 22 is shown the relationship between the solution low frequency specific conductance, $K_c$, and the oscillometer responses, for solutions of 1-1, 2-1 and 3-1 electrolytes at a resonant frequency of 100 Mc/sec

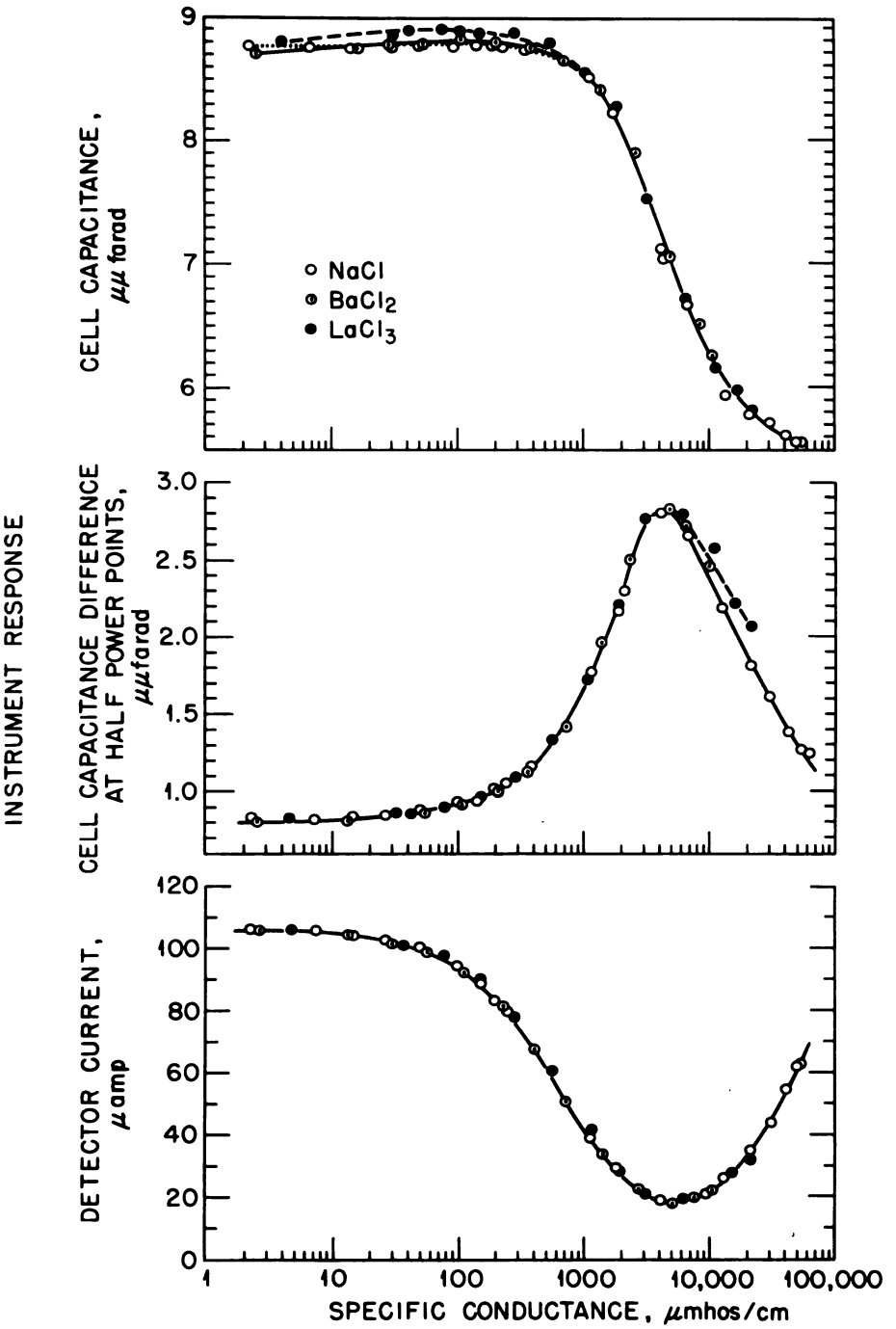


Figure 22. Oscillometer Responses versus Low Frequency Conductivity of Aqueous Solutions of 1-1, 2-1, and 3-1 Electrolytes (Freq. : 100 Mc/sec)

and 25°. As shown in Fig. 22, for an aqueous system the instrument response is independent of the nature of the electrolyte and dependent upon the solution conductivity. A general interpretation of the oscillometer responses is based upon equation (47 ) which relates the electrical properties of the cell solution network, as shown in Fig. 8, to the solution conductivity. The observed changes in oscillometer response are directly attributed to changes in electrical behavior of the cell-solution network.

As predicted by equation (49), the equivalent high frequency conductance, $G_p$, of the cell-solution network approaches zero at very small and large values of the solution conductivity, $K$. At a value of the solution conductivity, $K_{(peak)}$, given by equation (52), the equivalent high frequency conductance is a maximum, $G_{p_{(max)}}$, as given by equation (53). A change in $G_p$ will result in a proportional change in the total equivalent conductance of the oscillometer, $G_t$, as given by equation (A-29). Since the cell capacitance difference at half power is directly proportional to the total equivalent conductance of the oscillometer (equation (29), a change in $G_p$ will result in a proportional change in $\Delta C_{0.707}$.

The maximum change in $\Delta C_{0.707}$ is related to the equivalent parallel conductance of the oscillometer and is given by

$$(144) \qquad G_{p_{(max)}} = \frac{\omega\left|\Delta C_{0.707(max)} - \Delta C_{0.707(min)}\right|}{2} = \frac{\omega \Delta C_{(max)}}{2}$$

where $\Delta C_{(max)}$ is equal to the difference between the minimum value, $\Delta C_{0.707(min)}$, where $K_c$ is equal to zero and the maximum value, and

$\Delta C_{0.707(max)}$ which corresponds to $K_{o(peak)}$.

As would be expected, a change in the total equivalent conductance of the oscillometer results in a change in the detector current, $I$, at resonance. As shown in Fig. 22, the detector current decreases with an increase in solution conductivity, reaches a minimum, and then increases thereafter with increasing solution conductivity. The value of the solution conductivity, $K_{o\ min}$, where $I$ is a minimum, corresponds exactly to $K_{(peak)}$ for the $\Delta C_{0.707}$ response curve.

Theory predicts that the equivalent parallel capacitance, $C_p$, of the cell-solution network should remain essentially constant at very small values of $K$, then increase with increasing $K$ and finally reach a limiting value at very large value of $K$ (refer to Fig. 8). The difference between the extreme values of $C_p$ is equal to $\Delta C_p$ and is given by equation (56).

As previously stated, a change in solution parameters (conductivity or dielectric constant) will detune the oscillometer from resonance. The change in cell capacitance necessary to reestablish resonance will be exactly equal, but opposite in sign to the change in $C_p$. Therefore, an increase in $C_p$ as shown in Fig. 8 (for an increase in $K$) will result in a decrease in the oscillometer cell capacitance as shown in Fig. 22. At very large values of the solution conductivity, $C_p$ should approach a maximum limiting value as given by equation (55). Therefore, the cell capacitance should approach a minimum limiting value at large values of the solution conductivity.

In Fig. 22, the cell capacitance response curve has not reached a limiting value at the highest solution conductivity tested but appears

to approach it. Specific conductivity data beyond approximately 50,000 micromhos $-cm^{-1}$ could not be obtained with any degree of certainty with the conductivity bridge employed.

A comparison of the observed oscillometer response to that predicted by theory can be accomplished most conveniently by use of the data given in Table VI.

The experimental value for $\Delta C_{0.707\ (max)}$, $K_{c\ (peak)}$, $\Delta C_p$, $K_{c\ (mid\text{-}point)}$, $I_{(min)}$ and $K_{c\ (min)}$ were obtained from the response data given in Fig. 22. The experimental values for $K_{(peak)}$, $K_{(mid\text{-}point)}$ and $K_{(min)}$ were calculated by use of the expression

$$K = K_c \cdot a/l \tag{145}$$

where $K$ is equal to the solution conductance (mhos); $K_c$ is equal to the specific solution conductance; $a/l$ is equal to the effective cell constant of the condenser-type cell (cm); $a$ is equal to the effective area of the smaller of the two electrodes ($cm^2$) and $l$ is the effective distance between the electrodes (cm).

The cell constant, $a/l$ was evaluated for the condenser-type cell by use of the expression[61]

$$C = \frac{\varepsilon}{4\pi} \cdot \frac{a}{l} \tag{146}$$

or

$$C = 0.0885\,\varepsilon \cdot \frac{a}{l} \tag{147}$$

Table VI. Oscillometer Response Data for Aqueous Solutions of NaCl at 100 Mc/sec

| Response Measured | Quantity | Experimental | *Theoretical |
|---|---|---|---|
| Cap. Diff. at Half Power Points | $\Delta C_{0.707(max)}$, picofarads | 2.02 | 2.11 |
| | $G_{p(max)}$, micromhos | 635 | 662 |
| | $K_{o(peak)}$, micromhos $-cm^{-1}$ | 1,450 | 4,780 |
| | $K_{(peak)}$, micromhos | 52,100 | 172,000 |
| Cell Cap. | $\Delta C_p$, picofarads | >3 | 2.11 |
| | $K_{o(mid-point)}$, micromhos $-cm^{-1}$ | 1,450 | 4,780 |
| | $K_{(mid-point)}$, micromhos | 52,100 | 172,000 |
| Detector Current | $I_{(min)}$, microamp | 17.0 | ----- |
| | $K_{o(min)}$, micromhos $-cm^{-1}$ | 1,500 | 4,780 |
| | $K_{(min)}$, micromhos | 53,900 | 172,000 |

*Values used in calculations

$C_g$ = 24.02 picofarads (Table V)

$C_o$ = 3.182 picofarads (Table V)

$\varepsilon_{H_2O}$ = 78.54 (25°C.)

where $C$ is equal to the effective capacitance of the cell and $\varepsilon$ is equal to the dielectric constant of the medium contained in the cell. When the cell contains air, the effective capacitance of the cell is given by

$$C_o = 0.0885 \frac{a}{l} \tag{148}$$

where $C_o$ is equal to the capacitance due to the sample space of the vessel and is therefore equal to the experimental cell parameter, $C_o$, given in Table V. The effective cell constant based upon the experimental value for $C_o$ and equation (145) is equal to 36.0 cm.

As indicated in Table VI, the experimental values of the cell parameters $C_o$ and $C_g$ were used in the calculations for the theoretical data. The theoretical value for $I_{(min)}$ could not be evaluated due to the fact that the resistive and reactive impedances of the complex oscillometer network necessary to evaluate $I_{(min)}$ were not known.

As predicted by theory, the experimental values for $K_{o_{(peak)}}$, $K_{o_{(mid\text{-}point)}}$, and $K_{o_{(min)}}$ are approximately equal to each other. However, there is a significant difference between the experimental conductivity values for $K_{o_{(peak)}}$, $K_{o_{(mid\text{-}point)}}$ and $K_{o_{(min)}}$, and the corresponding theoretical values. The difference may be due, in part or in whole, to the erroneous experimental values of $C_g$ and $C_c$ (Table III) used in the calculations of the theoretical values of $K_{o_{(peak)}}$ and $K_{o_{(mid\text{-}point)}}$.

The experimental value calculated for $G_{p_{(max)}}$ is in good agreement with the theoretical value. The agreement in the data can be explained on the basis of the measurements involved in the calculation. For the

measurement of $\Delta C_{0.707}$, the main dial capacitor, $C_t$, was fixed, and the precision vernier screw capacitor, $C_v$, was varied. Since $\Delta C_{0.707}$ is the difference between two $C_v$ values, the error associated with the individual $C_v$ measurements are partially cancelled when the difference is taken. As a consequence, the absolute error in the value of $\Delta C_{0.707}$ will be less than the absolute error of either of the two $C_v$ values.

As shown in Table VI, the experimental value of $\Delta C_p$ is approximately 1.5 times greater than the theoretical value. The discrepancy between the experimental and theoretical values is probably due, in part or whole, to erroneous values of $C_g$ and $C_o$ used in the calculations of the theoretical value for $\Delta C_p$, and to the errors in the cell capacitance measurements.

It is interesting to note that if the experimental value of $G_{p\,(max)}$ is employed to calculate $\Delta C_p$ (refer to equation (60), one obtains a value for $\Delta C_p$ equal to 2.02 picofarads which is in good agreement with theory. This agreement would further indicate that the error involved in the cell capacitance is primarily due to error involved in the measurement of $C_t$.

Effect of Solvent Dielectric Constant upon the Oscillometer Response. In Fig. 23 is shown the relationship between the oscillometer response and the solution specific conductance for aqueous and methanolic solutions of sodium chloride. The response data for the aqueous solutions of sodium chloride are the same data as shown in Fig. 22 and was included in Fig. 23 for comparative purposes.

Due to difficulties encountered in balancing the conductivity bridge circuit at conductivity values greater than 12,000 micromhos $-cm^{-1}$ for the methanolic solutions, sufficient response data was not obtained to

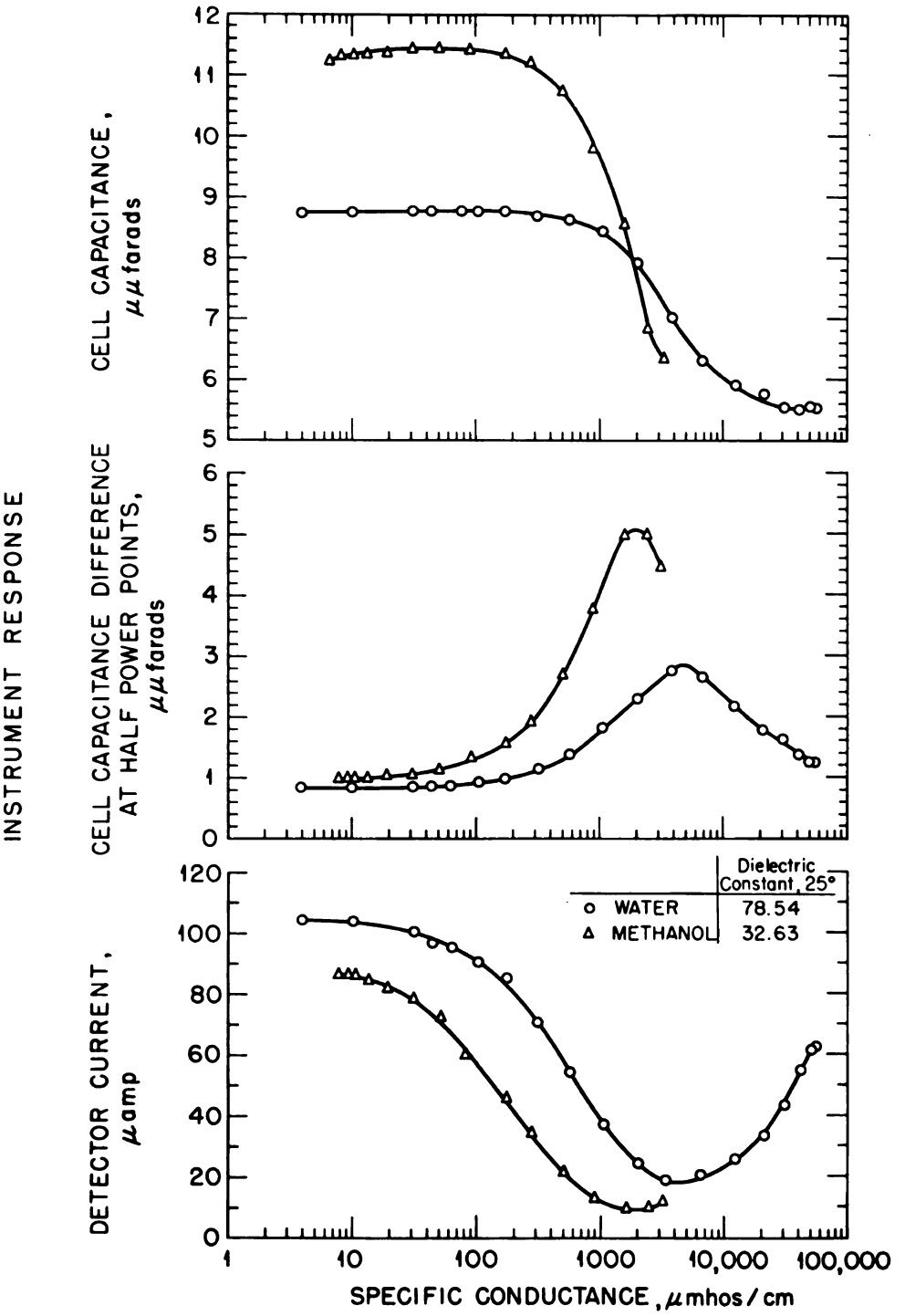


Figure 23. Effect of Solvent Dielectric Constant upon Oscillometer Response: Instrument Response versus Low Frequency Conductivity of Aqueous and Methanolic Solutions of Sodium Chloride (Freq. : 100 Mc/sec)

completely define the response curves. However, the cell capacitance difference at half power points response curve exhibits a maximum, the detector current response curves, exhibits minimum and the cell capacitance response curves appears to approach a limiting value at large conductivity values.

As predicted by theory, and shown in Fig 23, a decrease in the dielectric constant of the solution results in an increase in $\Delta C_p$, as indicated by the cell capacitance response, and an increase in $G_{p_{(max)}}$, as indicated by the cell capacitance difference at half power points response. Due to the increase in $G_p$ with increasing solution dielectric constant, a decrease in the oscillometer $Q$-factor is observed and is indicated by the detector current response.

In Table VII are given the experimental and theoretical oscillometer response data for methanolic solutions of sodium chloride at a resonant frequency of 100 Mc/sec. The agreement between the experimental and theoretical response data for methanol is comparable to the agreement observed for the aqueous response data given in Table V. With the exception of $\Delta C_{0.707(max)}$ or $G_{p_{(max)}}$, the agreement between the experimental and theoretical data is not exceptionally good. As stated previously, the lack of agreement is due, in part or whole, to the use of erroneous values for $C_g$ and $C_o$ in the calculations of the theoretical quantities and to errors in the cell capacitance measurements.

In Table VIII, comparisons of the experimental and the theoretical response data for methanol and water are given. The experimental data necessary to evaluate the various quantities are given in Tables VI and VII. The theoretical data were evaluated by means of the expression indicated.

Table VII. Oscillometer Response Data for Methanolic Solutions of NaCl at a Resonant Frequency of 100 Mc/sec

| Response Measured | Quantity Measured for Methanol | Experimental | * Theoretical |
|---|---|---|---|
| Cell Cap. Diff. at Half power point | $\Delta C_{0.707(max)}$, picofarads | 4.10 | 4.49 |
| | $G_{p(max)}$, micromhos | 1,290 | 1,420 |
| | $K_{O(peak)}$, micromhos $-cm^{-1}$ | 1,100 | 2,230 |
| | $K_{(peak)}$, micromhos | 39,500 | 80,300 |
| Cell Cap. | $\Delta C_p$, picofarads | 5.5 | 4.51 |
| | $K_{O(mid\text{-}point)}$, micromhos $-cm^{-1}$ | ~1,000 | 2,230 |
| | $K_{(mid\text{-}point)}$, micromhos | ≈36,000 | 80,300 |
| Detector Current | $I_{(min)}$, microamps | 9.0 | |
| | $K_{O(peak)}$, micromhos $-cm^{-1}$ | 1,100 | 2,230 |
| | $K_{(peak)}$, micromhos $-cm^{-1}$ | 39,500 | 80,300 |

*Values used in calculations.

$C_g$ = 24.02 picofarads (Table V)

$C_o$ = 3.182 picofarads (Table V)

$\varepsilon_{methanol}$ = 32.63 (25°C.)

Table VIII. Effect of Dielectric Constant on the Oscillometer Response (Solvents: Methanol and Water - Solute: NaCl Frequency: 100 Mc/sec)

| Ratio | *Theoretical | | Experimental |
|---|---|---|---|
| $\frac{K_{(peak)_{methanol}}}{K_{(peak)_{water}}}$ | $\frac{C_g + C_o\varepsilon_{methanol}}{C_g + C_o\varepsilon_{water}}$ | 0.467 | 0.733 |
| $\frac{G_{p_{(max)_{methanol}}}}{G_{p_{(max)_{water}}}}$ | $\frac{C_g + C_o\varepsilon_{water}}{C_g + C_o\varepsilon_{methanol}}$ | 2.14 | 2.03 |
| $\frac{\Delta C_{p_{methanol}}}{\Delta C_{p_{water}}}$ | $\frac{C_g + C_o\varepsilon_{water}}{C_g + C_o\varepsilon_{methanol}}$ | 2.14 | ≈1.8 |

*Values used in calculations.

$C_g$ = 24.02 picofarads (Table III)

$C_o$ = 3.182 picofarads (Table III)

$\varepsilon_{water}$ = 78.54 (25°C)

$\varepsilon_{methanol}$ = 32.63 (25°C)

As one would expect, the experimentally observed ratios of $G_{p_{(max)methanol}}$ to $G_{p_{(max)water}}$ and $\Delta C_{p_{methanol}}$ to $\Delta C_{p_{water}}$, are greater than unity, and the ratio of $K_{(peak)_{methanol}}$ to $K_{(peak)_{water}}$ is less than unity,

The surprisingly good agreement between the theoretical value calculated for the ratio of $G_{p_{(max)methanol}}$ to $G_{p_{(max)water}}$ and the value experimentally derived is fortuitous. The poor agreement between the theoretical and experimental value for $\frac{K_{(peak)methanol}}{K_{(peak)water}}$ and $\frac{\Delta C_{p_{methanol}}}{\Delta C_{p_{water}}}$ are thought to be due to errors associated primarily with the capacitance measurement of the main dial capacitor, $C_t$.

Effect of Resonant Frequency upon the Oscillometer Response. In Fig. 24 is shown the relationship between the instrument response at 75 and 100 Mc/sec and the solution low frequency conductance for aqueous solutions of electrolytes. The response data at 100 Mc/sec are the same data as shown in Fig. 22.

As predicted by theory, a decrease in the resonant frequency results in a decrease in $K_{(peak)}$ and $G_{p_{(max)}}$. The effect of frequency upon these parameters is clearly indicated by the cell capacitance difference at half power point response curves. For any given solution specific conductance, the equivalent parallel conductance of the cell-solution network, equal to $\frac{\omega \Delta C}{2}$ will be smaller at 75 Mc/sec than at 100 Mc/sec.

A decrease in $G_p$ with decreasing frequency is also indicated by the increase in the detector current response. The minimum of the detector current response curves at 75 and 100 Mc/sec correspond exactly to the

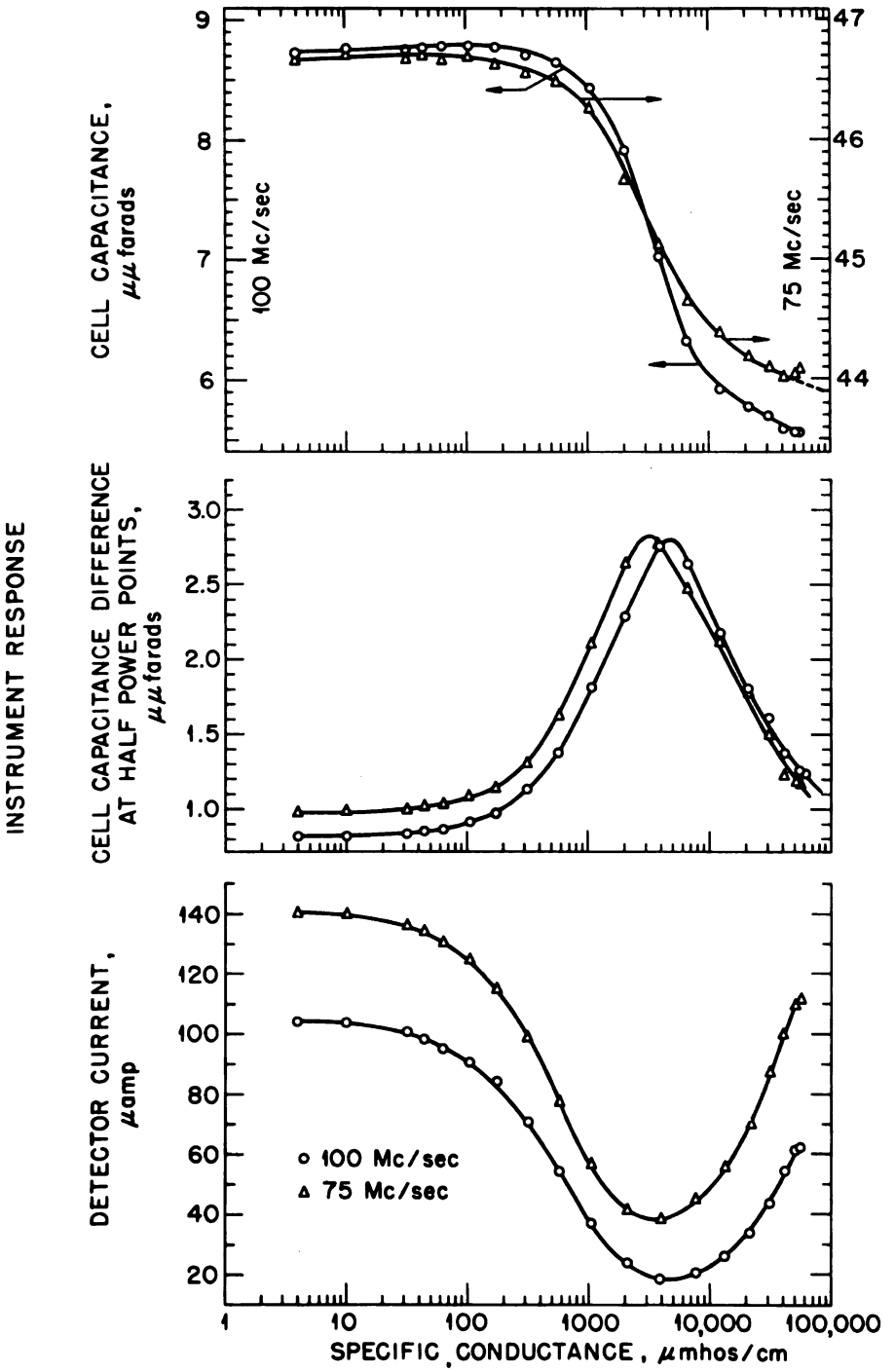


Figure 24. Effect of Resonant Frequency upon Oscillometer Response versus Low Frequency Conductivity of Aqueous Solutions of Sodium Chloride at 75 and 100 Mc/sec

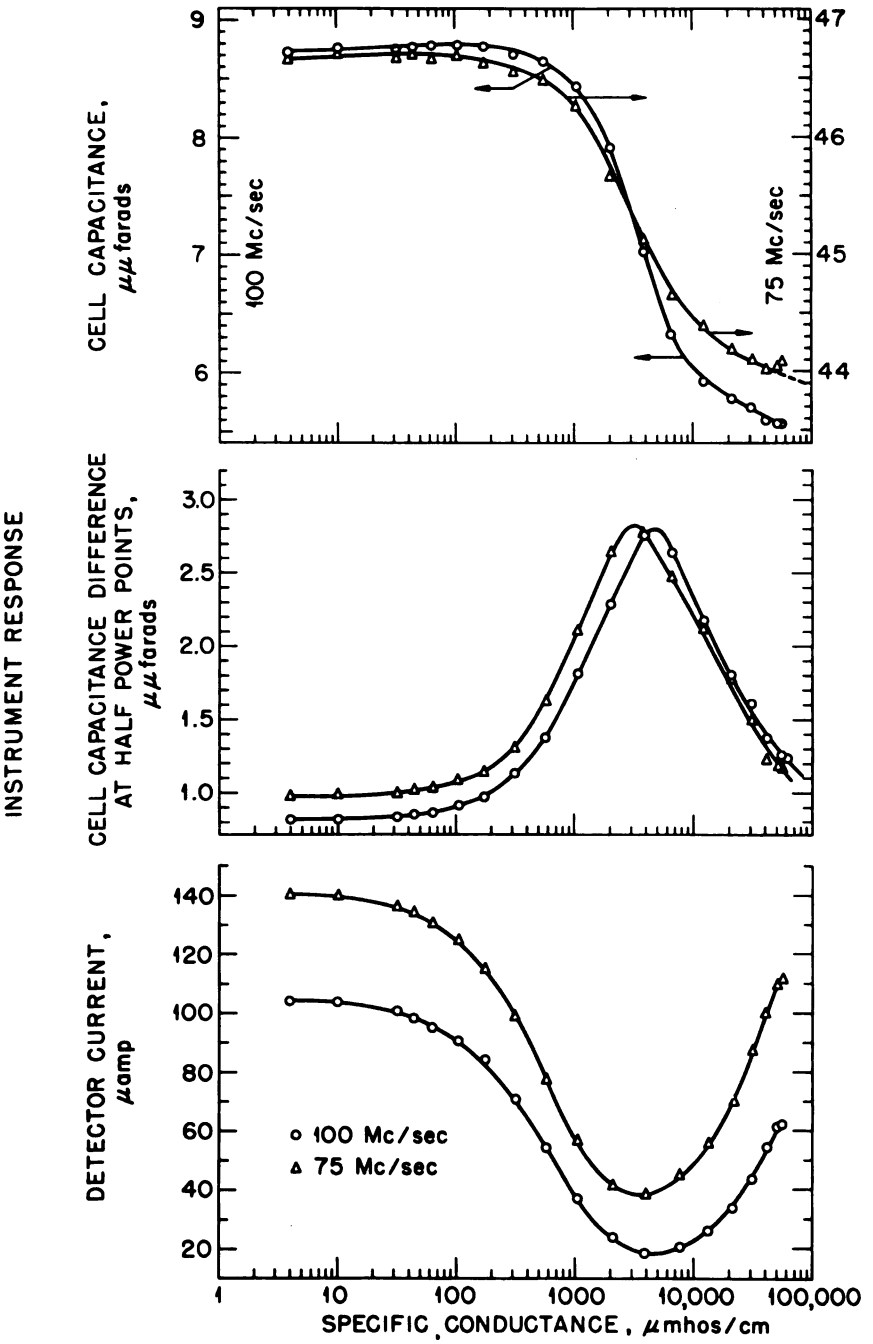


Figure 24. Effect of Resonant Frequency upon Oscillometer Response versus Low Frequency Conductivity of Aqueous Solutions of Sodium Chloride at 75 and 100 Mc/sec

maximum of the reflective cell capacitance difference at half-power point response curves.

As shown in Fig. 24, the cell capacitance curves at 75 and 100 Mc/sec have not reached limiting values at the highest conductivity solution conductivity tested but appear to approach them. As a result, it is not possible to evaluate the effect of frequency upon $\Delta C_p$. However, it can be shown that at 75 and 100 Mc, the difference in cell capacitance between the limiting value at small values of solution conductance and the cell capacitance corresponding to maxima of the $\Delta C_{0.707}$ response curves (or $K_{(peak)}$) are equal. One may assume, therefore, that $\Delta C_p$ would be independent of the resonant frequency as indicated by equation (56).

In Table IX are given the experimental and theoretical oscillometer response data for a resonant frequency of 75 Mc/sec. The experimental data necessary to evaluate $G_{p_{(max)}}$ and $\Delta C_p$ were obtained from the response curves shown in Fig. 24. The experimentally derived values of $C_g$ and $C_o$ given in Table V were employed in the calculations of the theoretical data.

In all cases, the agreement between the experimental and theoretical data is not exceptionally good. The large differences observed between the experimental and theoretical data is due, in fact or whole, to the erroneous values of $C_g$ and $C_o$ employed in the evaluation of the theoretical data and the errors associated with the cell capacitance measurements.

A comparison of the experimental and theoretical response data for resonant frequencies of 75 and 100 Mc/sec is given in Table X. The experimental data necessary to evaluate the various ratio are given in

Table IX. Oscillometer Response Data for Aqueous Solutions of NaCl at a Resonant Frequency of 75 Mc/sec

| Response Measured | Quantity Measured or Evaluated | Experimental | *Theoretical |
|---|---|---|---|
| Cap. Diff. at Half Power Points | $\Delta C_{0.707}$, picofarads | 1.85 | 1.57 |
| | $G_{p(max)}$, micromhos | 436 | 369 |
| | $K_{o(peak)}$, micromhos $-cm^{-1}$ | 1,200 | 3,540 |
| | $K_{(peak)}$, micromhos | 43,700 | 129,000 |
| Cell Cap | $\Delta C_p$, picofarads | 2.7 | 1.57 |
| | $K_{o(mid\text{-}point)}$, micromhos $-cm^{-1}$ | 1,200 | 3.540 |
| | $K_{(mid\text{-}point)}$, micromhos | 43,700 | 129,000 |
| Detector Current | $I_{(min)}$, microamps | 38 | ---- |
| | $K_{o(peak)}$, micromhos $-cm^{-1}$ | 1,250 | 3,540 |
| | $K_{(peak)}$, micromhos | 45,500 | 129,000 |

*Values used in calculations.

$C_g$ = 20.72 picofarads (Table V)

$C_o$ = 3.224 picofarads (Table V)

$\varepsilon_{H_2O}$ = 78.54 (25°C.)

Table X. Effect of Resonant Frequency on Oscillometer Response

(Solvent: Water - Solute: NaCl - Frequencies: 75 and 100 Mc/sec)

| Ratio | a) Theoretical | | b) Experimental |
|---|---|---|---|
| $\frac{K_{(peak)_{(75)}}}{K_{(peak)_{(100)}}}$ | 0.75 | 0.75 | 0.84 |
| $\frac{G_{p_{(max)_{(75)}}}}{G_{p_{(max)_{(100)}}}}$ | 0.75 | 0.56 | 0.69 |
| $\frac{\Delta C_{p_{(75)}}}{\Delta C_{p_{(100)}}}$ | 1.00 | 0.74 | 1.2 |

a) Values of $C_o$, $C_g$, and $\varepsilon_{H_2O}$ assumed to be constant and independent of frequency.

b) Experimental values of $C_g$ and $C_o$ (Table III) used in theoretical calculations. The dielectric constant of water assumed to be independent of frequency, equal to 78.54 at 25°C.

Table VII and IX.

Under the columns labeled "Theoretical", two values are given for each of the ratios evaluated. In column (a), the ratios were evaluated on the basis of $C_o$ and $C_g$ being constant and independent of the frequency. In column (b), the ratios were evaluated on the basis of the values of $C_g$ and $C_o$ experimentally derived at 75 and 100 Mc/sec and given in Table III. A comparison of column (a) to column (b) values of $\frac{G_{p(max)75}}{G_{p(max)100}}$ and $\frac{\Delta C_{p_{75}}}{\Delta C_{p_{100}}}$ indicate that the experimental values of $C_g$ and $C_o$ evaluated at 75 and 100 Mc/sec are in error. It is furtuitous that the column (a) and column (b) values for $\frac{K_{(peak)75}}{K_{(peak)100}}$ are equal.

The agreement between the experimental and theoretical quantities given in Table X is poor and is due to errors in the cell capacitance measurements used to evaluate the experimental quantities.

Oscillometer Response Curves for Perchloric Acid, Sodium Acetate and p-Nitroaniline in Glacial Acetic Acid. In Fig. 25 is shown the relationship between the oscillometer response obtained at 100 Mc/sec and the low frequency specific conductance of perchloric acid, sodium acetate and p-nitroaniline in glacial acetic acid at 25°. The data were obtained as described on page 71.

Only in the case of perchloric acid was sufficient data obtained to clearly define the shapes of the response curve and permit a comparison to the predicted response (Fig. 8). Due to the limiting conductivity of p-nitroaniline and sodium acetate in glacial acetic acid[63], specific conductivity data beyond 1 micromho $-cm^{-1}$ and 100 micromhos $-cm^{-1}$, respectively, could not be obtained. The largest conductivity values indicated in Fig. 25 for p-nitroaniline and sodium acetate correspond to

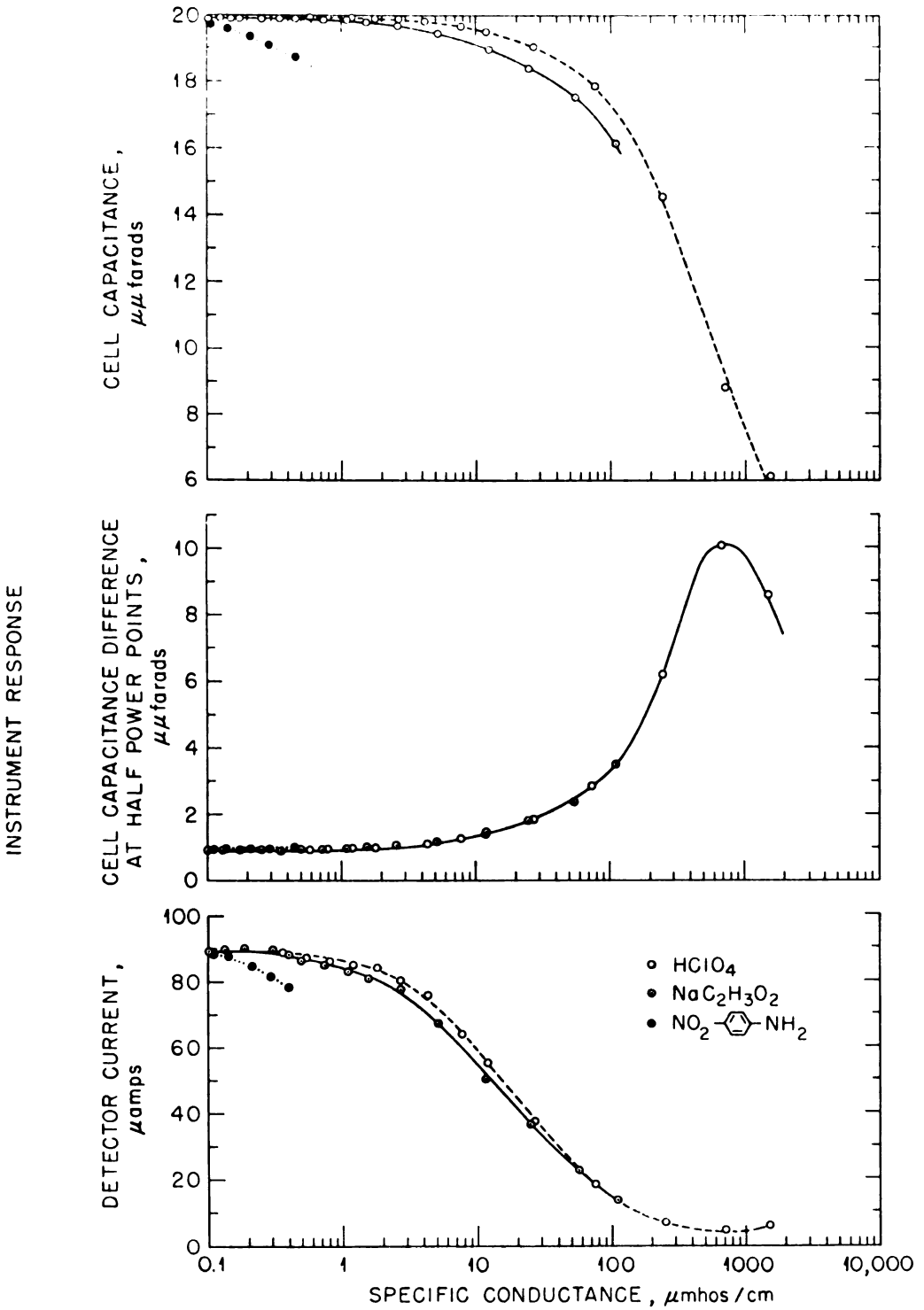


Figure 25. Oscillometer Response versus Low Frequency Specific Conductivity of Glacial Acetic Acid Solutions of Perchloric Acid, Sodium Acetate, and p-Nitroaniline (Freq. : 100 Mc/sec)

saturated solutions.

In general, it can be said that with an increase in solution conductance, the decrease in cell capacitance and detector current is greatest for p-nitroaniline and least for perchloric acid. Also, with an increase in solution conductance, the increase in the cell capacitance difference at half power points is greatest for p-nitroaniline and least for perchloric acid. The relatively small differences observed between the cell capacitance difference at half power point response curves for three solutes are not readily apparent as shown in Fig. 25.

As expected, the general shapes of the response curves for perchloric acid in glacial acetic acid are comparable to the response curves obtained for aqueous solutions of electrolytes. However, due to the low dielectric constant of glacial acetic acid, equal to approximately 6 as compared to 80 for water, $K_{(peak)}$ observed for the glacial acetic acid solution is less than $K_{(peak)}$ observed for the aqueous solutions. Also, $\Delta C_p$ and $G_{p(max)}$ is greater for the glacial acetic solution as compared to the respective values for water.

The difference between the various response curves for p-nitroaniline, sodium acetate and perchloric acid is readily apparent even though sufficient data were not obtained to clearly define the curves. The differences observed in response for these solutes is probably due to ion-pair formation and dipole interaction[63].

## APPLICATION

To test the performance of the oscillometer, a simulated aqueous titration of sodium hydroxide with hydrochloric acid and a nonaqueous (glacial acetic acid) titration of sodium acetate with perchloric acid were performed and the dielectric constants of some pure solvents were evaluated at a resonant frequency of 100 Mc/sec and 25°C.

In the oscillometric titration method, it is common practice to first obtain oscillometer response curves for the titration system to be studied, which show the relationship between the instrument response and the solution conductivity (or concentration) of the substance to be titrated, titrant, or product. Having obtained a response curve it is possible to select the proper conductivity (or concentration) range in which the substance titrated, titrant or product must fall to obtain straight line titration curves. A quantitative interpretation of the oscillometric titration curves can be accomplished by means of the oscillometer response curves and the low frequency conductance titration curves obtained for the titration system.[13,24]

To evaluate the dielectric constant of a test solvent, two methods may be employed.

The first method[11] involves the use of a calibration curve which relates cell capacitance at resonance to the dielectric constant of the solvent. To evaluate the dielectric constant of an unknown, the test sample is introduced into the cell assembly vessel and the cell capacitance at resonance measured. The dielectric constant of the test sample is determined by use of the calibration curve.

In the second method,[13,24] the cell parameters, $C_o$ and $C_g$, are evaluated as described on page 69. Having obtained $C_o$ and $C_g$, it is then possible to evaluate the dielectric constant of an unknown by use of equation (68) as described on page 71.

In this investigation, the second method was employed to evaluate the dielectric constants of some pure solvent in order to demonstrate the use of equation (68) and to observe the error in the derived dielectric constant measurement which result from errors in the cell capacitance and cell parameter measurements.

Oscillometric Titrations. To illustrate the application of the response curves for the simulated aqueous titration of sodium hydroxide with hydrochloric acid, the oscillometric response data presented for sodium chloride in Fig. 22 was selected and is shown in Fig. 26. The only difference between the response curves shown in Fig. 22 and 26 is that in Fig. 22, the abscissa is scaled in logarithmic units of specific conductivity, whereas, in Fig. 26, the abscissa is linear. In general, a linear relationship between the instrument response and solution conductivity is preferred to the semi-log relationship when the response curves are employed to interpret oscillometric titrations curves.

As shown in Fig. 26, the oscillometer responds with maximum sensitivity in a nearly linear manner through the conductivity range A to B. Therefore, in an oscillometric titration, the concentration of substance to be titrated, titrant or product, should be selected to fall in this region of solution conductivity in order to obtain straight line titration curves. Through the interval A to B, the cell capacitance and detector current decrease and the cell capacitance difference at half

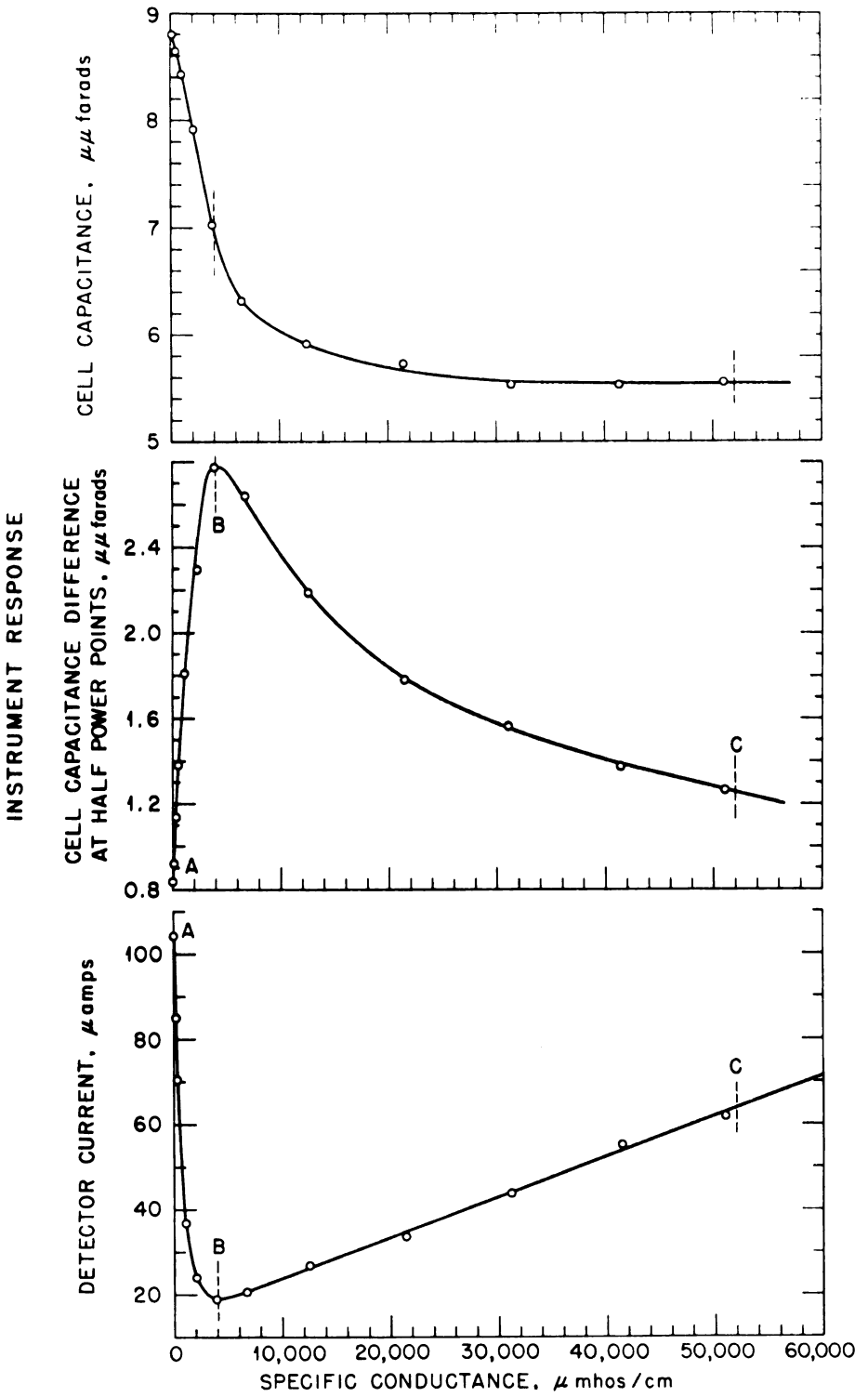


Figure 26. Oscillometer Response Curves for Aqueous Solutions of Sodium Chloride (Freq. : 100 Mc/sec)

power points increase.

At point B on the response curves, the cell capacitance difference is a maximum, the detector is a minimum, and the cell capacitance is equal to the mid-point value between the extremes. In the conductivity region corresponding to B, the cell capacitance difference at half power points and the detector current are least sensitive to changes in solution conductivity. This region of conductivity is to be avoided in oscillometric titrations because the oscillometric titration curves obtained for the detector current and cell capacitance difference at half power points will be M-shaped or W-shaped. When these types of oscillometric curves are obtained, it is difficult to locate the equivalence point.

Through the conductivity region B to C, the cell capacitance and cell capacitance difference at half power points decreases in a non-linear manner, whereas, the detector current increases linearly. If during the titration, the conductivity of the system falls in this interval, the oscillometric titration curves obtained for the cell capacitance and cell capacitance difference at half power points will consist of curved lines where as titration curves obtained for the detector current will consist of straight lines.

In Fig. 27 are shown the three oscillometric titration curves obtained for the simulated aqueous titration of sodium hydroxide with hydrochloric acid. The difference in the curve shapes are readily apparent. A general interpretation of these curves are based on Fig. 28, the low frequency conductivity titrations and Fig. 26, the response curves relating oscillometer response to the solution specific

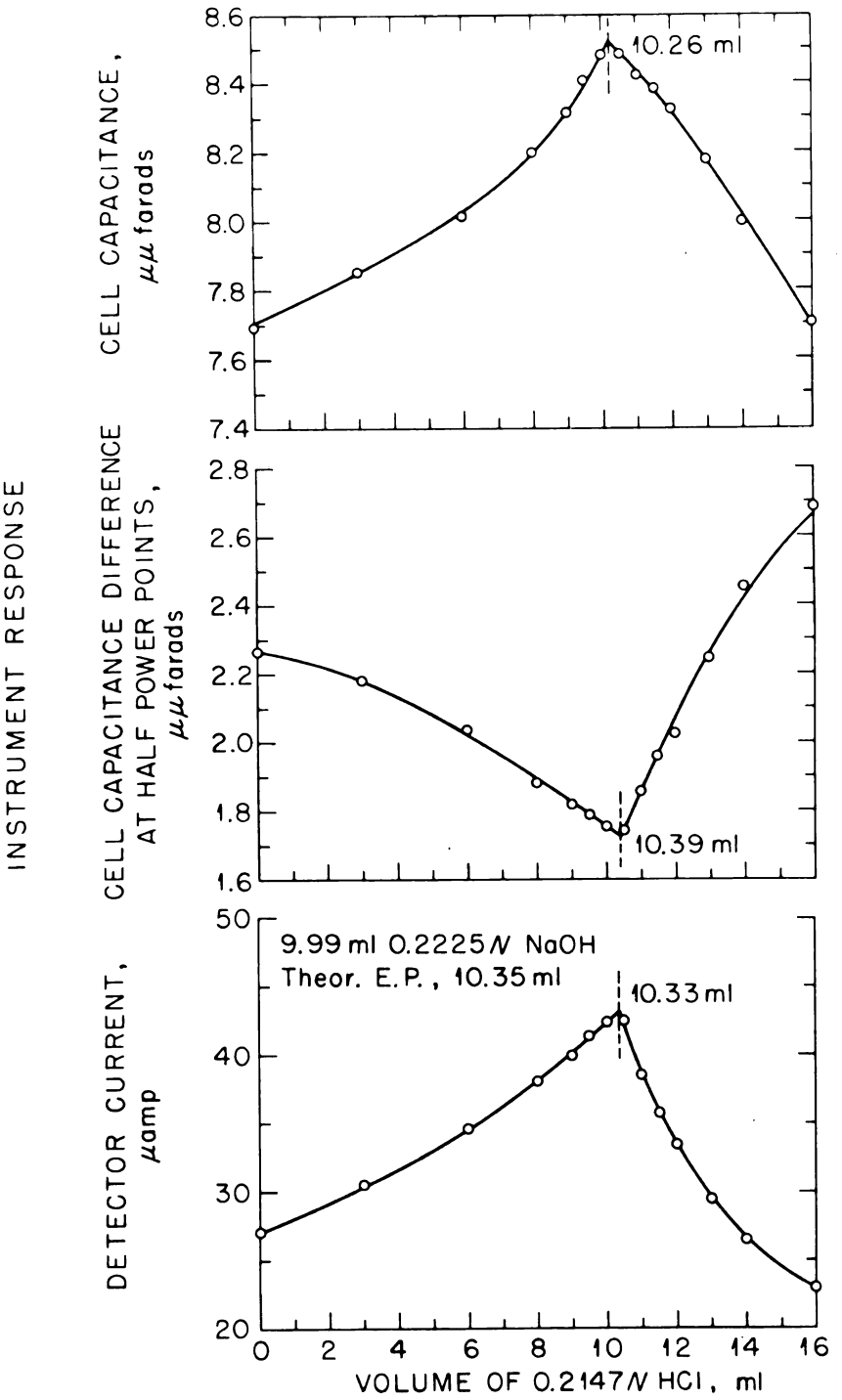


**Figure 27. Simulated Oscillometric Titration of Sodium Hydroxide with Hydrochloric Acid in Water (Freq. : 100 Mc/sec)**

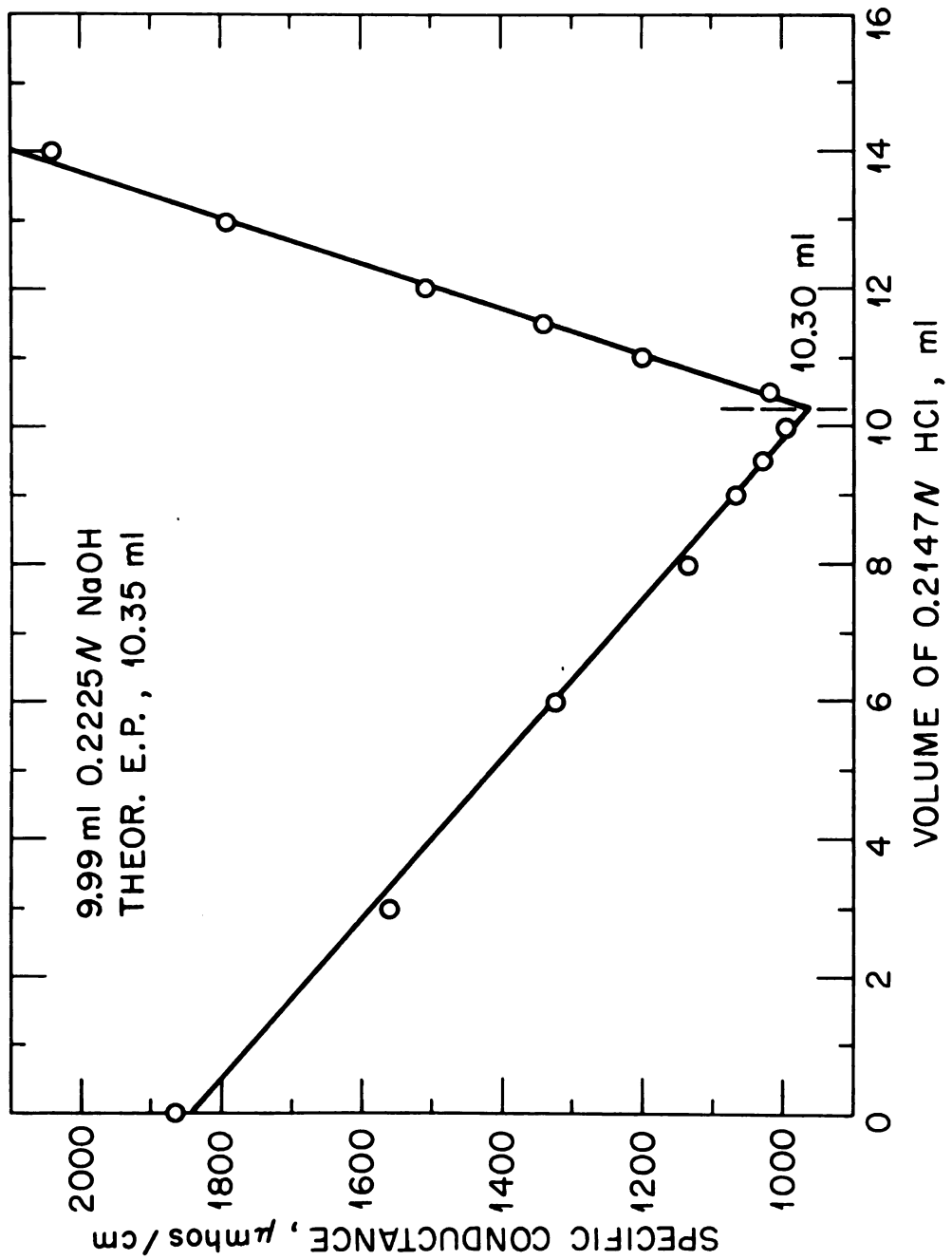


Figure 28. Simulated Low Frequency Conductometric Titration of Sodium Hydroxide with Hydrochloric Acid in Water

conductance. The low frequency conductivity titration curve shown in Fig. 28 was obtained with an identical series of solutions as used to obtain the oscillometric titration curves.

Through the course of the neutralization reaction, the solution low frequency specific conductivity decreases and the oscillometer cell capacitance and detector current increase, whereas, the cell capacitance difference at half power points decreases.

Beyond the equivalence point, the solution specific conductivity increases and the cell capacitance and detector current decrease, whereas, the cell capacitance difference at half power points increases. It follows that oscillometric titration curves relating cell capacitance or detector current to volume of titrant should be inverted V-shaped curves and that the oscillometric titration curve relating cell capacitance difference to volume of titrant should be V-shaped as shown in Fig. 27.

In Fig. 29 are shown the oscillometric titration curves obtained for the simulated titration of sodium acetate with perchloric acid in glacial acetic at 100 Mc/sec and 25°.

A general interpretation of these curves are based upon Fig. 30, the simulated low frequency conductometric titration and Fig. 23, the oscillometric response curves and may be accomplished in the manner as discussed for the aqueous titration.

Dielectric Constant Measurements. In Table XI are given the dielectric constants of some pure solvents evaluated at 100 Mc/sec and 25°. The method employed to evaluate the dielectric constants is described on page 71.

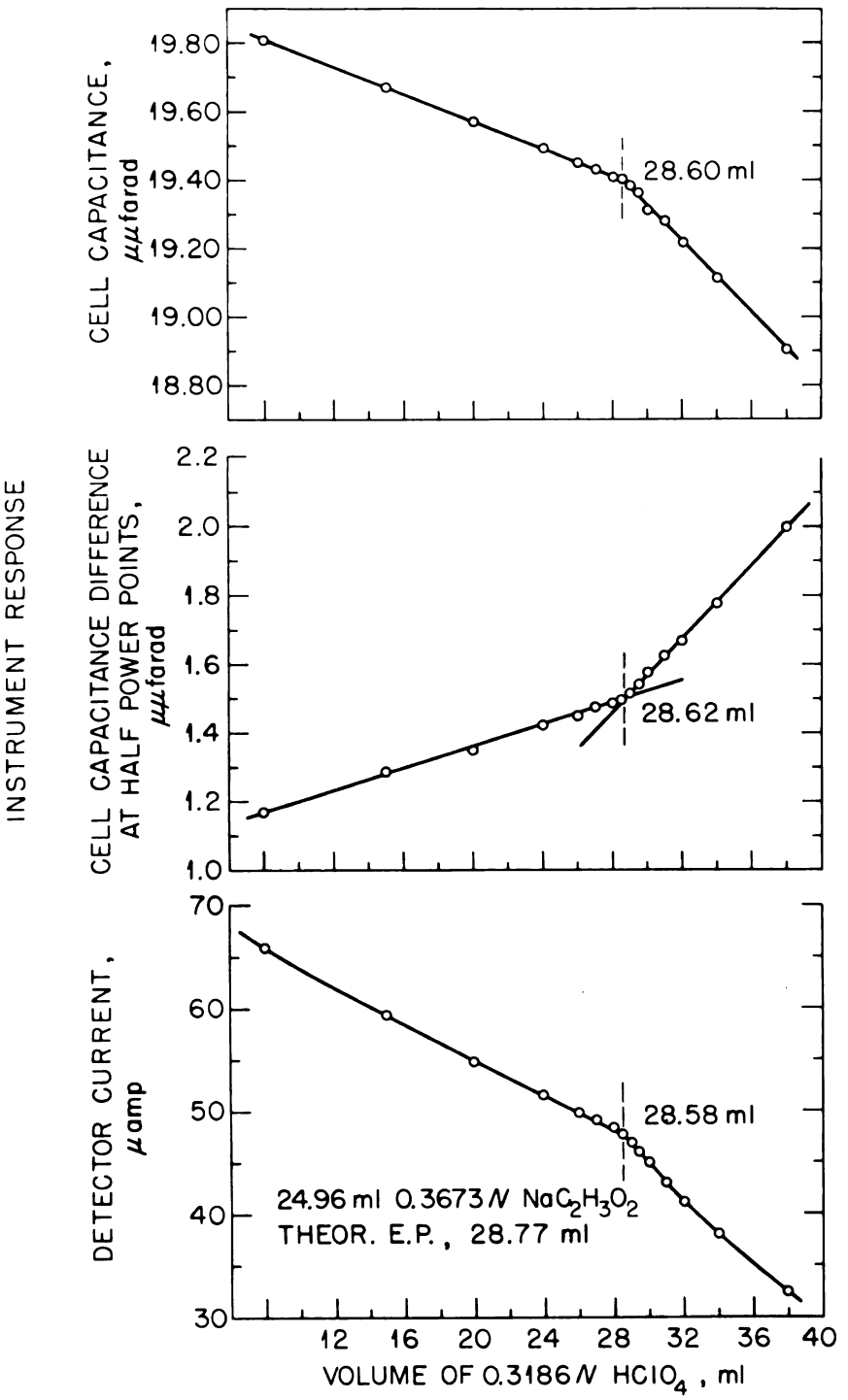


**Figure 29. Simulated Oscillometric Titration of Sodium Acetate with Perchloric Acid in Glacial Acetic Acid (Freq. : 100 Mc/sec)**

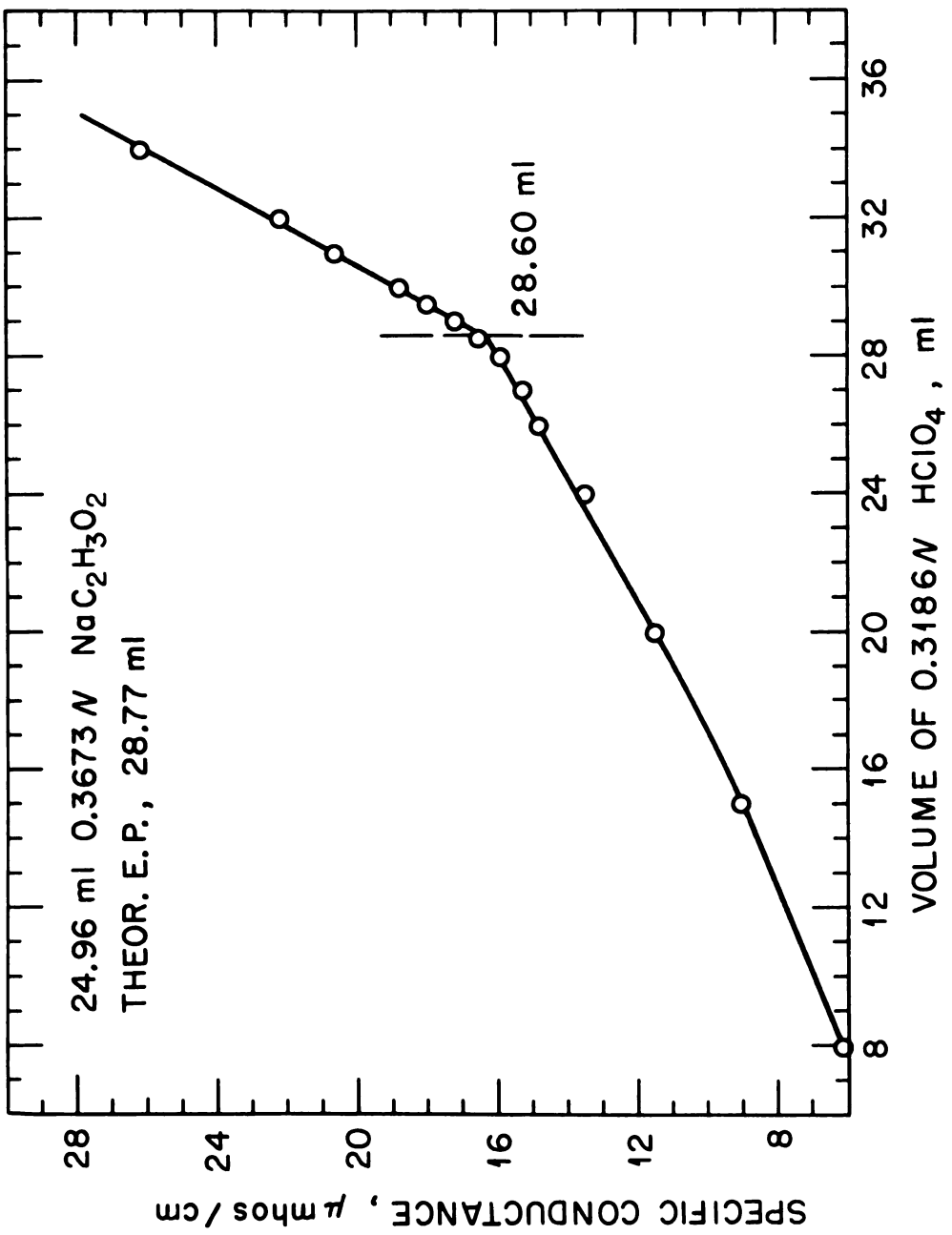


Figure 30. Low Frequency Conductometric Titration of Sodium Acetate with Perchloric Acid in Glacial Acetic Acid

Table XI. Dielectric Constants of some Purified Solvents

Evaluated at 100 Mc/sec and 25°

| | Dielectric Constant | | Relative Error |
|---|---|---|---|
| | a) Literature | b) Experimental | Per Cent |
| Benzene | 2.275 | 2.278 | +0.1 |
| Chloroform | 4.806 | 4.790 | -0.3 |
| Chlorobenzene | 5.621 | 5.586 | -0.6 |
| 1,2 Dichloroethane | 10.36 | 10.21 | -1.5 |
| Acetone | 20.71 | 20.79 | +0.4 |
| Nitrobenzene | 34.82 | 35.21 | +1.0 |
| Water | 78.54 | 79.80 | +1.6 |

a) Reference 62.

b) Average of three determinations.

Although the cell capacitance measurements and the cell parameter values $C_g$ and $C_o$ employed in the calculation of the dielectric constants (equation (68) are thought to be in error, the experimentally derived dielectric constants are in good agreement with literature values. The relative error of the measurements is shown to be largest for the solvents of high dielectric constant. This apparent increase in the relative error of the measurement with increasing dielectric constant is primarily due to the errors associated with the quantity $|\Delta C_a - \Delta C_s|$ in equation (68). The greater the difference between $\Delta C_s$ and $\Delta C_a$, the larger the absolute error in $|\Delta C_a - \Delta C_s|$. As discussed on pages 108-113, the error in the cell capacitance measure associated with the main dial capacitor, $C_t$, appears to increase with increasing separation of the electrodes. When a material with a high dielectric constant is contained in the cell assembly vessel, the separation of the electrodes of $C_t$ at resonance will be large as compared to the separation of the electrodes at resonance for the empty vessel. As a consequence, the error in $\Delta C_s$, will be large as compared to $\Delta C_a$.

If the main dial capacitor, $C_t$, and vernier screw capacitor, $C_v$, were calibrated, it would be possible to accurately measure the cell capacitance values, $\Delta C_a$, $\Delta C_s$, and $\Delta C_{H_g}$ and then evaluate precisely cell parameters, $C_o$ and $C_g$. In turn, the dielectric constant of a test material could be determined precisely.

# CONCLUSIONS

A prototype high frequency oscillometer operating at 100 megacycles per second was developed. A cylindrical reentrant cavity was employed as the resonant circuit element. High frequency voltage was induced in the cavity by inductive coupling of the cavity to a constant voltage and constant frequency generator. The current flowing in the cavity was indicated by a tuned detector circuit which was capacitively coupled to the cavity. The high frequency energy received by the detector probe is rectified and applied to the grid circuit of a dc amplifier tube which is part of a modified Wheatstone Bridge circuit. Bridge unbalance is linearly related to signal intensity.

One electrode of a precision variable capacitor was directly connected to the inner cylinder and the other electrode was connected to the outer cylinder of the cavity. Connected in parallel with the precision variable condenser was a condenser-type cell. When the oscillometer was initially tuned to resonance, a change in conductivity and/or dielectric constant of the solution contained in the cell detuned the oscillometer. Resonance was reestablished by adjustment of the precision condenser as indicated by maximum detector current.

Equivalent circuits are proposed to represent the signal generator, cavity, detector and cell-solution networks. A qualitative interpretation of the instrument response in terms of these circuits is presented.

The net effect of coupling the tuned detector circuit to the resonant cavity is to lower the $Q$-factor of the resonant cavity (or to increase the equivalent shunt conductance of the cavity). Optimum detector

current at resonance is obtained when the reactance of the cavity and detector circuits are equal to zero (i.e., when both circuits are tuned to resonance).

The oscillometer response curves obtained indicate that the changes in instrument response, effective detector current at resonance, cell capacitance at resonance and cell capacitance at half power points are related to changes in admittance of the cell-solution network as described by Reilly and McCurdy. The design of the instrument is such that changes in susceptance and high frequency conductance of the cell-solution network can be measured directly.

Equations were derived and a method described and used to evaluate the cell parameters $C_g$, the capacitance due to the walls of the vessel, and, $C_o$, the capacitance due to the annular sample spaces containing air. Also, an equation was derived and used to evaluate the dielectric constant of some pure solvents.

In the present study, no attempt was made to calibrate the main dial and vernier screw capacitors of the dielectric sample holder at 100 Mc/sec. The calibration data supplied by the manufacturer and obtained at 1000 cycles per second was employed in all capacitance measurements. In order to obtain precise capacitance measurements, it is imperative that the dielectric sample holder be calibrated at 100 Mc/sec. In turn, precise dielectric constant measurements would be possible.

Instrument performance was satisfactorily tested with a simulated titration of an aqueous solution of hydrochloric acid with sodium hydroxide and a simulated titration of a glacial acetic acid solution of sodium acetate with perchloric acid. Interpretation of the oscillometric

titration curves were accomplished by use of the oscillometer response curves and low frequency conductance titration curves.

It is without question that certain improvements in the mechanical arrangements and design can be made to improve the performance of the resonant cavity oscillometer, such as: (1) A practical titration cell be designed to permit stirring of the solutions. (2) For an instrument to be used primarily for titrations, the resonant cavity can be positioned vertically and the titration vessel inserted into the end of the cavity so that the test solution is located in the gap formed by the end closures of the inner and outer cylinders. In this position, the electrostatic field existing within the cavity is most dense. Consequently, the interaction between the electrostatic field and the test solution should be greatest in this position. (3) To increase the $Q$-factor of the oscillometer, a crystal diode detector and vibrating reed electrometer can be used. By proper selection of the resistive and capacitive components in the crystal diode circuit, it should be possible to minimize the resistive impedance coupled into the cavity as compared to the tuned detector circuit employed in the present study. (4) To extend the concentration ranges in which the oscillometer responds with maximum sensitivity in a linear manner, a smaller resonant cavity can be employed. The resonant frequency of the cavity will be inversely proportional to its mechanical dimensions.

## LITERATURE CITED


1. P.H. Sherrick, D.A. Dawe, R. Karr and F. Ewen, "Manual of Chemical Oscillometry", E.H. Sargeant and Co., Chicago, Illinois (1954).

2. G.A. Harlow and D.H. Morman, Anal. Chem. 38, 485R (1966).

3. A. Bellomo and O. Klug, Chem. Anal. (Warsaw) 9, 879 (1966).

4. M.F.C. Ladd and W.H. Lee, Talanta 12, 941 (1965).

5. M. Szczepanik, Przemyls Chem. 44, 542 (1965).

6. V.A. Zarinski and I.A. Ger'es, Zavodskaya Lab. 29, 1157 (1963).

7. E. Pungor, J. Electranal Chem. 3, 189 (1962).

8. M.F.C. Ladd and W.H. Lee, Talanta 4, 274 (1960).

9. A. Timnick, L.L. Fleck and E.R. Hooser, Chemistry in Canada, March, 23. (1960).

10. A. Bellomo and G. D'Amore, Atti Soc. Peloritana Sc. fis, mat nat., 5, 119 (1959).

11. E.H. Sargeant and Company, Scientific Apparatus and Methods 9, 1 (1957).

12. V.A. Zarinski and I.R. Mandelberg, Zavodskaya Lab. 22, 262 (1956).

13. C.N. Reilly in "New Instrumental Methods in Electrochemistry" by P. Delahay, Interscience Publishers, New York, N.Y., (1954), pp. 319-345.

14. G.G. Blake, "Conductometric Analyses at Radio Frequency", Chemical Publishing Co., Inc., New York, N.Y. (1952).

15. E. Pungor and L. Balazs, Magy. Kem Folyocrant 72, 257 (1966).

16. M. Syczepanik, Przemyal Chem. 44, 471 (1965).

17. K. Nakano and H. Tadano, Nippon Kagaku Zasshi 85, 485 (1964).

18. V.I. Ermakov. P.A. Zagorets, and N.I. Smernov, Russ. J. Phys. Chem. 36, 625 (1962).

19. R. Huber and K. Cruse, Z. phys. Chem. 12, 273 (1957).

20. R. Huber and K. Cruse, Angew. Chem. 66, 625 (1954).

21. R. Huber and K. Cruse, Angew. Chem. 66, 625 (1954).

22. J.L. Hall, J.A. Gibson, H.O. Phillips and F.E. Gritchfield, Anal. Chem. 26, 1539 (1954).

23. S. Fujiwara and S. Hayaski, Anal. Chem. 26, 239 (1954).

24. C.N. Reilly and W.H. McCurdy, Jr., Anal. Chem. 25, 86 (1953).

25. W.J. Blaedel and H.V. Malmstadt, Anal. Chem. 24, 455 (1952).

26. M.L. Mittal and S.S. Dube, Bull. Chem. Soc. Japan 39, 1064 (1966).

27. A. Bellomo and G'Amore, Chem. Tech. (Berlin) 14, 340 (1962).

28. L.O. Graniskaya and B.A. Lopatin, Zavadskaya Lab. 29, 9 (1960).

29. A.H. Johnson and A. Timnick, Anal. Chem. 28, 889 (1956).

30. E. Pungor and K. Huber, A. Anal. Chem. 154, 1 (1957).

31. S.S. Lane, Analyst 82, 406 (1957).

32. D.J. Fisher, M.T. Kelley, R.W. Stelzner, and E.B. Wagner, I.S.A. Journ. of Instr., Auto Control and Automation 4, 474 (1957).

33. M. Pancek, Chem. Listy 52, 1367 (1958).

34. R.W. Stelzner: Private communication, Oak Ridge National Laboratory, Oak Ridge, Tenn., Sept., 1959.

35. W.J. Blaedel and H.V. Malmstadt, Anal. Chem. 22, 1413 (1950).

36. C.N. Works, T.W. Dakin, and F.W. Baggs, Proceedings of the I.R.E., April, 245 (1945).

37. A.H. Johnson: Private communication, Michigan State University, East Lansing, Michigan, Sept., 1956.

38. F.E. Terman, "Electronic and Radio Engineering", 4th Ed. McGraw-Hill Book Co., New York, N.Y. (1955).

39. C.G. Cannon, "Electronics for Spectroscopists", Hilger and Watts Ltd., London (1960).

40. T.E. Terman, "Radio Engineers Handbook" 1st Ed., McGraw-Hill Book Co., New York, N.Y. (1943).

41. W.L. Barrow and W.W. Mieher, Proceedings I.R.E. 28, 184 (1940).

42. W.W. Hensen, J. Appl.Phys. 9, 654 (1938).

43. R.I. Sarbacher and W.A. Edson, "Hyper and Ultrahigh Frequency Engineering", John Wiley and Sons, Inc., New York, N.Y. (1946), p. 389.

44. J.C. Slater, "Forced Oscillations in Cavity Resonators", Rad. Lab. (MIT), Report No. 188, Dec. 31, 1942.

45. G.B. Collins, "Microwave Magnetrons", McGraw-Hill Book Company, Inc., (1948), p. 310.

46. C.G. Montgomery, "Technique of Microwave Measurements", MIT Radiation Laboratory Series, McGraw-Hill Book Company, Inc., New York, N.Y. (1947) pp. 285-319.

47. S.I. Pearson and G.J. Maler, "Introduction to Circuit Analyses", Jonh Wiley and Sons, Inc. (1965).

48. R.N. Kerchner and G.F. Corcoran, "Alternating-Current Circuits", 4th Ed., John Wiley and Sons, Inc., New York, N.Y. (1960).

49. K.G. Stone, "Determination of Organic Compounds", McGraw-Hill Book Co., Inc. , New York, N.Y., p. 92.

50. A.I. Vogel, "Practical Organic Chemistry", Longmans, Green and Co., Inc., New York, N.Y. (1948), p. 558.

51. N.J. Leonard and L.E. Sutton, J. Am. Chem. Soc. 70, 1564 (1948).

52. K.B. McAlpine and C.P. Smyth, J. Chem. Phys. 3, 55 (1935).

53. C.P. Smyth, R.W. Dornte, and E.B. Wilson, J. Am. Chem. Soc. 53, 4242 (1931).

54. R.J. Livingston, J. Am. Chem. Soc. 69, 1220 (1947).

55. "The Radio Amateur's Handbook", 33rd Ed. American Relay League, West Hartford, Conn. (1956), p. 84.

56. W.I. Orr, "The Radio Handbook", 16th Ed., Editors and Engineers, Ltd., Summerland, California (1962), pp. 232-33.

57. ASTM Standards, "Electric Insulation, Plastics, Rubber", Part 6, ASTM Designation: D150-47T, American Society for Testing Materials, Philadelphia, Pa., (1949).

58. L. Hartshorn and W.H. Ward, Proceedings, I.E.E. (London) 79, 597 (1936).

59. "Operating Instructions for Type 1690-A, Dielectric Sample Holder", General Radio Company, Cambridge, Mass. (1954).

60. 1966 Book of ASTM Standards "Electrical Insulating Materials", Part 29, ASTM Designation: D-150-65T, American Society for Testing Materials, Philadelphia, Pa. (1966).

61. A.E. Knowton "Standard Handbook for Electrical Engineers", 8th Ed., McGraw-Hill Book Company, New York, N.Y. (1949), p. 64.

62. A.A. Maryott and E.A. Smith, "Table of Dielectric Constants of Pure Liquids", National Bureau of Standards Circular 514, (1951).

63. S. Glasstone, "Physical Chemistry", 2nd Ed., D. Van Nostrand Co., Inc., New York, N.Y. (1946).

## APPENDIX I

### Sample Derivation for Universal Resonance Curves*

The effective impedance of a series resonance circuit as shown in Fig. 1 is given by

$$Z = \left| R^2 + \left| \omega L - \frac{1}{\omega C} \right| \right| \tag{3}$$

At resonance,

$$\omega L_0 = \frac{1}{\omega C_0} \tag{8}$$

and

$$Z_o = R \tag{10}$$

where the subscript zero denotes resonance. If the inductance, $L$, and resistance, $R$, of the series circuit are constant and independent of the frequency, the circuit may be tuned to resonance by adjusting the series circuit capacitance, $C$.

Equation (3) may be rearranged to express the impedance of the circuit in terms of the circuit $Q$ and the fractional capacitative tuning which is given by

$$\gamma = \frac{C}{C_o} \tag{15}$$

---

*The equation numbers appearing in the Appendices correspond to equation numbers appearing in the body of the text with the exception of equations prefaced by A which are new expressions and appear only in the Appendices.

where $C$ is the actual capacitance and $C_o$ is the capacitance at resonance.

Rearrangement of equation (1) in terms of the fraction tuning yields

$$(A\text{-}1) \qquad Z = \left[R^2 + \left[\omega L - \frac{1}{\omega C_o}\left|\frac{1}{\gamma}\right|\right]^2\right]^{1/2}$$

or

$$(A\text{-}2) \qquad Z = R\left[1 + \left[\frac{\omega L}{R} - \frac{1}{\omega C_o R}\left|\frac{1}{\gamma}\right|\right]^2\right]^{1/2}$$

Since the inductance $L$ is constant and is equal to $L_o$, the above equation may be rearranged in terms of $Q$, as given by

$$(A\text{-}3) \qquad Z = R\left[1 + \left[Q - Q\left|\frac{1}{\gamma}\right|\right]^2\right]^{1/2}$$

where

$$(8) \qquad Q = \frac{\omega L_o}{R} = \frac{1}{\omega C_o R}$$

Thus, the ratio of the actual impedance to the impedance at resonance is

$$(A\text{-}4) \qquad \frac{Z}{Z_o} = \frac{R\left[1 + Q^2\left[1 - \frac{1}{\gamma}\right]^2\right]^{1/2}}{R}$$

Factoring out the $R$ terms, the ratio of the actual impedance to the impedance of the $RLC$ series resonant circuit is given by

$$(16) \qquad \frac{Z}{Z_o} = \sqrt{1 + Q^2\left[1 - \frac{1}{\gamma}\right]^2}$$

The universal resonance curves for the series and parallel *RLC* circuit, obtained from equations (17), (18), and (19) and equations (26), (27), (28), and (29) may all be derived in a similar way by rearrangement of the appropriate expression for the quantities involved, in terms of the circuit $Q$ and fractional capacitative tuning.

## APPENDIX II

### Parts list for the Resonant Cavity Oscillometer

$C_R$ - Cavity resonator, Fig. 12

$C_s$ - Condenser-Type Cell, Fig. 13

$P_1$, $P_2$ - Coupling Probes, Fig. 12

$C_t$, $C_v$ - Type 1960-A Dielectric Sample Holder, General Radio Co., Fig. 14

$C_1$ - 250 pfd, 21 plate air condenser

$C_2$ - 500 pfd, 500 V.

$C_3$ - 0.1 mfd, 400 V.

$C_4$ - 0.5 mfd, 400 V.

$C_5$, $C_6$ - 0.1 mfd, 400 V.

$R_1$ - 4.7 megohms, 0.5 watt

$R_2$ - 3.3 megohms, 0.5 watt

$R_3$ - 20,000 ohms, 0.5 watt potentiometer

$R_4$ - 10,000 ohms, 0.5 watt

$R_5$ - 47,000 ohms, 0.5 watt

$R_6$ - 390 ohms, 0.5 watt

$R_7$ - 4700 ohms, 0.5 watt

$R_8$ - 25,000 ohms, 0.5 watt potentiometer

$R_9$, $R_{10}$ - 6800 ohms, 0.5 watt

$L_1$ - R. F. choke, 16 turns, No. 22 enamel

$T_1$ - Primary 115 V., 60 cycles: secondary No. 1: 180-0-180V; Section No. 2: 6.3 V., 1.2 amps

$M_1$ - 0.30 microammeter

$M_2$ - 0-200 microammeter, 0-0051 microamp/div

$V_1$ - 955

$V_2$ - 6SQ7

$V_3$ - 6 x 5-GT

$S.W._1$ - DPST toggle switch

$S.W._2$ - DPST toggle switch

## APPENDIX III

### Operating Procedure for the Resonant Cavity Oscillometer

1. Connect the input terminal of the cavity resonator to the source of high frequency oscillation (Refer Appendix V, Operating Procedure for the Hewlett Packard Model 608A VHF Signal Generator).
2. Set the ammeter toggle switch to HIGH SEN. and the high sensitivity galvanometer switch to OFF.
3. Connect the power cable to a source of 115 volt 60 cycle current, and turn the power switch ON. Allow 10 to 15 minutes warm up for the 6SQ7 tube to stabilize.
4. Rotate the detector SENSITIVITY control to the extreme counter clockwise position (lowest detector sensitivity).
5. Set the ammeter toggle switch to the LOW SENS. position. The detector current is indicated by the 0-30 microammeter.
6. Turn the detector capacitance dial to 250.
7. Rotate the main dial of the dielectric sample holder until a maximum meter indication is obtained. If the meter indication initially is less than zero, rotate the ZERO SET control until the meter indication is greater than zero.
8. Set the high sensitivity galvanometer, 0.200 microamps, to the X0.001 sensitivity position and rotate the ZERO ADJ. control until the meter reads zero. Set the meter toggle switch to HIGH SENS.

9. Adjust the detector SENSITIVITY control to give a desired meter indication with the oscillometer tuned to resonance. It may be necessary to rotate the vernier screw of the dielectric sample holder to tune precisely the oscillometer to resonance as indicated by a maximum meter indication (refer to Fig. 19).

10. Detune the cavity from resonance by rotating the main dial of the dielectric sample holder until a minimum meter indication is observed. Increase the galvanometer sensitivity by step switching, as the meter indications decrease, to determine precisely the minimum meter indication.

11. Rotate the ZERO SET control until the meter indication is zero (clockwise rotation of the ZERO SET control will increase the meter indication). The ZERO SET control most be readjusted for every change in the setting of the SENSITIVITY control.

12. Set the galvanometer sensitivity switch to X0.001.

13. Turn the detector capacitance dial to a new setting. Then, rotate the main dial of the dielectric sample holder until a maximum meter indication is observed. Rotate the vernier screw to precisely determine the maximum. Repeat this procedure until a maximum meter indication is observed for a given setting of the detector capacitance dial when the oscillometer is tuned to resonance (refer to Fig. 20).

14. After having determined the setting of the detector capacitance to give maximum oscillometer response, as described above, high frequency measurements can be made.

APPENDIX IV

## Hewlett-Packard Model 608A VHF Signal Generator Specifications

### Frequency Range

10 to 500 megacycles in 5 ranges

Ranges: 10-21 Mc, 21-45 Mc, 45-100 Mc, 100-230 Mc, 230-500 Mc

### Calibration Accuracy

Within ± 1%. Frequency settings can be duplicated within 0.2%.

### Output Voltage

0.1 microvolt to 1.0 volt, continuously variable, Direct Reading controls calibrated in voltage and dbm.

### Rated Load Impedance

50 ohms resistive

### Internal Impedance

50 ohms; maximum VSWR 1.2

### Output Voltage Accuracy

Within ± 1 db rated load over entire frequency range.

### Leakage

Negligible

### Power Supply Rating

Voltage - 115/230 volts ± 10%

Frequency - 50-60 cycles/sec

Wattage - 150 watts

RF Output Connector

Amphenol No. SO-239 CPH-49194, 83-1H Series UHF

APPENDIX V

## Operating Procedure for the Hewlett-Packard Model 608A VHF Signal Generator

1. Connect the OUTPUT terminal of the Model 608A generator to the cavity resonator power input terminal by means of a RG8/U coaxial cable terminated with Amphenol 83-1SP (PL-259 CPH-49190) connectors.
2. Connect the power cable to a source of 110 volts - 60 cycles current, and turn the POWER switch ON. Allow 10 to 15 minutes warmup for the output frequency and level to stabilize.
3. Set the RANGE control to the desired frequency range.
4. Rotate the frequency control until the desired frequency is indicated by the frequency dial.
5. Set the CW, PULSE 400 ≈, 1000 ≈, Ext. MOD switch to the CW position (output without modulation).
6. Adjust the OUTPUT LEVEL control until a reading is obtained on the output voltmeter. Do not bring this level up to a full scale reading on the meter.
7. Adjust the TRIMMER knob for a maximum reading on the output voltmeter.
8. Set the OUTPUT LEVEL control to SET LEVEL point on the output voltmeter and adjust the ATTENUATOR control so its dial reads 500 millivolts.
    a. Periodically readjust the TRIMMER knob for a maximum reading on the output voltmeter to

insure output frequency stability.

b. Readjust the OUTPUT LEVEL control to the SET LEVEL whenever a change in output is indicated by the output voltmeter.

## APPENDIX VI

## Sample Derivation for the Cell Parameters Equations $\left[C_o \text{ and } C_g\right]$

At resonance, the total equivalent capacitance of the resonant cavity oscillometer for any given frequency is given by

$$C_{(total)} = C_x + C_s + \left(C_t - C_v\right)_s \tag{A-5}$$

where $C_x$ is the total equivalent capacitance of the oscillometer excluding the capacitance associated with the cell-solution load, $C_s$, and the capacitance associated with the dielectric sample holder, $\left(C_t - C_v\right)_s$. The capacitance term $C_x$ includes the distributed capacitance of the resonant cavity and also includes the equivalent capacitance as a result of capacitive reactance coupled into the cavity by the signal generator and the detector circuits. The magnitude of the capacitance terms $C_{(total)}$ and $C_x$ are unknown. However, at a given frequency, they are assumed to be constant and operate independently of the capacitance terms $C_s$ and $\left(C_t - C_v\right)_s$.

The capacitance term $\left(C_t - C_v\right)_s$ is the difference in capacitance between the reading of the main micrometer dial, $C_t$, and the vernier screw, $C_v$, of the dielectric sample holder and represents the capacitance value measured for the test sample contained in the cell.

The capacitance term, $C_s$, represents the capacitance of the condenser-type cell and is given by

$$C_s = \frac{C_g C_o \varepsilon_s}{C_g + C_o \varepsilon_s} \tag{A-6}$$

where $C_g$ is the capacitance due to glass walls of the cell, $C_o$ is the capacitance of the cell containing air and $\varepsilon_s$ is the dielectric constant of the test sample contained in the cell. Equation (A-6) is identical in form to equation (54) and assumes that the resistance of dielectric contained is so large as to be negligible in the equivalent parallel capacitance term for the condenser-type cell (Refer to equation (50).

In general, when a dielectric is contained within the cell, the total capacitance is thus given by

$$C_{(total)} = C_x + \frac{C_g C_o \varepsilon_s}{C_g + C_o \varepsilon_s} + \Delta C_s \tag{A-7}$$

where $\Delta C_s$ is equal to the capacitance difference between $C_t$ and $C_v$, $\left(C_t - C_v\right)_s$, which is measured for the particular dielectric.

When air is contained in the cell, the total equivalent oscillometer capacitance at resonance is given by

$$C_{(total)} = C_x + \frac{C_o C_g}{C_o + C_g} + \Delta C_a \tag{A-8}$$

where $\Delta C_a$ is equal to the capacitance difference $\left(C_t - C_v\right)_a$ measured for air.

When mercury is contained in the cell, the equivalent parallel capacitance of the cell (equation (51) is reduced to $C_g$, and the total equivalent oscillometer capacitance is given by

$$C_{(total)} = C_x + C_g + \Delta C_{H_g} \tag{A-9}$$

where $\Delta C_{H_g}$ is equal to the capacitance difference, $\left(C_t - C_v\right)_{H_g}$ measured for mercury.

By use of equations (A-7), (A-8) and (A-9) one may derive the cell constants $C_o$ and $C_g$ in the following manner:

Equation (67),

$$C_o = \frac{C_g^2 - C_g\left(\Delta C_a - \Delta C_{H_g}\right)}{\left(\Delta C_a - \Delta C_{H_g}\right)}$$

is obtained by equating equations (A-8) and (A-9) to eliminate the constant terms $C_{(total)}$ and $C_x$. The resulting expression is solved for $C_o$ in terms of $C_g$, $\Delta C_a$, and $\Delta C_{H_g}$.

Equation (66),

$$C_g = \frac{\left(\varepsilon_s - 1\right)\left(\Delta C_s - \Delta C_{H_g}\right)}{\varepsilon_s\left(\frac{\Delta C_s - \Delta C_{H_g}}{\Delta C_a - \Delta C_{H_g}}\right) - 1}$$

is obtained by equating equations (A-7) and (A-8) in order to eliminate the constant $C_{(total)}$ and $C_x$. The resulting expression is solved for $C_g$ in terms of $C_o$, $\Delta C_s$, $\Delta C_{H_g}$, and $\varepsilon_s$. The value of $C_o$, given by equation (67) is substituted into the expression obtained for $C_g$ and $C_g$ reevaluated in terms of $\Delta C_s$, $\Delta C_{H_g}$, $\Delta C_a$, and $\varepsilon_s$.

The value of $C_g$ may be calculated by measurement of $\Delta C_a$ for air, $\Delta C_{H_g}$ for mercury, and $\Delta C_s$ for a material of known dielectric constant, $\varepsilon_s$. Having determined the value of $C_g$ by use of equation (67), it is then possible to substitute the value of $C_g$, $\Delta C_a$, $\Delta C_{H_g}$ into equation (66) and calculate the value of $C_o$.

Equation (68),

$$\varepsilon_s = \frac{C_g}{C_o}\left[\frac{\left(\Delta C_a - \Delta C_s\right) + \frac{C_g C_o}{C_g + C_o}}{C_g - \left(\Delta C_a - \Delta C_s\right) - \frac{C_g C_o}{C_g + C_o}}\right]$$

is obtained by equating equations (A-7) and (A-8) to eliminate the constants $C_{(total)}$ and $C_x$. The resulting expression is solved for $\varepsilon_s$ in terms of $C_g$, $C_o$, $\Delta C_a$, and $\Delta C_s$.

## APPENDIX VII

## Susceptance Variance Method[57-58] and Derivation of Equations

When a constant alternating voltage, $V_2$, is applied between the terminals, $a$ and $b$, of a series resonance circuit as shown in Fig. A-1, the current flowing in the circuit is given by

$$(A\text{-}10) \qquad I_2 = \frac{V_2}{Z_t} = \frac{V_2}{R_2 + j\omega L_2 + \dfrac{R_p}{1 + j\omega C_2 R_p}}$$

In this equivalent circuit representation the subscript 2 denotes the resonant cavity and therefore, is consistant with previous circuit representations. However, the voltage source $V_2$, the resistance $R_2$, the inductance $L_2$, and the capacitance $C_2$, all represent the total equivalent series parameters of the oscillometer. In this representation the parallel resistance, $R_p$, would be analogous to the equivalent parallel cell solution load (equation (47) THEORY).

The voltage drop, $V'$, across the capacitance $C_2$ (or across points c-d) is given by

$$(A\text{-}11) \qquad V' = I_2 \left( \frac{R_p}{1 + j\omega C_2 R_p} \right)$$

or

$$(A\text{-}12) \qquad V' = \left( \frac{\dfrac{R_p}{1 + j\omega C_2 R_p}}{R_2 + j\omega L_2 + \dfrac{R_p}{1 + j\omega C_2 R_p}} \right) V_2$$

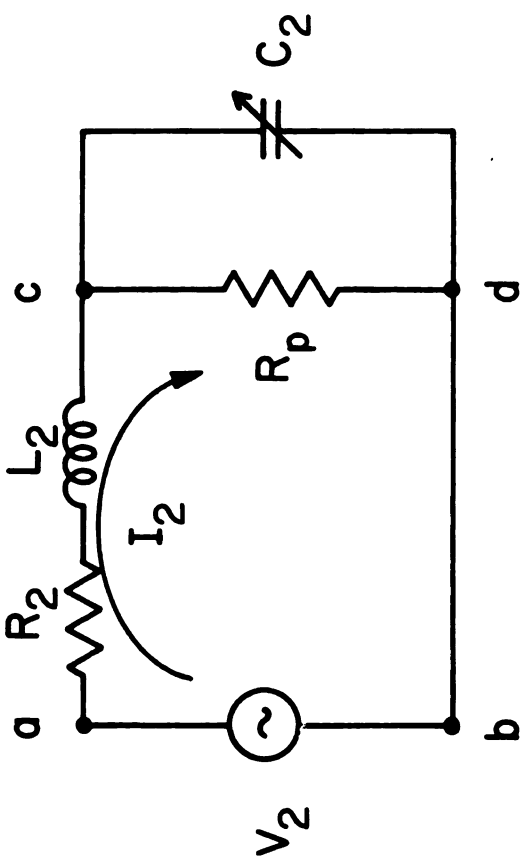


Figure A-1. Equivalent Series Resonant Circuit to Represent the Resonant Cavity Oscillometer and Equivalent Shunt Resistance of the Cell-Solution Circuit

Rearrangement of the terms in equation (A-12) yields

$$V' = \frac{\frac{V_2}{R_2 + j\omega L_2}}{\frac{1}{R_p} + j\omega C_2 + \frac{1}{R_2 + j\omega L_2}} \tag{A-13}$$

If the quantity $\frac{1}{R_2 + j\omega L_2}$ is rationalized and the terms of the equation (A-14) are grouped into the real and imaginary parts, the voltage $V'$ is equal to

$$V' = \frac{\left[\frac{R_2}{R_2^2 + \omega^2 L_2^2} - j\,\frac{L_2}{R_2^2 + \omega^2 L_2^2}\right] V_2}{\frac{1}{R_p} + \frac{R_2}{R_2^2 + \omega^2 L_2^2} + j\omega\left[C_2 - \frac{L_2}{R_2^2 + \omega^2 L_2^2}\right]} \tag{A-15}$$

Since the quantity $\frac{1}{R_p}$ is equal to $G_p$, the parallel shunt conductance, and the quantity $\frac{R_2}{R_2^2 + \omega^2 L_2^2}$ is equal to the equivalent shunt conductance, $G_e$, of the $R_2 - L_2$ network, equation (A-15) is reduced to

$$V' = \frac{\left[G_e - \frac{j\omega L_2}{R_2^2 + \omega^2 L_2^2}\right] V_2}{G_t + j\omega\left[C_2 - \frac{L_2}{R_2^2 + \omega^2 L_2^2}\right]} \tag{A-16}$$

where $G_t$ is equal to the total equivalent shunt conductance, and

$$G_t = \frac{1}{R_p} + \frac{R_2}{R_2^2 + \omega^2 L_2^2} = G_p + G_e \tag{A-17}$$

Resonance is obtained when the capacitance $C_2$ is adjusted to yield maximum effective voltage $V'_{(res)}$ under condition of constant applied

voltage, $V_2$, at angular frequency, $\omega$. It is evident from equation (A-17) that the value of the capacitance, $C_{2(res)}$, that will yield maximum effective voltage, $V'_{(res)}$, is equal to

$$C_{2(res)} = \frac{L_2}{R_2^2 + \omega^2 L_2^2} \tag{A-18}$$

The maximum effective voltage at resonance is then equal to

$$V'_{(res)} = \frac{\left| G_e - j\left| \frac{\omega L_2}{R_2^2 + \omega^2 L_2^2} \right| \right| V_2}{G_t} \tag{A-19}$$

The ratio of the voltage for any given value of $C_2$, to the voltage at resonance is given by

$$\frac{V'}{V'_{(res)}} = \frac{G_t}{G_t + j\omega\left| C_2 - \frac{L_2}{R_2^2 + \omega^2 L_2^2} \right|} \tag{A-20}$$

or

$$\left| \frac{V'}{V'_{(res)}} \right|^2 = \frac{G_t^2}{G_t^2 + \omega^2 \left| C_2 - \frac{L_2}{R_2^2 + \omega^2 L_2^2} \right|^2} \tag{A-21}$$

The value of $C_2$, for any given value of $\frac{V'}{V'_{(res)}}$ is given by

$$C_2 = \frac{L_2}{R_2^2 + \omega^2 L_2^2} \pm \frac{G_t}{\omega}\left| \frac{1}{\left| \frac{V'}{V'_{(res)}} \right|^2} - 1 \right|^{1/2} \tag{A-22}$$

Since the quantity $\frac{L_2}{R_2^2 + \omega^2 L_2^2}$ is equal to $C_{2(res)}$, equation (A-22) is reduced to

$$C_2 = C_{2(res)} \pm \frac{G_t}{\omega}\left[\left(\frac{1}{\frac{V'}{V'_{(res)}}}\right)^2 - 1\right]^{1/2} \tag{A-23}$$

If for a given value of $\frac{V'}{V'_{(res)}}$, $C_a$ and $C_b$ are chosen to represent the two capacitance values of $C_2$ to satisfy the conditions of equation (A-23), their values may be given by

$$C_a = C_{(res)} + \frac{G_t}{\omega}\left[\left(\frac{1}{\frac{V'}{V'_{(res)}}}\right)^2 - 1\right]^{1/2} \tag{A-24}$$

and

$$C_b = C_{2(res)} - \frac{G_t}{\omega}\left[\left(\frac{1}{\frac{V'}{V'_{(res)}}}\right)^2 - 1\right]^{1/2} \tag{A-25}$$

It is evident from equations (A-24) and (A-25) that the capacitance at resonance, $C_{2(res)}$, is equal to

$$C_{2(res)} = 1/2\left[C_a + C_b\right] \tag{A-26}$$

and that the total equivalent shunt conductance $G_t$, is equal to

$$G_t = \frac{\omega\left[C_a - C_b\right]}{2\left[\left(\frac{1}{\frac{V'}{V'_{(res)}}}\right)^2 - 1\right]^{1/2}} = \frac{\omega\Delta C_{ab}}{2\left[\left(\frac{1}{\frac{V'}{V'_{(res)}}}\right)^2 - 1\right]^{1/2}} \tag{A-27}$$

If the capacitance values $C_a$ and $C_b$ are the two capacitance values of $C_2$ (on either side of resonance) which correspond to $\frac{V'}{V'_{(res)}} = 0.707$, (the half power points), the value of $G_t$ is equal to

$$G_t = \frac{\omega \Delta C_{0.707}}{2} \tag{A-28}$$

The $Q$-factor for the cavity resonance circuit (Fig. 1) is related to the capacitance difference at the half power points by

$$Q = \frac{\omega C_{2(res)}}{G_t} = \frac{2C_{2(res)}}{\Delta C_{0.707}} \tag{A-29}$$

APPENDIX VIII

## Fundamental Equivalent Circuit Representation of the Resonant Cavity Oscillometer and Derivation of the Circuit Equations (for the Capacitive Coupling)

The fundamental equivalent circuit drawn to represent the resonant cavity oscillometer is shown in Fig. A-2.

The subscript 1 denotes the signal generator circuit. The constant applied signal generator voltage is given by $V_1$. $R_1$ and $L_1$ represent the total equivalent resistance and inductance of the loop probe used to couple the signal generator to the resonant cavity. The mutual inductance between the inductor $L_1$ and inductor $L_2$ is represented by $M_{12}$.

The subscript 2 refers to the resonant cavity circuit. $L_2$ represents the total distributed inductance of the resonant cavity. $R_2$ represents the total equivalent series resistance of the resonant cavity and includes not only the distributed resistance of the cavity but also includes the equivalent series resistance of the condenser-type cell-solution load (refer to Fig. 11). The variable capacitance, $C_2$, represents the total equivalent series capacitance of the cavity network and includes the total distributed capacitance of the cavity, the parallel capacitance network of the dielectric sample holder $\{C_t$ and $C_v\}$ and the equivalent capacitance associated with the condenser-type cell-solution load (refer to Fig. 11).

The subscript 3 refers only to that portion of the detector circuit (Fig. 11) which preceeds the detector tube $V_3$. The variable capacitance $C_3$, represents the detector probe capacitance which is connected to the

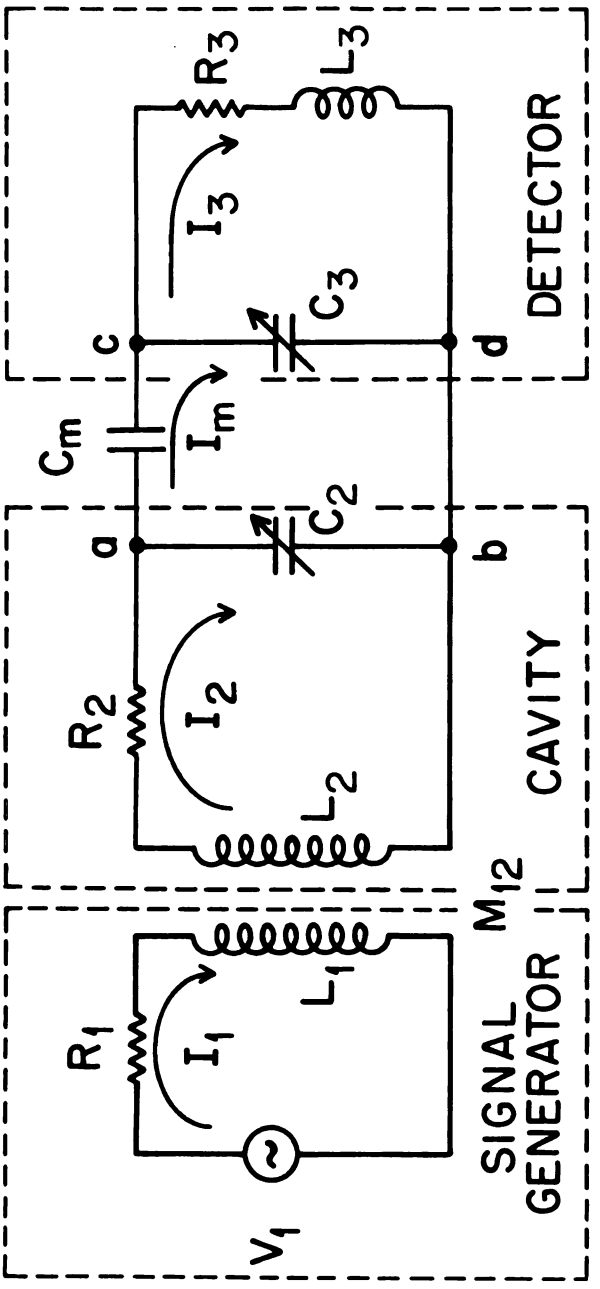


Figure A-2. Fundamental Equivalent Circuit to Represent the Resonant Cavity Oscillometer (Detector Coupled Capacitively to the Cavity)

rod probe. The resistance $R_3$ and inductance $L_3$ represent the total distributed resistance and inductance associated with the detector network.

The circuit representation shown in Fig. A-2, differs from that shown in Fig. 16 in that the detector is capacitively coupled to the cavity by capacitance, $C_m$. Whereas, in Fig. 16, the detector is shown to be inductively coupled. As previously stated, the same qualitative interpretations of the coupled resonance circuit (Fig. 16 or Fig. A-2) may be derived for either form of coupling, inductive or capacitive. For the inductively coupled circuits, it is much simpler to show the relationship between the voltage, current, and impedances of the various loops.

For the circuit shown in Fig. A-2, the following equation may be written to represent the voltage and current relationships of the four loops (circuit 1, 2, 3, and the capacitive coupling network consisting of $C_2$, $C_M$, and $C_3$)

(A-30) $$V_1 = I_1\left[R_1\right] + I_1\left[jX_{l_1}\right] + I_2\left[jX_{M_{12}}\right]$$

(A-31) $$0 = I_2\left[R_2\right] + \left[I_2 - I_m\right]\left[-jX_{c_2}\right] + I_2\left[jX_{l_2}\right] + I_1\left[jX_{M_{12}}\right]$$

(A-32) $$0 = I_m\left[jX_{c_m}\right] + \left[I_m - I_3\right]\left[-jX_{c_2}\right] + \left[I_m - I_2\right]\left[-jX_{c_2}\right]$$

(A-33) $$0 = I_3\left[R_3\right] + I_3\left[jX_{l_3}\right] + \left[I_3 - I_m\right]\left[-jX_{c_3}\right]$$

Then rearrangement of the terms yields the following equations

(A-30a) $$V_1 = \left[R_1 + jX_{l_1}\right]I_1 + \left[jX_{M_{12}}\right]I_2$$

(A-31a) $$0 = \left(jX_{M_{12}}\right)I_1 + \left(R_2 + j\left(X_{l_2} - X_{c_2}\right)\right)I_2 + \left(jX_{c_2}\right)I_m$$

(A-32a) $$0 = \left(jX_{c_2}\right)I_2 + \left(-j\left(X_{c_2} + X_{c_m} + X_{c_3}\right)\right)I_m + \left(jX_{c_3}\right)I_3$$

(A-33a) $$0 = \left(jX_{c_m}\right)I_m + \left(R_3 + j\left(X_{l_3} - X_{c_3}\right)\right)I_3$$

These simultaneous equations are of the general form

(A-30b) $$A = a_{11}I_1 + a_{12}I_2 + a_{13}I_m + a_{14}I_3$$

(A-31b) $$B = a_{21}I_1 + a_{22}I_2 + a_{23}I_m + a_{24}I_3$$

(A-32b) $$C = a_{31}I_1 + a_{32}I_2 + a_{33}I_m + a_{34}I_3$$

(A-33b) $$D = a_{41}I_1 + a_{42}I_2 + a_{43}I_m + a_{44}I_3$$

where:

$A = V$

$B = 0$

$C = 0$

$D = 0$

$a_{11} = Z_1 = R_1 + jX_{l_1}$

$a_{12} = jX_{M_{12}}$

$a_{13} = 0$

$a_{14} = 0$

$a_{21} = jX_{M_{12}}$

$a_{22} = Z_2 = R_2 + j\left(X_{l_2} - X_{c_2}\right)$

$a_{23} = jX_{c_2}$

$a_{24} = 0$

$a_{31} = 0$

$a_{32} = jX_{c_2}$

$a_{33} = -j\left(X_{c_2} + X_{c_m} + X_{c_3}\right)$

$a_{34} = jX_{c_3}$

$a_{41} = 0$

$a_{42} = 0$

$a_{43} = jX_{c_m}$

$a_{44} = Z_3 = R_3 + j\left(X_{l_3} - X_{c_3}\right)$

These simultaneous equations may be solved for $I_1$, $I_2$, $I_m$ and $I_3$ by the use of determinates. For example for $I_1$

$$I_1 = \frac{\begin{vmatrix} V & a_{12} & 0 & 0 \\ 0 & a_{22} & a_{23} & 0 \\ 0 & a_{32} & a_{33} & a_{34} \\ 0 & 0 & a_{43} & a_{44} \end{vmatrix}}{\begin{vmatrix} a_{11} & a_{12} & 0 & 0 \\ a_{21} & a_{22} & a_{23} & 0 \\ 0 & a_{32} & a_{33} & a_{34} \\ 0 & 0 & a_{43} & a_{44} \end{vmatrix}} \tag{A-34}$$

or

$$I_1 = \left| \frac{a_{22}a_{33}a_{44} - a_{22}a_{34}a_{43} - a_{23}a_{32}a_{44}}{a_{11}a_{22}a_{33}a_{44} - a_{11}a_{22}a_{34}a_{43} - a_{11}a_{23}a_{32}a_{44} - a_{12}a_{21}a_{33}a_{44} + a_{12}a_{21}a_{34}a_{43}} \right| V_1 \tag{A-35}$$

In a similar manner, the value of $I_2$, $I_m$ and $I_3$ may be determined and are given by

$$I_2 = \left| \frac{-a_{21}a_{33}a_{44} + a_{21}a_{34}a_{43}}{a_{11}a_{22}a_{33}a_{44} - a_{11}a_{22}a_{34}a_{43} - a_{11}a_{23}a_{32}a_{44} - a_{12}a_{21}a_{33}a_{44} + a_{12}a_{21}a_{34}a_{43}} \right| V_1 \tag{A-36}$$

$$I_m = \left| \frac{a_{21}a_{32}a_{44}}{a_{11}a_{22}a_{33}a_{44} - a_{11}a_{22}a_{34}a_{43} - a_{11}a_{23}a_{32}a_{44} - a_{12}a_{21}a_{33}a_{44} + a_{12}a_{21}a_{34}a_{43}} \right| V_1 \tag{A-37}$$

$$(A\text{-}38) \qquad I_3 = \left| \frac{-a_{21}\, a_{32}\, a_{43}}{a_{11}\, a_{22}\, a_{33}\, a_{44} - a_{11}\, a_{22}\, a_{34}\, a_{43} - a_{11}\, a_{23}\, a_{32}\, a_{44} - a_{12}\, a_{21}\, a_{33}\, a_{44} + a_{12}\, a_{21}\, a_{34}\, a_{43}} \right| V_1$$

To illustrate the complexity and difficulty in handling the above equations, one need only substitute the proper impedance and reactance value for each of the coefficients. For example, the denominator for equations (A-35) - (A-38) is given by

$$(A\text{-}39) \qquad \text{Denominator} = Z_1 Z_2 Z_3 \left| -j X_{c_2} + X_{C_m} + X_{c_3} \right| + Z_1 Z_2 X_{c_3} X_{c_m} + Z_1 Z_3 X^2_{c_2} + X^2_{M_{12}} Z_3 \left| -j X_{c_2} + X_{c_m} + X_{c_3} \right| + X^2_{M_{12}} X^2_{c_3}$$

To determine the absolute magnitude for the respective current values, all manipulations must be carried out vectorially, which in turn introduce many more terms as compared to the current obtained for $I_2$ (equation (117) in the treatment of the inductive coupled circuits (refer to DISCUSSION AND RESULTS).

The value of $X_{c_2}$ or $X_{c_3}$ which will produce maximum effective detector current may be found by differentiating the expression for $I_3$ (as given in equation (A-35), and in which the proper values of resistances and reactances are substituted) with respect to the proper $X$ and equating $dI_3/dX$ equal to zero. For example, the value of $X_c$ which will produce partial resonance may be determined by equating $dI_3/dX_2$ equal to zero and solving for $X_2$ in terms of the other parameters. Having determined

the value of $X_2$ which will produce partial resonance, it is then possible to determine the value of $C_2$ which will yield the given value of $X_2$ (refer to equation (131), RESULTS AND DISCUSSION).

To use the susceptance-variance technique to measure the high frequency shunt conductance across the variable cell capacitance $\left(C_t \text{ and } C_v\right)$, it is necessary to show that the detector voltage, $V_{c_3}$, is directly proportional to the voltage drop across the equivalent cavity capacitance, $C_2$.

The voltage across the detector probe capacitance, $C_3$, and the voltage across the cavity capacitance, $C_2$, are given by

$$V_{c_3} = -jX_{c_3}\left(I_m - I_3\right) \tag{A-40}$$

$$V_{c_2} = -jX_{c_2}\left(I_2 - I_m\right) \tag{A-41}$$

The ratio of the voltages is then equal to

$$\frac{V_{c_3}}{V_{c_2}} = \frac{\left(I_m - I_3\right) - X_{c_3}}{\left(I - I_m\right)X_{c_2}} \tag{A-42}$$

If one substitutes into equation (A-42) the values of $I_2$, $I_m$, and $I_3$ given by equations ( A-36), (A-37) and (A-38) respectively, the ratio of the voltage is then given by

$$\frac{V_{c_3}}{V_{c_2}} = \left[\frac{a_{32}\left(a_{44} + a_{43}\right)}{a_{34}a_{43} - a_{33}a_{44} - a_{32}a_{44}}\right]\frac{X_{c_3}}{X_{c_2}} \tag{A-43}$$

Furthermore, if the value of reactance, resistance, and impedance corresponding to the appropriate coefficients are substituted in equation (A-43), the ratio of the voltage is shown to equal

$$(A\text{-}44) \qquad \frac{V_{c_3}}{V_{c_2}} = \left| \frac{-jX_{c_m} X_{c_3}^{\,2} Z_3}{X_{c_m} X_{c_3} - j\left[X_{c_m} + X_{c_3}\right] Z_3} \right|$$

The significance of equation (A-44) is that for a given value of $C_3$, assuming that $C_m$, $R_3$, and $L_3$ are fixed and operate independently of each other, the voltage measured across the detector probe capacitance, $C_3$, is directly proportional to the voltage across the cavity capacitance, $C_2$.

Thus, it is possible to use the susceptance variance technique to determine the capacitance difference at the half power points and relate this value to the equivalent high frequency shunt conductance of the oscillometer (refer to APPENDIX VII for derivation of equation for the susceptance variance method).